40236

National Library of Canada
Bibliothèque nationale du Canada

CANADIAN THESES ON MICROFICHE

THÈSES CANADIENNES SUR MICROFICHE

NAME OF AUTHOR/*NOM DE L'AUTEUR* FRANCIS JOSEPH McVeA

TITLE OF THESIS/*TITRE DE LA THÈSE* ELECTRICAL PROPERTIES OF THE ATHABASCA TAR SANDS

UNIVERSITY/*UNIVERSITÉ* University of Alberta

DEGREE FOR WHICH THESIS WAS PRESENTED/ *GRADE POUR LEQUEL CETTE THÈSE FUT PRÉSENTÉE* Masters of Science

YEAR THIS DEGREE CONFERRED/*ANNÉE D'OBTENTION DE CE GRADE* 1978

NAME OF SUPERVISOR/*NOM DU DIRECTEUR DE THÈSE* Dr CHUTE AND Dr Vermeulen

Permission is hereby granted to the NATIONAL LIBRARY OF CANADA to microfilm this thesis and to lend or sell copies of the film.

The author reserves other publication rights, and neither the thesis nor extensive extracts from it may be printed or otherwise reproduced without the author's written permission.

L'autorisation est, par la présente, accordée à la BIBLIOTHÈQUE NATIONALE DU CANADA de microfilmer cette thèse et de prêter ou de vendre des exemplaires du film.

L'auteur se réserve les autres droits de publication; ni la thèse ni de longs extraits de celle-ci ne doivent être imprimés ou autrement reproduits sans l'autorisation écrite de l'auteur.

DATED/*DATÉ* June 12/78 SIGNED/*SIGNÉ* F J McVea

PERMANENT ADDRESS/*RÉSIDENCE FIXE*
1585 LAKEWOOD ROAD WEST
EDMONTON ALBERTA
T6K 2V7

NL-91 (3-74)

National Library of Canada

Cataloguing Branch
Canadian Theses Division

Ottawa, Canada
K1A 0N4

Bibliothèque nationale du Canada

Direction du catalogage
Division des thèses canadiennes

NOTICE

The quality of this microfiche is heavily dependent upon the quality of the original thesis submitted for microfilming. Every effort has been made to ensure the highest quality of reproduction possible.

If pages are missing, contact the university which granted the degree.

Some pages may have indistinct print especially if the original pages were typed with a poor typewriter ribbon or if the university sent us a poor photocopy.

Previously copyrighted materials (journal articles, published tests, etc.) are not filmed.

Reproduction in full or in part of this film is governed by the Canadian Copyright Act, R.S.C. 1970, c. C-30. Please read the authorization forms which accompany this thesis.

THIS DISSERTATION
HAS BEEN MICROFILMED
EXACTLY AS RECEIVED

AVIS

La qualité de cette microfiche dépend grandement de la qualité de la thèse soumise au microfilmage. Nous avons tout fait pour assurer une qualité supérieure de reproduction.

S'il manque des pages, veuillez communiquer avec l'université qui a conféré le grade.

La qualité d'impression de certaines pages peut laisser à désirer, surtout si les pages originales ont été dactylographiées à l'aide d'un ruban usé ou si l'université nous a fait parvenir une photocopie de mauvaise qualité.

Les documents qui font déjà l'objet d'un droit d'auteur (articles de revue, examens publiés, etc.) ne sont pas microfilmés.

La reproduction, même partielle, de ce microfilm est soumise à la Loi canadienne sur le droit d'auteur, SRC 1970, c. C-30. Veuillez prendre connaissance des formules d'autorisation qui accompagnent cette thèse.

LA THÈSE A ÉTÉ
MICROFILMÉE TELLE QUE
NOUS L'AVONS REÇUE

NL-339 (3/77)

THE UNIVERSITY OF ALBERTA

ELECTRICAL PROPERTIES OF THE ATHABASCA TAR SANDS

by

©

FRANCIS JOSEPH MCVEA

A THESIS
SUBMITTED TO THE FACULTY OF GRADUATE STUDIES AND RESEARCH
IN PARTIAL FULFILMENT OF THE REQUIREMENTS FOR THE DEGREE
OF MASTER OF SCIENCE
IN
ELECTRICAL ENGINEERING

DEPARTMENT OF ELECTRICAL ENGINEERING

EDMONTON, ALBERTA
FALL, 1978

THE UNIVERSITY OF ALBERTA

FACULTY OF GRADUATE STUDIES AND REASEARCH

The undersigned certify that they have read, and recommend to the faculty of Graduate Studies and Reasearch, for acceptance, a thesis entitled "Electrical Properties of the Athabasca Tar Sands" submitted by Francis Joseph Mcvea in partial fulfilment of the requirements for the degree of Master of Science in Electrical Engineering.

S Chute
Supervisor

F. E. Vermeulen
Supervisor

C. G. Englefield

C. E. Capjack

External Examiner

Date June 6/78

DEDICATION

This thesis is dedicated to my brother Christopher who was killed in his second year of Electrical Engineering. Christopher was always prepared to face new challenges and would put everything he had into the struggle. His kindness, willingness to help others and uncompromising efforts will long be remembered.

ABSTRACT

The conductivity and dielectric permittivity of samples of tar sand from the Athabasca tar sands in northern Alberta have been measured at low frequencies as part of a study of the feasibility of in situ separation of bitumen from tar sand using electromagnetic fields.

A study of existing measuring procedures and of problems associated with low frequency measurements in general led to the selection of a two electrode measuring technique employing copper electrodes mated to the tar sand samples with blotters soaked in a copper sulphate solution.

Results for conductivity and dielectric permittivity over a frequency range from 10^2 Hz to 10^7 Hz are included.

ACKNOWLEDGEMENTS

The research described in this thesis was carried out at the Department of Electrical Engineering, University of Alberta, under the joint supervision of Dr. F. E. Vermeulen and Dr. F. S. Chute to whom the author is indebted for their patient assistance and guidance.

The author would also like to thank his wife for her support and patience and, of course, for typing this thesis.

TABLE OF CONTENTS

CHAPTER PAGE

INTRODUCTION 1

1 MEASUREMENT OF ELECTRICAL PARAMETERS 9

1.1 General 9

1.2 Laboratory Measurements 12

1.2.1 The Capacitance Test Cell 12

1.2.2 Resonance Methods 17

1.2.3 Four Electrode Methods 22

1.2.4 Transmission Line Methods 25

1.2.5 Waveguides and Resonators 31

1.3 In Situ Measurements 36

1.3.1 Wave Tilt Method 36

1.3.2 Field Strength Method 39

1.3.3 Four Probe Methods 39

2 MEASUREMENT ERRORS 42

2.1 General 42

2.2 Electrode Contact Errors 45

2.3 Electrode Polarization 51

2.4 Polarization Errors 59

3 MEASUREMENT TECHNIQUES 64

3.1 General 64

3.2 Two Electrode Measurement Cell 65

3.2.1 Cell Construction 65

3.2.2 Electrode Preparation 68

TABLE OF CONTENTS continued

3.2.3 Sample Preparation 75

3.2.4 Measuring Instruments 78

3.3 Coaxial Measurement Cell 85

3.4 Tar Sand Sample Analysis 87

4 EXPERIMENTAL RESULTS 90

4.1 General 90

4.2 Capacitive Cell Results 90

4.3 Coaxial Cell Results 95

4.4 Discussion of Results 97

4.5 Conclusions 101

LIST OF REFERENCES 146

LIST OF FIGURES

Figure Page

1.1 Measurement Cell 14

1.2 Measurement Cell of Figure 1.1 14

1.3 Test Cell Representation With Sample 15

1.4 Resonant Measurement Circuit 18

1.5 Voltage Resonance 21

1.6 Four Electrode Cell 24

1.7 Four Electrode Measurement System 24

1.8 Transmission Line Representation 26

1.9 Transmission Line 31

1.10 Waveguide Measurement 32

1.11 Transmission Bridge 35

1.12 Wave Tilt Technique 37

1.13 Four Electrode Array 40

2.1 Electrode Contact Representation 46

2.2 Electrode Contact Circuit 46

2.3 Circuit for Air Gap Methods 47

2.4 Apparent Capacitance Versus Frequency 48

2.5 Metal Electrode Interface 51

2.6 Ionic Double Layer 54

2.7 Overvoltage Versus Net Current 56

2.8 Interface Impedance 59

3.1 Test Cell Holder 67

3.2 Mid-range Measurements 80

LIST OF FIGURES continued

3.3 Low Frequency Measurement Arrangement 84
4.1 Tar Sand Samples 4M1 4M2 104
4.2 Tar Sand Samples 4M1 4M3 105
4.3 Tar Sand Samples 4T1 4T2 106
4.4 Tar Sand Samples 4W1 4W1a 107
4.5 Composite Graph of Batch 1 108
4.6 Tar Sand Samples 4R2 4R2a 109
4.7 Tar Sand Samples 4R3 4R3a 110
4.8 Tar Sand Samples 4F1 4F1a 111
4.9 Tar Sand Samples 5T1 5T1a 112
4.10 Tar Sand Samples 5T2 5T2a 113
4.11 Tar Sand Samples 5W2 5W2a 114
4.12 Tar Sand Samples 5W1 5W3 115
4.13 Tar Sand Samples 5W2 5W3 116
4.14 Tar Sand Samples 5R1 5R1a 117
4.15 Tar Sand Samples 5R2 5R2a 118
4.16 Tar Sand Samples 5F1 5F1a 119
4.17 Tar Sand Samples 6M1 6M1a 120
4.18 Tar Sand Samples 6T1 6T1a 121
4.19 Tar Sand Samples 6T1a 6T2 122
4.20 Composite Graph Of Batch 2 123
4.21 Tar Sand Samples 6R1 6R1a 124
4.22 Tar Sand Samples 6R2 6R2a 125
4.23 Tar Sand Samples 6F1 6F2 126
4.24 Tar Sand Samples 6F1 6F3 127

LIST OF FIGURES continued

4.25 Tar Sand Samples 6F3 6F4 128

4.26 Tar Sand Samples 7M1 7M1a 129

4.27 Composite Graph of Batch 3 130

4.28 Drying Test Results 131

4.29 Pure Bitumen Sample Results 132

4.30 Tar Sand Sample F1-1 133

4.31 Tar Sand Sample F3-1 134

4.32 Tar Sand Sample F3-2 135

4.33 Tar Sand Sample F3-3 136

4.34 Tar Sand Sample F3-4 137

4.35 Composite Graph of Batch 4 138

4.36 Tar Sand Sample F4-1 139

4.37 Tar Sand Sample F4-2 140

4.38 Tar Sand Sample F4-3 141

4.39 Composite Graph of Batch 5 142

4.40 First Drying Test 143

4.41 Second Drying Test 144

4.42 Parameter Limits 145

LIST OF PHOTOGRAPHIC PLATES

Plate	Description	Page
1	Capacitive Test Cell Assembly	66
2	Instrument Arrangement for Measurements	83
3	Coaxial Measurement Cell	86
4	Tar Sand Analysis Unit	88

INTRODUCTION

THE ATHABASCA TAR SANDS

The tar sands of Alberta consist of a dense viscous conglomerate of sand, clay, and heavy oil. Although tar sands are found throughout the world, the largest body and only deposit undergoing commercial development is located in northeastern Alberta.

The Alberta Energy Resources Conservation Board places the proven resources at about 350 billion barrels. At present only one process utilizing mined tar sand is used for bitumen recovery. There are two factors which limit the amount of tar sand which can be mined. The first of these is the bitumen saturation. Current policy is to select plant feed with bitumen saturation of 10% or greater by weight. This policy excludes about 30% of the tar sands from mining development. The second quantity which limits mining development is the thickness of overburden covering the tar sand. Using present techniques, an overburden depth of 120 feet is generally accepted as the economic limit for stripping.[1] These two limits reduce the amount which can be mined to about 10% of the proven resources. Tar sand mining requires manipulation of vast amounts of material under harsh climatic conditions and has become viable only with the rising demand for crude oil.

To fully exploit the tar sands, an in situ recovery technique must be developed. Currently, the most promising methods under study employ thermal heating of the tar sand in place to reduce the bitumen viscosity to a point where conventional production techniques can be used.

In situ production of bitumen from the tar sands is very similar to secondary oil production in that some form of drive energy must be provided to force the oil to the surface. In secondary production this drive energy has been expended during initial production while in the tar sands this energy never existed. Most in situ proposals to recover bitumen envision a pattern of injection wells into which air or steam is forced to drive the oil to a production well where it is collected. The injection wells are expected to surround the production well in some regular geometric pattern. For example, four injection wells could be placed at each corner of a square with the production well at the center.

There are several methods which can furnish the required drive energy. The forward combustion method forces air into the injection wells. The bitumen is ignited and the resulting high temperature zone moves towards the production well, pushing the oil ahead of it as it moves. The tar sand bed must be sufficiently permeable to allow the oil to flow without blockage. The peak temperature as well as the combustion zone velocity are functions of the rate at which air is forced into the injection wells. The combustion reaction consumes both the heavier fractions of the bitumen and the residue coke. The bitumen is therefore partially distilled and an upgraded product is collected.

A further development of this plan is the combination of forward combustion and water flood (COFCAW). After forward combustion has raised the local reservoir temperatures sharply, a water and air mixture is forced into the injection wells. The water serves to distribute the high local temperatures throughout a greater portion of the oil reservoir. The subsequent lowering of viscosity allows the oil to be driven to a production well under the action of the air and water. The efficiency of this proposal depends on heat losses from the formation. If the losses upward through the overburden or downward through the basement rock are excessive, the combustion zone temperature will drop sufficiently that self-sustaining combustion will cease. The insulation required to minimize the heat loss may limit this process to tar sand areas covered by thick layers of overburden.[2]

The reverse combustion method consists of igniting the bitumen at the production well, thus forcing the burning front to propagate towards the injection well. In this method only air must pass through the unburned bed; the combustion products travel through the previously heated portion of the formation. The blockage problem encountered in the forward combustion method no longer exists since the path to the production well has been swept clean previously. The product is regained in a gaseous form and requires little upgrading. However, reverse combustion consumes a middle fraction of the bitumen and leaves an unburned residue behind. Also, a significant amount of energy is left behind the combustion front in the form of heat.

A second approach for in situ production uses steam or some other driver fluid to increase the mobility of the bitumen and allow production. The fluid injection method is a relatively low temperature recovery technique. Although a hydrocarbon dilutent could be used to lower the viscosity of the tar sand, the initial cost of the solvent plus the loss of solvent associated with the procedure preclude this method from current investigation. Much more promising is an oil water emulsion formed by forcing either hot water or steam into the injection well. Steam is particularily attractive because its high latent heat allows high energy transfer to the bitumen formation. This thermal energy mobilizes the bitumen permitting an emulsion to form. The viscosity of such an emulsion is essentially that of the water component which is very mobile and could be forced to the production well relatively easily. Problems arise, however, since the feedwater must be softened to remove excess minerals before being heated to steam in a boiler. Large amounts of waste water are produced which require cleaning before recycling or disposal. Also a portion of the recovered bitumen must be consumed as fuel to continue the process. Again a thick insulating blanket of overburden may be required to prevent excessive heat losses from the tar sand.[3]

The preceeding proposals for in situ development show that some form of energy must be introduced to reduce the viscosity of the bitumen and that adequate communication must exist between the production and injection wells. If the tar sand permeability is low, some form of path must be established between the wells along which energy can propagate and bitumen may flow. This energy will be conducted radially outwards along the path so as to heat a large area.

Recently there has been interest in the direct application of electrical energy to the tar sands. An electrical in situ technique could consist of two electrodes, one at an injection well and one at the production well. If a sufficiently high voltage were applied across these electrodes, significant current would flow in the intervening tar sand material. The current flow would result in a carbonized path between the two wells. This technique was initially used to gassify coal.

As well, Davis[4] reported that a potential of 2300 volts with an electrode spacing of thirty feet was sufficient to distill petroleum from oil reservoir rocks. Once an electrical path between injection and production wells exists, electrical heating may be continued to reduce the viscosity of bitumen surrounding the path. Initial communication between two wells thus having been established by electrical methods, conventional steam or water drive may prove more economical for the continuation of the bitumen heating. Flock[5] suggests that a surface nuclear plant would provide not only the low cost electrical energy required but also a great amount of waste thermal energy. This thermal energy could be utilized at some further stage of the in situ process.

The low frequency electrical heating method just described is based on electrical conduction. That is, electrical energy propagation and ohmic heating occur due to current flow between the two electrodes. As the frequency of the electric field is increased other mechanisms become responsible for energy propagation. In the upper audio frequencies currents are induced in the material; thus a direct conductive path is not required between electrodes to produce heat. As the frequency is further increased to radio and microwave frequencies, the energy is transferred to the tar sand by electromagnetic radiation. The heating effect is primarily due to dielectric rather than ohmic heating.

Direct electrical heating at high frequencies would be advantageous since the radiated energy could selectively heat the tar sand but not the overburden or basement formations. This advantage comes about because the volume into which energy is directed can be selected by judicious choice of antennas. Unlike steam or combustion methods which transfer energy radially outward along a path between the injection and production wells, electrical radiation heats the water contained within the tar sand directly without need of a permeable path. Thus bitumen from previously inaccessible areas may be produced. Abernathy,[6] using theoretical heat flow models, suggests that a much more uniform temperature distribution between injection and production wells can be obtained through electromagnetic radiation. To properly design an in situ system based on direct electrical heating, the electrical properties of the tar sand must be known over a wide frequency range. These properties depend on a variety of factors such as water content and bitumen saturation.

The purpose of this thesis is to ascertain the electrical parameters of tar sands. The first and second Chapters will deal with the various methods available to determine the parameters and the causes of measurement errors. Although measuring techniques over a wide frequency range are described, the primary interest in this thesis lies in the lower frequencies. The third Chapter will give a complete description of the actual measuring equipment used, and will also describe the various types of electrodes which were tested in order to minimize measurement error. The fourth Chapter will present the measurement results. These results primarily include the conductivity and permittivity of tar sand versus frequency. Measurements taken on pure bitumen samples and tar sand samples allowed to dry are also included. The fourth Chapter will also attempt to interpret the data obtained in terms of the physical tar sand parameters.

CHAPTER ONE

MEASUREMENT OF ELECTRICAL PARAMETERS

1.1 GENERAL

Physically, tar sand consists of water-wetted sand particles which are in turn surrounded by a bitumen cover. The space between the bitumen-covered sand particles contains free water and mineral material. The sand makes up about 83% by weight of the tar sand while the bitumen and water combination remains relatively constant at approximately 17%. The material between the bitumen-covered grains contains clay-like mineral referred to as fines. The higher the bitumen saturation, the lower the amount of fines.[7]

The preceeding discussion of electrical in situ techniques suggests that a comprehensive tabulation of electrical parameters of tar sand over a wide frequency range is required. At low frequencies, for a given driving voltage, the resistivity of the tar sand will determine the heating rate. For instance, the resistivity increases as the water is evaporated from the tar sand and the heating rate will decrease. At high frequencies the electrical properties will also determine the heating rate and in addition set the depth to which energy can propagate. The electrical parameters and their variation with change in the physical properties of the tar sand are evidently of paramount importance in any system design. Also, the determination of the electrical parameters of various samples of tar sand may give information regarding the bitumen or water saturation and thereby eliminate time consuming physical extraction and analysis procedures.

The electrical parameters which characterize a dielectric are the conductivity, the permittivity, and the permeability. The magnetic permeabilities of most materials vary little from that of free space and are seldom tabulated. The permittivity or dielectric constant is a measure of the polarization of a substance. When a material is placed in an electric field the relative displacement of positive and negative charge centers causes the material to become polarized. The total polarization is made up of different components which in turn depend on the nature of the charges which are displaced. *Electronic polarization* is due to the relative displacement of the electron cloud and the nuclei of the atom. *Atomic polarization* involves displacement of atoms within a molecule by bending or stretching bonds between atoms. For an ionic solid, atomic polarization would be seen as the displacement of the component ions. If the material is dipolar there is an additional form of polarization, *orientational polarization*. Rather than being in random thermal motion, the dipole moments tend to align with the applied electric field. In a heterogeneous dielectric where the electrical properties of the constituent parts differ, a fourth type of polarization, interfacial, is noted. Interfacial polarization occurs in heterogeneous dielectrics where charge movement varies between component phases of the material. Charge will accumulate along interface boundaries where conductivities differ. In material with electrolytic conduction the charged particles responsible for interfacial polarization are ions. A material such as tar sand has many interfaces between sand or clay particles and electrolytes where interfacial polarization will occur. However, if such polarization forms at the sample-electrode interface, the electrodes are altering the sample and a measurement error exists. This type of error will be discussed in Chapter Two.

Generally speaking, each of these polarization components contributes to the dielectric constant over different frequency ranges. At high frequencies, only electrons can accelerate quickly enough to follow the alternating field and, hence, high frequency polarization is predominantly electronic. As the driving frequency is lowered, the other mechanisms of polarization begin to contribute as well. Because these mechanisms of polarization are frequency dependent, the dielectric permittivity increases with decreasing frequency and the term 'dielectric constant' is a misnomer. In addition to the displacement of charge caused by a time varying electric field, there is a dielectric loss. This loss results from friction due to ionic movement within the material and is responsible for the dielectric heating noticed at high frequencies.

1.2 LABORATORY MEASUREMENTS

There is no single measuring technique which will yield the dielectric permittivity or the conductivity over the wide frequency range required to characterize a material. The remainder of this chapter will discuss the measuring techniques available in the various frequency ranges of interest. For audio to low radio frequencies a capacitor test cell is widely used. Above this range into the hundreds of MHz, a transmission line method is employed. At microwave frequencies either a resonant cavity or a dielectric loaded waveguide is used.

In addition, field techniques capable of measuring the electrical parameters of earth materials averaged over many meters are described, as well as bore hole techniques developed primarily for oil and mineral prospecting.

1.2.1 The Capacitive Test Cell

At low frequencies, where circuit theory approximations hold, a capacitor test cell is used. The capacitance of the test cell increases when a dielectric is introduced between the electrodes. From the physical size of the capacitor and the change in capacitance between empty and full measurements, the dielectric permittivity may be obtained. The conductivity is measured in a similar manner.

The capacitor test cell is generally of the parallel plate or coaxial cylinder type. A retaining ring of low loss material such as plexiglass or teflon is used with the parallel plate cell to contain semi-solid materials and hold the plates in a parallel configuration. The dielectric permittivity, ε_r , is the ratio of the capacitance of the cell including the sample, to that of the empty cell. Any extra capacitances which are measured in addition to the sample capacitance must be accounted for. These extra capacitances are indicated in the following figure which depicts a typical measurement test cell. They include the interlead capacitance resulting from the measuring leads and also a term, C_{oh}, which accounts for the capacitance in the overhang region including the effect of the retaining ring and retaining bolts.

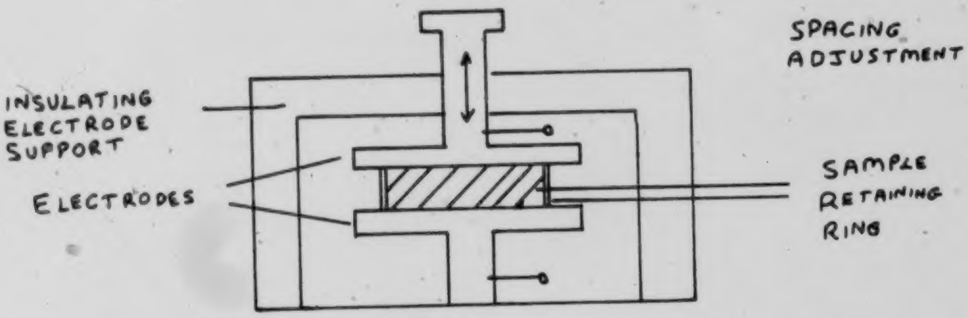
SPACING ADJUSTMENT
INSULATING ELECTRODE SUPPORT
ELECTRODES
SAMPLE RETAINING RING

Figure(1.1) Measurement Cell

This cell is represented schematically in Figure 1.2:

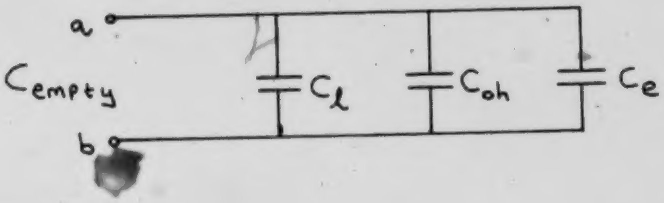
a
C_{empty}
b
C_l
C_{oh}
C_e

Figure(1.2) Measurement Cell of Figure 1.1

The capacitance of the sample area with no dielectric inserted is given by Ce, while the total empty capacitance including leads and overhang is given by Cempty.

Figure 1.3 shows the measuring arrangement once the sample has been inserted between the plates.

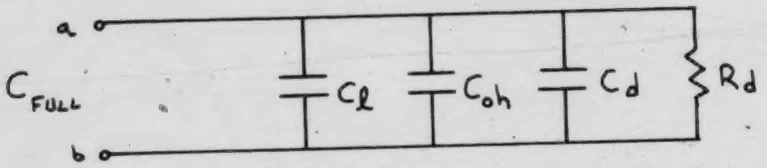

Figure(1.3) Test Cell Representation With Sample

C_d and R_d are the capacitance and resistance of the dielectric sample. Since all the extraneous capacitances are in parallel with the sample, the total capacitance of the filled test cell at terminals a, b becomes:

$$C_{FULL} = C_{\ell} + C_{oh} + C_d \tag{1.1}$$

The capacitance measured with no tar sand inserted is:

$$C_{EMPTY} = C_{\ell} + C_{oh} + C_e \tag{1.2}$$

Therefore:

$$C_{FULL} - C_{EMPTY} = C_d - C_e$$

$$C_d = C_{FULL} - C_{EMPTY} + C_e \tag{1.3}$$

Since the dielectric permittivity, ε_r, is the ratio of the full cell capacitance to the empty cell capacitance, then:

$$\varepsilon_r = C_d = \frac{C_{FULL} - C_{EMPTY} + C_e}{C_e}$$

$$\varepsilon_r = \frac{C_{FULL} - C_{EMPTY}}{C_e} + 1$$

(1.4)

The extra capacitances C_ℓ and C_{oh} are common to both measurements and thus their numerical values are not required for the determination of ε_r. The sample conductivity, σ, may be determined from the resistance measured with the sample inserted, R_d, and the test cell geometry. The expression for σ becomes:

$$\sigma = \frac{1}{R_d} \times \frac{d}{A} \qquad (1.5)$$

where d is the spacing between electrodes and A is the electrode area covered by the sample.

Either a direct or a comparison method may be used to measure the empty and full capacitances at terminals a,b. A direct reading places a voltage across terminals a,b and measures the magnitude and phase of the resulting current. A similar measurement is taken across the empty cell. From these two readings the electrical parameters may be derived. Alternatively, a bridge compares the current through a variable capacitor and variable resistor with the current through the unknown impedance. When the bridge is balanced, as indicated by a null meter deflection, the variable components have the same impedance as the unknown sample. Since the variable components are calibrated, the unknown sample values may be read directly off the bridge.

1.2.2 Resonance Methods

The bridge method referred to above relies on two calibrated circuit elements. However, as the measurement frequency is increased, additional impedances due to circuit leads and imperfect circuit elements produce uncertainties in the calibration of these elements. For example, resistors exhibit series inductance and higher resistance at high frequencies. These errors are so large that only a Schering bridge which employs calibrated capacitors can be used accurately above 100kHz.

In order to conduct measurements of electric parameters of dielectrics between 10 and 100kHz, Hartshorn and Ward[8] have suggested a resonant circuit technique. Although there are several different resonance methods available, all attempt to measure the capacitance of a test cell by resonating it in an inductive circuit. Resonance is first obtained with the sample in place, following which the circuit is reresonated with just the empty cell by adjusting the electrode spacing, usually with a micrometer drive. The various methods differ in the procedure by which the conductance is determined, however. Hartshorn and Ward used a reactance variation method for three reasons. First, air capacitors are the only calibrated standards required. Second, all components are connected in parallel which simplifies shielding between components and ground. Third, calibration of the apparatus at one frequency will hold over the entire frequency range. The basic measuring circuit used by Hartshorn and Ward is shown in figure 1.4:

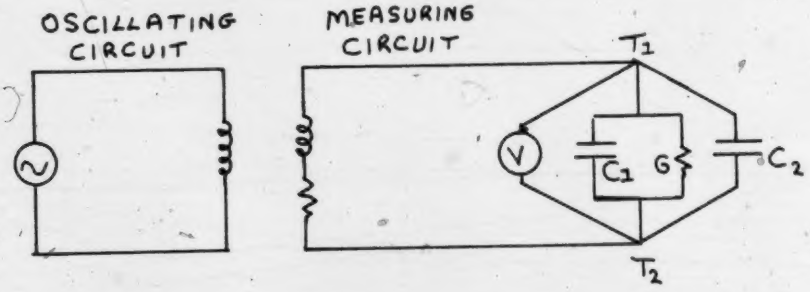

Figure(1.4) Resonance Measurement Circuit

The circuit consists of an oscillating circuit inductively coupled to the measuring circuit. C_1 is the test cell capacitance while C_2 is a small trimmer capacitor. G is the sample conductance. A high input impedance voltmeter, shown as V, is used to determine voltage resonance. If Voc is the open circuit voltage appearing across the terminals T_1 and T_2 when the cell is disconnected, the current which flows when the cell is connected is given by:

$$I = \frac{V_{oc}}{R + j\omega L_T + \frac{1}{G + j\omega C}} \tag{1.6}$$

where $C = C_1 + C_2$. The impedance $Z_T = R_T + j\omega L_T$ is the Thevenin equivalent impedance looking into the generator. The coil system and the capacitor holder system must be separately shielded from one another to prevent interaction between the impedances. The voltmeter between the terminal indicates:

$$V = \frac{I}{G + j\omega C} \tag{1.7}$$

which can be expressed as:

$$V = \frac{V_{oc}[G + j\omega C]}{Z_T[G + j\omega C] + 1} \times \frac{1}{G + j\omega C}$$

$$V = \frac{V_{oc}}{Z_T[G + j\omega C] + 1} \tag{1.8}$$

This expression may be rearranged to yield:

$$V = \frac{V_{oc}}{Z_T} \times \frac{1}{G + j\omega C + \frac{1}{Z_T}}$$

$$V = \frac{V_{oc}}{Z_T} \times \frac{1}{G + j\omega C + \frac{Z_T^*}{|Z_T|^2}} \tag{1.9}$$

where $Z_T^* = R_T - j\omega L_T$ is the complex conjugate of the Thevenin impedance.

$$V = \frac{V_{OC}}{Z_T} \times \frac{1}{G + \frac{R_T}{|Z_T|^2} + j\omega\left[C - \frac{L_T}{|Z_T|^2}\right]} \tag{1.10}$$

If all quantities are held constant while the capacitance is varied, the voltmeter will indicate a voltage maximum, Vr, when:

$$C = C_r = \frac{L_T}{|Z_T|^2} \tag{1.11}$$

where Cr is the total capacitance at voltage resonance. The ratio of the magnitude of the indicated voltage, V, squared at some other value of total capacitance, C, to the magnitude of the resonant voltage squared is given by:

$$\frac{V_r^2}{V^2} = \frac{\left[G + \frac{R_T}{|Z_T|^2}\right]^2 + \omega^2\left[C - \frac{L_T}{|Z_T|^2}\right]^2}{\left[G + \frac{R_T}{|Z_T|^2}\right]^2}$$

$$\frac{V_r^2}{V^2} = 1 + \frac{\omega^2\left[C - \frac{L_T}{|Z_T|^2}\right]^2}{\left[G + \frac{R_T}{|Z_T|^2}\right]^2} \tag{1.12}$$

If this squared voltage ratio is indicated by q, the capacitance at any value of q is indicated by:

$$C = \frac{L_T}{|Z_T|^2} \pm \frac{G + \frac{R_T}{|Z_T|^2}\sqrt{q-1}}{\omega} \tag{1.13}$$

$G + R_T/|Z_T|^2$ is just the equivalent total conductance, GT, of the circuit. The curve for voltage squared versus capacitance is shown in figure 1.5:

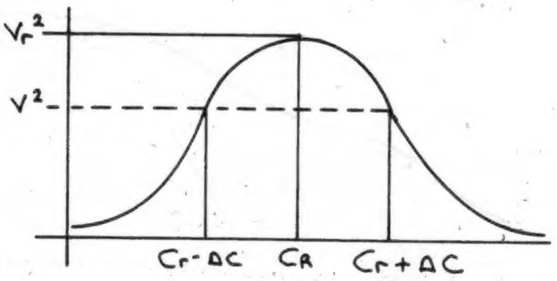

Figure(1.5) Voltage Resonance

For simplicity, the circuit is tuned off resonance by adjusting the small trimmer capacitor until a value V=.707Vr is indicated. The squared voltage ratio, q, is now two and the simplified expression for the total capacitance becomes:

$$C = C_r \pm \frac{G_T}{\omega} \tag{1.14}$$

The above equation can be solved for GT by substituting in the values of C which yields V=.707Vr on both sides of resonance to yield:

$$G_T = \omega \Delta C \tag{1.15}$$

With the dielectric sample between the electrodes, the circuit is tuned to resonance. The reading, Vr, of the voltmeter is noted. The circuit is detuned on both sides of resonance by means of the trimmer capacitor until V=.707Vr is noted. From equation 1.15 and these readings the total conductance is found. After again tuning to resonance the sample is removed and the circuit is reresonated by adjusting the electrode spacing of the test cell. At this resonance the total capacitance is identical to that measured with sample inserted. The ratio of this capacitance to the vacuum capacitance at the original 'sample inserted' spacing is the dielectric permittivity of the sample. The sample conductance, from which the conductivity may be calculated, is the difference between the 'sample in' conductance and the conductance without a sample.

Primarily resistive samples are difficult to measure accurately using a resonance technique due to the broadening of the resonant curve. Without a sharp peak, voltage resonance is determined by measuring symmetrically on both sides of the resonant peak and interpolating to find Vr.

The resonant method involves time-consuming measurements with the sample inserted and withdrawn at each frequency. Since certain physical parameters such as the water content of tar sand change very rapidly, a bridge technique was chosen because it permitted rapid measurements over a wide frequency range with little loss of accuracy compared to the resonant method. This technique will be described at a later stage.

1.2.3 Four Electrode Methods

Two electrode measurement techniques yield satisfactory results as long as the voltage measured by the electrodes truly represents the voltage across the sample. Unfortunately, unless excellent electrical contact is made between electrodes and sample, a nonlinear interface impedance develops. The error due to this impedance is then current-dependent. In addition, for samples in which conduction changes from electronic to ionic, an electrode polarization impedance develops due to ion accumulation. The ions accumulate along interfaces where conduction changes from ionic to electronic. Elaborate sample and electrode preparation techniques have been developed in an attempt to reduce this problem. These will be discussed in Chapter Two.

A different approach used by Schwan and Ferris,[9] and Ferris,[10] isolated the measuring circuit from the driving circuit by using a four electrode measuring arrangement. Two electrodes, one at either end of the sample, carry the current. Two voltage electrodes are placed within the sample to measure the potential difference across a known length of the sample. The input impedance of these electrodes, relative to the specimen, is so high that negligible current passes through them and electrode interface problems are minimized. A measuring arrangement similar to the one described by Ferris is illustrated in figure 1.6:

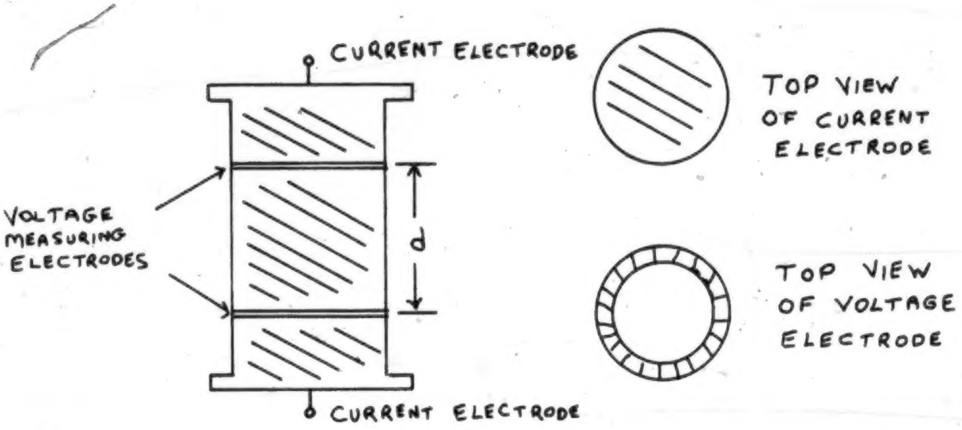
CURRENT ELECTRODE
VOLTAGE MEASURING ELECTRODES
d
CURRENT ELECTRODE
TOP VIEW OF CURRENT ELECTRODE
TOP VIEW OF VOLTAGE ELECTRODE

Figure (1.6) Four Electrode Cell

The measurement electrodes are placed in series with a variable capacitor and variable resistor. A typical arrangement is indicated in figure 1.7:

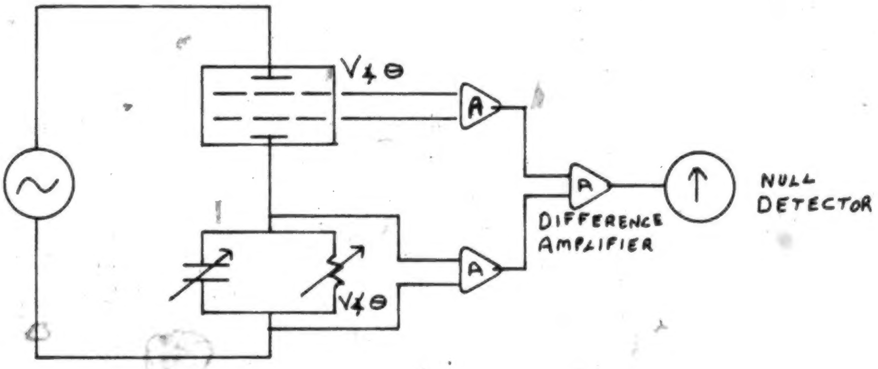
V∠θ
A
A
A
NULL DETECTOR
DIFFERENCE AMPLIFIER
V∠θ

Figure (1.7) Four Electrode Measurement System

The variable components are adjusted until a null indication on the detector is achieved. This null indicates that the adjustable impedance is identical with the unknown impedance of the sample between the separated voltage electrodes.

The critical elements in the system are the voltage amplifiers. In order to achieve very high input impedance values while ensuring stability, special operational amplifiers and circuit techniques must be used. The relative phase shift between amplifiers must be carefully matched in order to measure capacitances correctly. An oscilloscope or voltmeter which responds over the correct frequency range may be used as a null detector. Electrode polarization is generally only a serious problem below one kHz. Above this frequency ions can not respond to the rapidly changing electric field. Difficult problems associated with the four electrode technique include the design of suitably accurate measuring instrumentation. A second problem deals with coupling the voltage electrodes to the sample properly. With liquid samples, for which this technique is primarily used, close coupling is easily obtained. With solid samples, however, care must be exercised to prevent coupling impedances. The author decided that the electrode impedance problem could be controlled and chose the simpler two-electrode technique.

1.2.4 Transmission Line Methods

Measuring circuits at, and above radio frequencies can no longer be based on lumped circuit approximations. Rather, a transmission line concept in which the circuit elements are distributed along the line must be used. A circuit representation of a length of uniform transmission line is illustrated in figure 1.8:

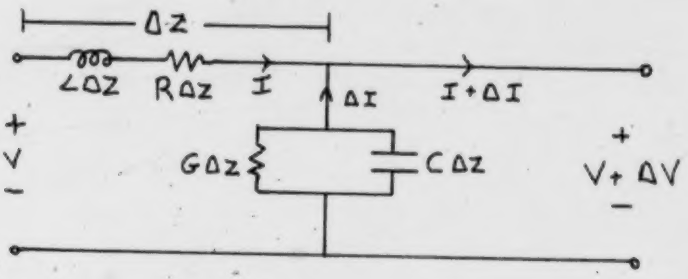

Figure(1.8) Transmission Line Representation

Along a differential length of line, dz, the voltage change, dV, is given by:

$$\frac{dV}{dz} = \left[R + j\omega L\right] I \qquad (1.16)$$

where R and L are the line impedances per unit of length.

In a similar manner, the differential current change, dI, is given by:

$$-\frac{dI}{dz} = \left[G + j\omega C\right] V \qquad (1.17)$$

where G and C are the per unit length conductance and capacitance, respectively. In the limit, as this differential length shrinks to zero, the solution to these differential equations can be shown as the sum of forward and backward travelling waves.[11] The voltage at any point $z = -\ell$ is given by:

$$V = V_1 e^{+\gamma \ell} + V_2 e^{-\gamma \ell} \qquad (1.18)$$

where V_1 is the incident wave and V_2 the reflected wave, and where it has been assumed that $z = 0$ corresponds to the load end of the transmission line. Thus, the length l is the distance from the load to the point in question. The propagation constant, γ, is a complex quantity which is expressed in terms of the line parameters:

$$\gamma = \sqrt{(R+j\omega L)(G+j\omega C)} \tag{1.19}$$

These constants are characteristics of the line and surrounding media. The media in which the transmission line is immersed will affect the wave propagation along the line by altering the parameters which make up the propagation constant. This fact may be used to determine the electrical properties of the substance surrounding the line.

Kirkscether[12] devised a method to measure the ground parameters by introducing a two wire balanced transmission line into the sample. The sample diameter had to be several times larger than the line spacing in order to effectively contain the fields of the transmission line. The input impedance of the dielectric filled line was obtained for two line terminations; namely, open circuit and short circuit.

Any text of electrical engineering (for example Everitt[13]) gives the input impedance at a distance l from the load on a transmission line as:

$$Z_{INPUT}(l) = Z_o \frac{Z_R \cosh \gamma l + Z_o \sinh \gamma l}{Z_o \cosh \gamma l + Z_R \sinh \gamma l} \tag{1.20}$$

The impedance is expressed in terms of the terminating impedance, Zr, and the characteristic impedance, Zo. Zo is the ratio of voltage to current for an infinite line, given by:

$$Zo = \sqrt{\frac{R+jwL}{G+jwC}} \quad (1.21)$$

The short circuit impedance, Zsc, found by setting Zr=0 in equation 1.20 is:

$$Zsc = Zo \tanh \gamma l \quad (1.22)$$

Similarly, the open circuit impedance, Zoc, is found by setting Zr = ∞:

$$Zoc = Zo \coth \gamma l \quad (1.23)$$

Therefore in terms of the measured values of Zsc and Zoc:

$$Zo = \sqrt{Zsc \times Zoc} \quad (1.24)$$

The hyperbolic tangent of γl can also be expressed in terms of the measured impedances Zsc and Zoc as:

$$\tanh \gamma l = \frac{Zsc}{Zo} = \sqrt{\frac{Zsc}{Zoc}} \quad (1.25)$$

An expression for finding the inverse of a hyperbolic tangent of a complex argument is given by Everitt.

From the expressions for propagation constant (equation1.19) and characteristic impedance (equation1.21) the following relation is found:

$$\frac{\gamma}{Zo} = G + j\omega C \quad (1.26)$$

Once G and C are found from the above expression the conductivity, σ, and dielectric permittivity, ε, are given by Kirkscether as:

$$\varepsilon = \frac{C}{C_0} \qquad \sigma = \frac{\varepsilon_0 G}{C_0} \tag{1.27}$$

where ε_0 is the free space permittivity and C_0 is the line capacitance per unit length in air.

The experimental technique consists of first measuring the characteristic impedance of the transmission line in free space. The line is then introduced into the medium to be tested and input impedance measurements of the short circuited and open circuited line are made. From these measurements the values of γ and Z_0 are determined using equations 1.24 and 1.25. Then G and C and thus ε and σ are found from equations 1.26 and 1.27.

If the line cannot be short circuited, for instance in a field measurement, the input impedance must be taken with the line at two different depths within the material. To simplify calculation the second depth is simply twice the first. The first measurement will yield:

$$Z_1 = Z_{OC_1} = \frac{Z_0}{\tanh \gamma l} \tag{1.28}$$

The second measurement with twice the length of transmission line in the material under study will yield:

$$Z_2 = Z_{OC_2} = \frac{Z_0}{\tanh 2\gamma l} \tag{1.29}$$

Now:

$$\frac{Z_2}{Z_1} \quad \frac{\tanh \gamma l}{\tanh 2\gamma l} \quad \frac{1}{2}\left[1 + \tanh^2 \gamma l\right] \tag{1.30}$$

Solving equation 1.30 gives:

$$\text{TANH}\ \gamma l \quad \sqrt{\frac{2Z_2 - Z_1}{Z_1}} \tag{1.31}$$

Since, from above:

$$Z_o = Z_1\ \text{TANH}\ \gamma l$$

$$Z_o = \sqrt{Z_1\,(2Z_2 - Z_1)} \tag{1.32}$$

Then the sample parameters may once again be found from Zo and γ as in the first case.

Kirkscether's method was developed in terms of a two wire line; however, such a line presents several difficulties. First, the line must be rigid to ensure uniform separation. Second, there may be difficulty in providing an adequate short circuit. Third, the sample must be large enough to contain all the fields associated with a two wire line.

A coaxial line may provide a simpler arrangement since the fields are contained within the inner and outer conductors. Only a sample sufficient to fill the region between the conductors is required. A short circuit is easily provided by means of a threaded end cap. The center conductor can be maintained in a uniform position.

The open and short circuit measurements can be made with an impedance meter or an admittance bridge. The leads connecting the measuring unit to the transmission line constitute an additional length of line as indicated in figure 1.9:

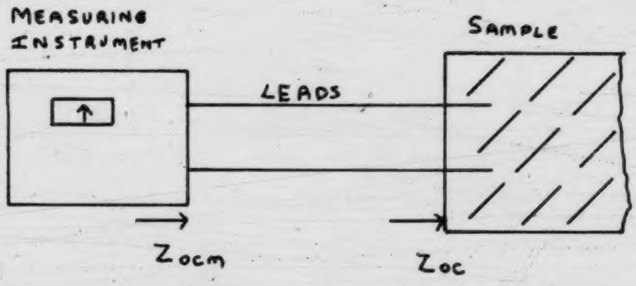

Figure(1.9) Transmission Line

The measured impedance Zocm must be corrected to the Zoc position.

Some of the results presented in this thesis were obtained using a coaxial transmission line operating at frequencies between 1MHz and 100MHz. Below this frequency it was felt the electrode contact impedances could be more easily controlled in a capacitor test cell such as described in section 1.2.1 .

1.2.5 Waveguides and Resonators

At frequencies above 1GHz the sample is measured within a section of waveguide or a resonant cavity. Propagation of an electromagnetic wave within a dielectric filled waveguide depends on the electrical properties of the dielectric sample and also the guide dimensions.

The dielectric properties of a sample can be obtained from slotted line measurements on a shorted section of waveguide containing the tar sand material in the manner illustrated in figure 1.10:

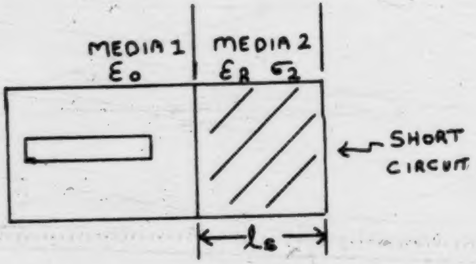

Figure(1.10) Waveguide Measurement

If media 1 is a lossless air filled guide, the load impedance, Z_ℓ, seen at the dielectric sample interface (x=0) can be expressed in terms of the reflection coefficient, Γ, as:

$$Z_\ell = Z_{01} \times \left[\frac{1+\Gamma}{1-\Gamma}\right] \tag{1.33}$$

where Z_{01} is the characteristic impedance in the air filled region. The reflection coefficient is generally a complex number whose magnitude, $|\Gamma|$, and phase, ϕ, can be determined using the relationships:

$$|\Gamma| = \frac{S-1}{S+1} \qquad \phi = 180^\circ - 2\beta\left[\ell + \ell_s\right] \tag{1.34}$$

where S is the ratio of the maximum electric (or magnetic) field to the minimum electric (or magnetic) field in the air filled region. ℓ_s is the sample length and ℓ is the distance that the position of a minimum of the electric (or magnetic) field shifts when a sample is inserted; both S and ℓ are easily measured using a slotted line.[14]

At the same time, since the waveguide is shorted, the impedance can be expressed in terms of the parameters of media 2 as:

$$Z\ell = Z_{o2} \ \mathrm{TANH}\ \gamma_2 \ell_s \tag{1.35}$$

Here Z_{o2} is the characteristic impedance in the dielectric filled region and γ_2 is the propagation function in this region given as:

$$\gamma_2^2 = \left[\frac{m\pi}{a}\right]^2 \left[\frac{n\pi}{b}\right]^2 + j\omega\mu\left[\sigma + j\omega\varepsilon\right] \tag{1.36}$$

for a rectangular waveguide. The integers m and n express the order of the propagating mode in the waveguide, ω is the angular frequency, and a and b are the waveguide dimensions. The parameters μ, σ and ε are the magnetic permeability, the conductivity and the dielectric permittivity of media 2 respectively. For tar sand it is generally assumed that $\mu = \mu_o$. Since measurements are generally carried out in the dominant or TE_{10} mode, m=1 and n=0. For TE modes, equations 1.33 and 1.35 may be equated to yield:

$$\frac{1}{\gamma_1 \ell_s} \times \frac{1+\Gamma}{1-\Gamma} = \frac{\mathrm{TANH}\ \gamma_2 \ell_s}{\gamma_2 \ell_s} \tag{1.37}$$

The left hand side of this equation is some complex function $C \measuredangle \psi$, derived from measurements of the sample thickness, the voltage standing wave ratio, the wavelength in the air filled region, and the distance 1, between the first minimum and sample interface. Von Hipple[15] presents charts of the transcendental equation 1.37 from which $\gamma_2 l_s$ may be determined as some complex number $T\angle T$. Thus, for the TE10 mode case:

$$\gamma_1^2 = \left[\frac{\pi}{a}\right]^2 + j\omega\mu_0\sigma - \omega^2\mu_0\varepsilon = \frac{T^2}{l_s^2}\angle 2T \tag{1.38}$$

The real components are equated to yield:

$$\left[\frac{\pi}{a}\right]^2 - \omega^2\mu_0\varepsilon = \frac{T^2}{l_s^2}\cos 2T \tag{1.39}$$

from which the dielectric permittivity is obtained as:

$$\varepsilon_r = \left[\frac{\lambda}{2a}\right]^2 - \left[\frac{T^2}{l_s^2}\right]\cos 2T\left[\frac{\lambda}{2\pi}\right]^2 \tag{1.40}$$

where λ is the free space wavelength. In a similar procedure, the imaginary components are equated to yield:

$$\sigma = \frac{T^2 \sin 2T}{l_s^2\,\omega\,\mu_0} \tag{1.41}$$

An alternate method is based on transmission measurements through two lengths of sample. The complex propagation constant given in equation 1.36 can be broken into an attenuation α nepers per meter and a phase shift β radians per meter. By using a variable attenuator and phase shifter the following bridge may be set up:

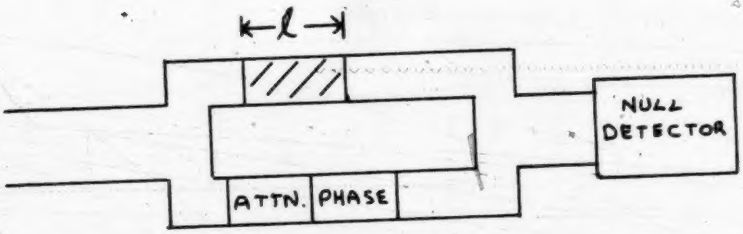

Figure(1.11) Transmission Bridge

The phase and attenuation is varied until a null output is achieved. The sample length is then increased and the bridge nulled again. From the attenuation and phase shift per meter, the parameters may be found from equation 1.36.

A cavity resonator is analogous to a resonant circuit. Any substance within the cavity will alter the resonant frequency and the Q of the resonator. The electrical parameters of the sample may be found by measuring the change in Q, and resonance frequency with and without a sample. The sample should be small enough not to alter the field magnitude within the cavity and the field must be uniform across the sample. A cavity may be used in any mode; however, some modes are particularly suited for certain samples. For example, a cavity in the TM_{010} mode which has an axial E field is suited to a cylindrical sample. Cavity measurements are restricted to a relatively narrow bandwidth about the resonant frequency of the cavity. Measurements at microwave frequencies were not undertaken since the concentration in this thesis was on lower frequencies.

1.3 IN SITU MEASUREMENTS

Laboratory methods may give a false picture of the electrical parameters of some materials because physical properties may no longer be the same as in the native environment. For example, the water content of tar sand changes rapidly when the tar sand is exposed to air. In addition, light hydrocarbon gases such as naptha can be easily lost to the atmosphere. A laboratory sample could have little resemblance to an in situ sample. Also, with laboratory testing it is difficult to simulate the actual in situ conditions with respect to temperature and pressure. Field techniques which yield parameters averaged over many meters may provide more representative values for non-uniform samples. Lytle[16] describes numerous in situ methods including borehole techniques which yield actual in place values and also surface techniques which give electrical properties averaged over many meters. Some of these methods are described briefly below.

1.3.1 Wave Tilt Method

The wave tilt method involves transmitting an electromagnetic wave along the surface of the earth. In a similar fashion to transmission line measurements (equation 1.19), the wave propagation is a function of the electrical parameters of the medium through which the wave travels. From measurements of the propagated wave the electrical parameters may be found. The measuring arrangement consists of a vertically oriented antenna above the earth's surface as shown in the following figure:

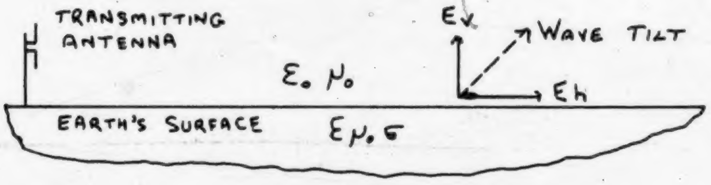

Figure (1.12) Wave Tilt Technique

The horizontal component of the field, E_h, arises because the earth's surface is not a perfect conductor. The wave tilt, W, is defined as:

$$W = \frac{E_h}{E_v} \tag{1.42}$$

where E_h and E_v are scalar components of the electric field. Generally, the vertical and horizontal conponents of the electric field will not be in phase, so that the fields above the earth will be elliptically polarized. To determine W, the ratio of the major to minor axis of the ellipse must be measured as well as the angle of inclination of the major axis with respect to the earth's surface. The ratio of the vertical component of the electric field to the horizontal magnetic field component is Zo, the free space characteristic impedance, and equals 120π ohms. However, the horizontal electric field is approximately related to the horizontal magnetic field by Ze, the surface impedance of the earth. Thus the wave tilt, W, becomes:

$$Z_o = \frac{E_v}{H_h} \quad \text{AND} \quad Z_\ell \simeq \frac{E_h}{H_h}$$

$$W = \frac{E_h}{E_v} = \frac{Z_\ell}{Z_o} \tag{1.43}$$

The impedance of the earth, Ze, is given by Jordan and Balmain[17] as:

$$Z_\ell \quad \sqrt{\frac{j\omega\mu_o}{\sigma + j\omega\varepsilon}} \tag{1.44}$$

where it has been assumed that the earth is non-magnetic. Therefore:

$$\frac{E_h}{E_v} \quad \frac{1}{120\pi}\sqrt{\frac{j\omega\mu_o}{\sigma + j\omega\varepsilon}} \tag{1.45}$$

and the measurement of the wave tilt can be related to the ground constants ε_r and σ. This technique gives the ground constants averaged over a large distance. By varying the frequency of the radio transmitter, the depth of penetration may be varied. Thus the variation of parameters with depth may be estimated.

1.3.2 Field Strength Method

The attentuation of an electromagnetic wave propagating along the surface of the earth depends on the conductivity and dielectric constant of the ground. Sommerfeld[18] describes the effect of the earth on radio wave attenuation in terms of the electrical properties of the earth. By measuring the attenuation of the fields of commercial radio stations with a field strength meter, a ground conductivity map of the United States was formed.[19] Some workers, for instance Feldman,[20] found this method unsatisfactory, probably due to the non-uniformity of the ground being measured.

1.3.3 Four Probe Methods

There are numerous four probe methods available for either surface or borehole measurements. These methods are very similar to the four electrode laboratory technique in that they use two probes to drive a current and two probes to measure the potential difference. These methods are used mainly in geophysical surveying.[21] One typical arrangement is shown in figure (1.13)

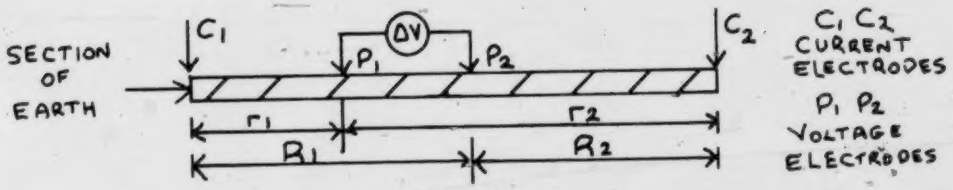

Figure (1.13) Four Electrode Array

From potential theory,[22] the expression for the average resistivity is:

$$\rho_a = \frac{2\pi\Delta V}{I}\left[\frac{1}{\frac{1}{r_1}-\frac{1}{r_2}-\frac{1}{R_1}+\frac{1}{R_2}}\right] \qquad (1.46)$$

If:

$$\text{LENGTH } r_1 = R_1 = r \quad \text{AND} \quad \text{LENGTH } r_2 = R_2 = r + \Delta r \qquad (1.47)$$

so that the spacing between the two probes while measuring potential becomes Δr, the expression for ρ_a becomes:

$$\rho_a = \frac{\pi\Delta V r^2}{I\Delta r} \qquad (1.48)$$

The survey involves separating the current electrodes widely, then measuring the potential difference over a small length. The potential probes are moved over the whole area of interest. From these measurements a plot of average resistivity may be constructed. This technique is used to indicate abrupt changes in resistivity due to a conducting mineral deposit underground. Although this method does not measure dielectric permittivity, Lytle[23] describes several alternative methods which do.

Chapter One has indicated a number of ways to measure the electrical parameters of the ground. Although this chapter described measuring techniques over various frequency ranges, the primary interest of this thesis is the low frequency range. A bridge technique on a two terminal measurement cell was chosen for tar sand because of its ease of construction and simplicity of calibration and operation. At higher frequencies a coaxial transmission line was used. These measurements were done in a laboratory, but the transmission line technique appeared most promising for field measurements as well.

CHAPTER TWO

MEASUREMENT ERRORS

2.1 GENERAL

Researchers have measured the electrical properties of homogeneous materials over a wide frequency range. Von Hippel,[24] for instance, has tabulated the dielectric properties of solids and liquids extensively. These homogeneous dielectrics generally show a rise in relative permittivity as the measuring frequency is lowered and the effects of additional polarization mechanisms are noticed. Also the dielectric permittivity, ε_r, seldom rises above 100 for uniform materials and changes by a factor of two or less over a wide frequency spectrum.

Lossy substances, such as rock or soil samples, yield results which have been the subject of considerable debate. Investigators found that as the measuring frequency was lowered below 1kHz extremely large values of dielectric permittivity were encountered. Smith-Rose[25] reported the dielectric permittivity of moist soil changes from about 30 at 10KHz to 100 000 at 50Hz. Keller and Licastro[26] measured permittivities of greater than 1 000 000 on core samples at the low end of the frequency spectrum. They felt that the observed dispersion was enhanced by water within the sample; when essentially all the moisture was removed from the rock sample by oven and vacuum drying, they noticed little change in ε_r with frequency. Howell and Licastro[27] also measured the dielectric properties of core samples. They noticed a maximum of 4 000 at 100Hz. Scott et al.[28] perfected a new measuring technique for rock samples. By careful consideration of electrode errors they tabulated results lower, by one order of magnitude, than values found by previous researchers.

These abnormally high values of permittivity are not only found in rock or soil samples. Fricke[29] reported dielectric permittivities greater than 1000 for biological cell suspensions. Koops[30] and Von Hippel[31] found large values of ε_r at low frequencies for artificial ferrites and meat samples, respectively. Johnson and Cole[32] described large permittivities for dielectric liquids with ohmic conduction. Reseachers have considered these large values of permittivity anomalous for two reasons. First, the large values cannot be completely explained in terms of the various mechanisms of polarization cited earlier. Second, the permittivity of lossy substances changes by several orders of magnitude as the frequency is lowered from radio frequencies to less than 1kHz. However, the permittivity of a homogeneous sample generally changes by less than a factor of two over this range.

Initially workers felt that measurement errors were causing these large permittivity readings. Howell and Licastro[33] believed polarization at the electrode sample interface could be responsible. Tarkhov[34] and Valeev and Parkhomenko[35] suggested the high dielectric values could simply be a result of contact errors at the sample-electrode interface. Scott et al.[36] believed electrodes form barriers which cause ions to pile up at the electrode interface. Other workers felt that the high values of permittivity could be explained by considering polarization occuring within the heterogeneous sample. This polarization is a property of the sample and thus the high permittivities are valid. Marshall and Madden[37] introduced the term "Membrane Polarization" to distinguish polarization occuring within the sample from electrode polarization. Keller and Licastro[38] suggested that clay-bearing samples could act as ion sieves allowing positive ions to travel more easily than negative ions. This sifting could lead to charge separation with the resulting large permittivities. Fuller and Ward[39] presented an interpretation which explained the large dielectric permittivities. Conduction current is normally considered the current due to the transport of free charge which is in phase with the electric field. Displacement current, associated with bound charges not free to drift through the sample, is out of phase with the electric field. Fuller and Ward suggested that ionic drift, influenced by factors such as pore viscosity and collisions, will produce a quadrature conduction component. The quadrature current measured, including the displacement and out of phase conduction current, is attributed solely to displacement current with the resulting large apparent dielectric permittivity. This theory is discussed further in Chapter Four.

The preceeding paragraphs describe several recent proposals to explain the anomalous results found when measuring lossy samples. At the present time there is no consistent point of view concerning these large values. Next, this chapter will describe electrode problems which lead to errors in the determination of permittivity and conductivity. Particular emphasis will be placed on electrodes in contact with samples with ohmic conductivities such as moist tar sand. Techniques developed by previous researchers to reduce electrode errors and to determine whether the anomalous values are representative of the samples will be discussed.

2.2 ELECTRODE CONTACT ERRORS

The first requirement for accurate measurements is to ensure that the electrode contacts the sample as intimately as possible. Such contact will prevent the formation of an air gap between the electrodes and the sample. However, due to irregularities in the surface of the sample, the electrode makes direct contact at a few points at best. An exaggerated representation is shown in figure 2.1:

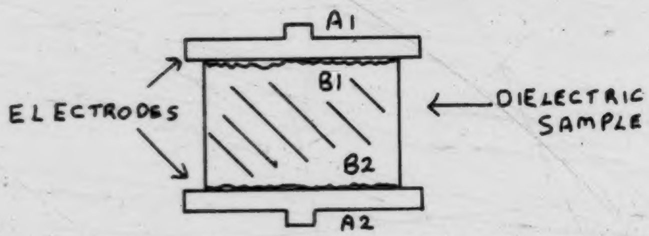

Figure(2.1) Electrode Contact Representation

The sample impedance of interest is between B_1 and B_2. The measuring circuit however, sees the impedance between A_1 and A_2. The contact between the sample and the electrode can be schematically represented by a capacitor due to the air gaps, in parallel with a resistor caused by the limited contact. The circuit seen by the measuring instrument now appears as:

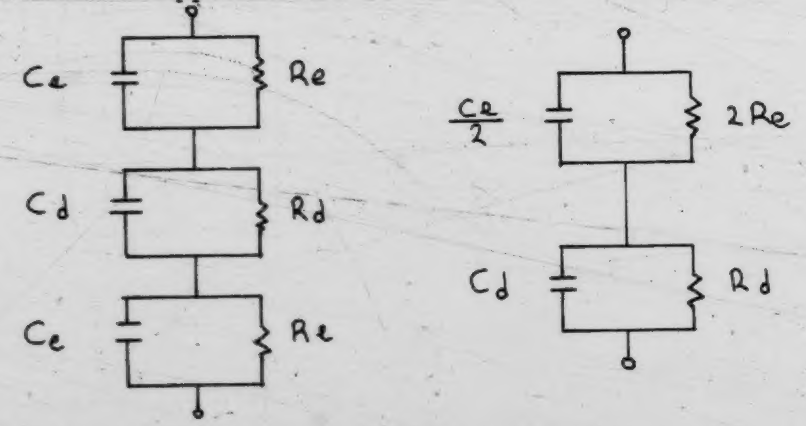

Figure(2.2) Electrode Contact Circuit

where C_d and R_d are the sample parameters and C_e and R_e

are the electrode impedances due to poor contact.

Reseachers expected the capacitance of the air gap to be much larger than that of the sample because the air gap spacing was very small. The air gap capacitance would present a small series impedance and alter the sample capacitance by only a small percentage. However, very serious errors can arise if the sample is lossy. In essence, the measuring circuit sees large capacitors due to the air gaps at each electrode separated by a dielectric which appears mainly resistive. If the measured capacitance is attributed solely to the sample, the dielectric permittivity will appear very large. An illustration of the error encountered by ignoring the air gap capacitance can be seen from the following example. The impedance of the circuit below, which contains typical values for electrode impedances, was determined numerically over a wide frequency range.

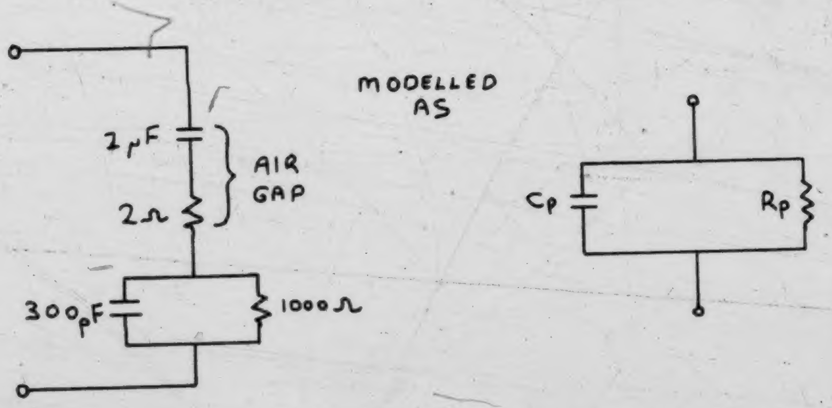

Figure (2.3) Circuit for Air Gap Methods

When this impedance is modelled strictly by a resistor and capacitor in parallel, the capacitance apparently rises to large values as the frequency is lowered. The apparent capacitance of the above circuit versus frequency is shown in figure 2.4:

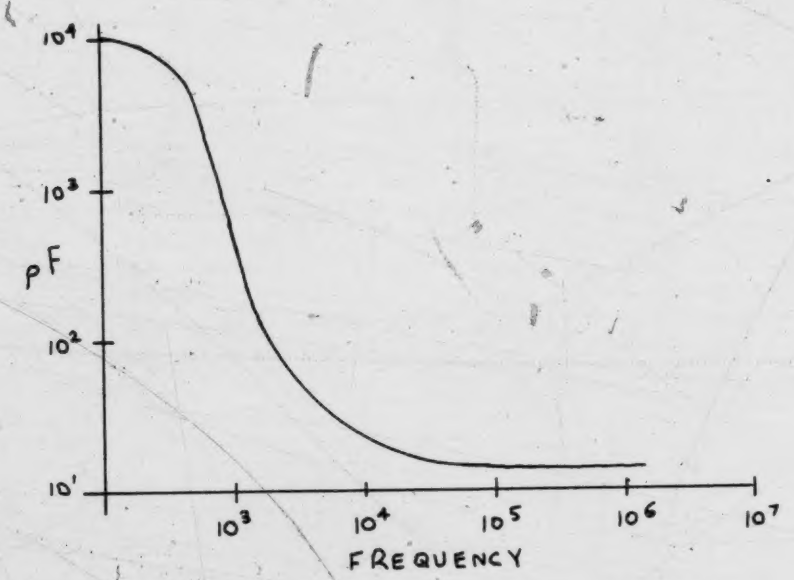

Figure(2.4) Apparent Capacitance versus Frequency.

If measured, the dielectric permittivity tabulated for such a capacitance would rise to large values at low frequencies. This rise at low frequencies is very similar to the rise reported for lossy dielectrics.

Various techniques have been developed by researchers to minimize the contact error problem. For samples which can be machined, the first requirement is to make the sample as plane as possible. Electrodes can be placed directly on the sample through the use of evaporated or sprayed-on metal, using suitable masks to outline the electrode area. Evaporated metal electrodes may require a backing electrode since the metal has low conductivity due to its extreme thinness. Both the sprayed-on and the evaporated electrodes adhere to a sample well; however, evaporation must take place in a vacuum chamber. This vacuum procedure may prove to be a disadvantage as much of the moisture within the sample will be removed.

An alternate electrode arrangement consists of floating the sample on a pool of mercury. A second electrode is formed by pouring mercury within suitable retaining rings on top of the sample. Mercury will closely follow the sample irregularities, providing an intimate contact. However, mercury has a high surface tension and often will not "wet" the sample surface. Moreover, the mercury surface becomes contaminated easily. Mercury electrodes will be discussed further in Chapter Three.

Conducting silver paint has been successfully applied to dielectrics. The paint consists of silver flecks suspended in a carrying solvent. When the paint is applied, the solvent evaporates leaving the silver adhering to the sample. Two disadvantages are that overnight drying is required and the solvent may attack some samples.

Thin metal foil applied with a minimum amount of petroleum jelly has been recommended by the American Society for Testing Materials (ASTM) as a suitable material for solids. The foil is applied directly to the sample and cut to the correct size using a sharp blade. Any wrinkles in the foil can be eliminated by a roller, ensuring intimate contact with the sample.

For moisture bearing substances such as tar sand, none of the preceeding methods are completely satisfactory. Any electrode preparation technique which requires drying or baking will alter the physical state and thus the electrical parameters of the sample. Also, tar sand samples cannot be formed easily with plane surfaces due to the pliable nature of the tar sand.

The author has found that a suitable arrangement for measuring moisture-bearing samples consists of placing moist blotters between each electrode and the sample. The blotters are soaked in an electrolytic solution to ensure low contact impedance between the electrodes and the sample. This blotter method will be described in greater detail at a later stage of the thesis.

Eliminating the error due to contact problems does not necessarily ensure satsifactory measurements. The moisture in dielectric samples generally contains ions in solution. Measurements on such samples are subject to a polarization error because current flow must change from ionic to electronic conduction at the electrode interface. The following section will present a brief outline of electrode polarization as it affects electrode impedances and dielectric measurements.

2.3 ELECTRODE POLARIZATION

At the instant a metal is immersed into an electrolyte, there is no potential difference across the metal electrolyte interface. Immediately, the metal loses electrons to the solution and ions in solution accept electrons in order to reach minimum free energy. These reactions are strictly chemical reactions brought about by thermodynamic forces. Once charge has been transferred, an electric field exists across the interface. This is illustrated in figure 2.5:

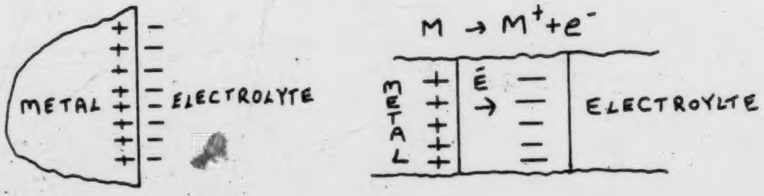

Figure(2.5) Metal Electrode Interface

Here M is any positive ion and e an electron donated by the metal. The electric field created in the interphase region by the initial electron transfers tends to discourage the reaction $M + M^{+} + e^{-}$ since additional electrons leaving the electrode must work against this electric field. The opposing reaction $M^{+} + e^{-} \rightarrow M$ is accelerated by the field. As the positive charge builds up on the metal decreasing the first reaction, the rate of the second reaction increases. The electric field and the opposing reaction interact with one another until energetic equilibrium is reached. There is some value of the electric field where the rate of losing electrons by the metal is balanced by the electrode's gain of electrons. The charge on the metal and the charge on the solution become equal and constant. An equilibrium potential which is a characteristic of the electrode and the solution exists across the interface. At this point, although there is no net current flow, equal exchange currents continue to cross the interface in both directions. The magnitude of the exchange currents is a function of the particular metal electrode and the electrolyte involved.

At equilibrium there will be a separation of charge in the interphase region. This charge separation has been called the *Ionic Double Layer* because of the earlier belief that the ionic charges were aligned in a sheet close to the electrode. The charge on the electrode, equal and opposite to that on the solution, kept the interphase region electrically neutral. Thus the early picture of the double layer consisted of two sheets of charge separated by a small distance. An energy barrier between the two layers of charge does not permit their instantaneous recombination.

The preceeding models of the double layer did not agree fully with experimental studies on electrode interfaces. The most recent model of the double layer consists of two separate regions in close proximity to the electrode. The innermost layer consists of water dipoles attracted to the excess charge on the electrode. In addition to the water molecules some ionic species may be adsorbed on the electrode. The plane formed by the centers of these ions and the water dipoles is referred to as the *inner Helmholtz plane*. The second layer consists of ions surrounded by water molecules (solvated ions). The plane through the center of these ions is known as the *outer Helmholtz plane*. This plane represents the plane of nearest approach for ions, because the water dipoles forming the *inner Helmholtz plane* block the electrode. At this outer plane the ion concentration will be maximum, decreasing away from the electrode as the coulombic forces weaken and thermal agitation disturbs the ions. Thus the excess charge is not fixed on the *outer Helmholtz plane* in close proximity to the electrode as in earlier models, but is dispersed in the solution adjacent to the electrode. This model is illustrated in figure 2.6:

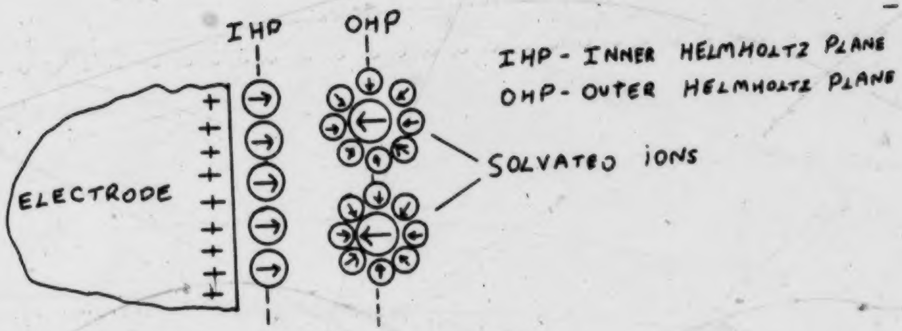

Figure(2.6) Ionic Double Layer

The ion separation, in effect, is a capacitor which remains charged due to equal reaction rates across the interface.

The previous discussion deals with the case of an isolated electrode unable to supply or sink additional electrons. When a sample measurement is required, a current must pass through the electrodes and the sample. Thus, the net current crossing the interphase region is no longer zero.

An electrode is called ideally polarizable if no charge crosses the interphase region when an external potential is applied. The change in potential only alters the charge separation in the double layer. An ideally polarized electrode behaves similarly to a perfect capacitor. As in an ideal capacitor, there is no conduction current; current flow is maintained through displacement current. If charge can freely exchange across an interface without altering the equilibrium potential across the interphase region, an electrode is called ideally non-polarizable. Such an electrode is analogous to a shorted capacitor. Current flow through the region is strictly by conduction. Any real electrode will exhibit behavior between these two extremes, having both conduction and displacement current. This behavior is analogous to a leaky capacitor. The polarization of an electrode depends on the rates of the oxidation and reduction reactions at the interface. These reactions determine the rate at which charge can cross the interface.

At equilibrium, the exchange current density, i_0, is a measure of the number of electrons crossing a unit of electrode area in a given time. The rates of the individual forward (losing electrons) and reverse (gaining electrons) reactions are equal and are designated by the same term i_0. A unique equilibrium potential difference exists across the interface region. In order for a net current to flow, the interface voltage must differ from its equilibrium value. The net current flow across an interface is a function of the non-equilibrium potential difference across the interface. This non-equilibrium potential difference consists of the equilibrium potential difference and the overvoltage; the potential by which the electrode departs from equilibrium.

The relationship between the net current density, i

(A/M^2),and the overvoltage, η (V), is given by the Butler-Volmer[40] equation. A plot of overvoltage versus current closely resembles a hyperbolic sine function. This plot is illustrated in figure 2.7:

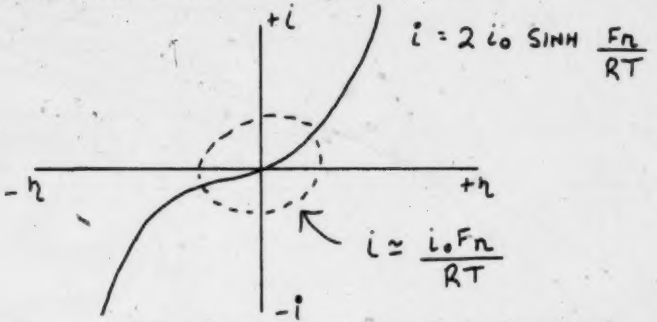

Figure(2.7) Overvoltage versus Net Current

The overvoltage is the excess voltage, above and beyond the equilibrium voltage, needed to drive a net current density. For low overvoltages the following linear relation with net current density may be derived by expanding the sinh expression in terms of exponentials and ignoring the higher order terms:

$$i \simeq i_0 \frac{F\eta}{RT} \tag{2.1}$$

Here i_0 is the exchange current density at equilibrium. F is Faraday's constant, the charge on a mole of electrons in Coulombs/Mole. η is the overvoltage in Volts and R is the Universal Gas constant (Joules/°K Mole). T is the absolute temperature in °K.

An electrode in which the voltage varies little from its equilibium voltage has previously been called non-polarizable. The linear expression can be rewritten as:

$$\frac{\eta}{i} = \frac{RT}{Fi_0} \equiv \rho_{m-s} \qquad (2.2)$$

The ratio η/i corresponds to an ohmic impedance, ρ_{m-s}, called the metal to solution resistivity. The impedance is mainly controlled by the exchange current density, i_0, which in turn determines the overvoltage required to produce the net current density $\mathring{i}$. If the exchange current density tends to infinity:

$$\rho_{m-s\atop i_0\to\infty} \simeq \frac{RT}{Fi_0} \Longrightarrow \rho_{m-s} \to 0 \qquad (2.3)$$

Hence, the metal solution resistance and the overvoltage tend to zero. At the other extreme, if the exchange current density tends to zero:

$$\rho_{m-s\atop i_0\to 0} \simeq \frac{RT}{Fi_0} \Longrightarrow \rho_{m-s} \to \infty \qquad (2.4)$$

Here the metal solution resistance tends to infinity which corresponds to a highly polarizable interface. The linear portion of the Butler-Volmer equation gives a qualitative view of how polarized an electrode is. The higher the exchange current density, the less polarized the interface and the lower the interface resistance.

The total impedance between the electrode and the bulk sample may now be examined in terms of its constituent parts. As discussed earlier, most electrodes are polarized to some extent. That is, the interphase region must carry both a conductive and a capacitive current simultaneously. The interfacial impedance consists of a capacitor due to the ionic double layer, in parallel with a series of components collectively called the _Faradaic_ impedance. The first component consists of the resistance to charge transfer across the double layer. The second component is a diffusion related impedance which arises because of the change in composition of the electrolyte near the double layer. Concentration gradients, which are equalized by diffusion, form in the solution. If the concentration changes, the charge transfer rate and thus the impedance changes. Dymond[41] notes this diffusion impedance varies as $\varsigma^{-1/2}$. The final impedance component is determined from the bulk sample characteristics and the test cell geometry. Within the bulk region, charge is carried mainly by ions and may consist of both capacitive and conductive currents. A representation of the total interface impedance is illustrated below:

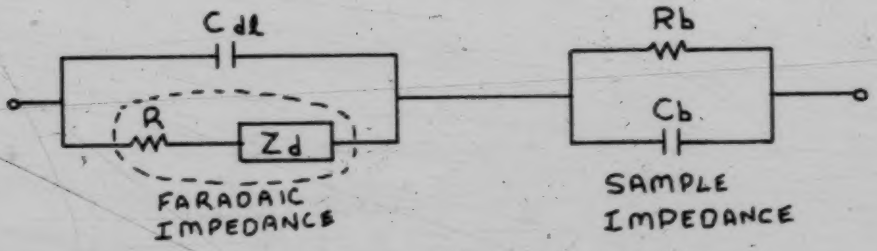

Figure(2.8) Interface Impedance

Here C_{dl} is the double layer capacitance, R is the resistance to charge transfer, Z_d is the diffusion impedance and R_b and C_b are the resistance and capacitance of the bulk sample, respectively.

2.4 POLARIZATION ERRORS

At frequencies below approximately 1kHz, the impedance of the double layer capacitance is very large and the impedance of the interface is largely that of the Faradaic impedance. Since at these low frequencies the Faradaic impedance is often greater than that of the bulk sample, it is apparent that large errors occur in the determination of R_b and C_b. As the frequency is increased the double layer capacitance becomes the controlling element in the interface impedance. At sufficiently high frequencies the series impedance associated with C_{dl} diminishes with respect to the bulk impedance of the sample. Polarization errors are negligible. Researchers first tried to eliminate the polarization error by taking measurements at two different electrode spacings. Assuming that the electrode polarization was independent of electrode spacing, the impedance $Z(\ell)$ measured at electrode spacing, ℓ, consists of:

$$Z(\ell) = Z_p + Z_s \tag{2.5}$$

where Z_p is the total polarization impedance which consists of both the double layer capacitance and the Faradaic impedance. Z_S is the sample impedance. When the spacing is doubled to 2ℓ, the interfacial impedance remains the same while the sample impedance doubles:

$$Z(2\ell) = Z_p + 2Z_s \tag{2.6}$$

This yields:

$$Z(2\ell) - Z(\ell) = 2Z_s - Z_s \tag{2.7}$$

from which the sample capacitance and conductivity may be determined. This correction technique is limited because the polarization impedance Z_p may become larger than the sample impedance Z_s. Small errors in the determination of $Z(\ell)$ and $Z(2\ell)$ may then cause large relative errors in Z_S.

A technique which the author found helpful to determine when polarization errors were influencing sample results, consisted of taking measurements at two sample lengths. The measurements were begun at high frequencies where serious polarization errors are unlikely. One sample was exactly twice the length of the other; their impedances were expected to differ by a factor of two. As the measuring frequency was lowered, any deviation in this impedance factor of two indicated polarization was evident.

Tarkhov[42] made, perhaps, the earliest attempt to eliminate polarization errors by eliminating direct contact and thus conductive currents between the metal electrodes and the moist sample. Thin mica discs were inserted between sample and electrode. Tarkhov felt the impedance of these discs would be much smaller than the sample impedance, allowing the sample impedance to be measured. In effect, these discs forced the interface current to be strictly capacitive and so remove errors associated with the Faradaic impedance. Incorrect development of his expression for sample impedance resulted in a term proportional to ω^2 being omitted from the denominator of his expression for sample permittivity. As his measuring frequency was lowered, extremely high values of permittivity were measured. Tarkhov then abondoned this technique as a failure. Scott et al.[43] detected Tarkhov's mistake and further developed this "blocking" electrode by using much thinner mylar insulators between the sample and the electrodes. They also experienced difficulty because the mylar insulators presented a much larger impedance than the sample. The sample values could not be accurately obtained. At this point they rejected the "blocking" electrodes and investigated nonpolarizing electrodes which would allow free exchange of charge between electrode and electrolyte. Scott et al. examined the polarization behavior of various metal electrodes in contact with blotters soaked in metal salt solutions. They found that for samples containing less than 10% water by weight, several electrode-electrolyte pairs gave low polarization impedance. However, for higher percentages of water the polarization error rose rapidly.

Scott et al. found that a platinized electrode together with a blotter soaked in a silver particle suspension and silver nitrate gave the lowest polarization impedance. Platinum has long been recognized as an ideal electrode material for two reasons. First, platinum has the highest exchange current density of any metal excluding palladium. Second, the surface area can be increased tremendously through platinization. Platinization is an electroplating technique which deposits colloidal platinum onto metallic platinum electrodes. The surface roughness thus produced can increase the effective electrode surface by as much as 10 000 times. This roughness increases the number of sites where charge may depart from the electrode surface, lowering the current density and subsequently polarization error. The measuring current density remains below the exchange current density and the electrode remains virtually nonpolarizing. Unfortunately, the cost of platinum electrodes is very high and the platinized surface is very fragile.

The added expense for platinized platinum electrodes could not be justified for this project. The electrodes finally chosen, copper in contact with a copper sulphate electrolyte, had sufficiently small electrode impedance considering the nonuniformity of the tar sand samples. As was described earlier, measurements were taken on two lengths of sample allowing a check for polarization errors.

CHAPTER THREE

MEASUREMENT TECHNIQUES

3.1 GENERAL

The primary aim of this thesis is to measure the low frequency behavior of tar sand from 100Hz to 10MHz. Measurements were carried out using the two-electrode bridge technique described in Chapter One. At the same time, measurements carried out by a summer student utilizing a coaxial transmission line extended the measuring range to 100MHz. The low frequency transmission line measurements also provided an independent check on the bridge results. Tar sand batches were obtained from the Syncrude research laboratory in Edmonton. The Syncrude stockpile consisted of a large amount of tar sand within a shed. The batches were obtained from within the pile, sealed in drums and stored in a refrigerated room to minimize moisture loss from the tar sand. There were sufficient variations in moisture and bitumen content between batches to indicate variations of electrical parameters as a function of these variables. Samples from each batch of tar sand were analysed to yield the water, sand and bitumen percentages.

3.2 TWO ELECTRODE MEASUREMENT CELL

3.2.1 Cell Construction

The original test cell consisted of two horizontally mounted aluminum electrodes threaded onto two aluminum support columns within a four sided plexiglass box. Each dimension of the box was approximately 1 foot. The top support was free to move through a threaded collar set into the top face of the plexiglass box. This threaded collar allowed the top electrode to move up and down which permitted measurements at various electrode spacings. The support columns were later changed to mild steel because the aluminum threads between the electrodes and support columns cold welded together. This weld made it extremely difficult to remove the electrode from the support column. The photograph on the following page illustrates the test cell assembly.

Because of the crumbly nature of the tar sand, a plexiglass ring was used to contain the material within the electrodes and to ensure uniform electrode separation. The electrodes were initially held together by nylon screws through the edge of the electrode into the plastic spacer. Since these screws tended to break off within the plastic, the electrode diameter was increased by 1/2 inch

PLATE 1 CAPACITIVE TEST CELL ASSEMBLY

and plastic bolts were used to connect the electrodes together directly.

The use of two complete sets of electrodes, each equipped with plexiglass rings of various lengths, allowed near simultaneous measurements on various sample thicknesses. The electrode leads were fixed to the cell holder in such a manner that their configuration remained the same from measurement to measurement. This feature assured that the interlead capacitance remained unchanged between measurements and thus its numerical value was not required for the impedance calculations. Connecting leads to three separate impedance instruments, with overlapping frequency ranges, were permanently fixed adjacent to the test cell allowing rapid connection. The three instruments, including two vector impedance meters and an impedance bridge, are fully described in a following section. The measurement arrangement is illustrated in figure 3.1:

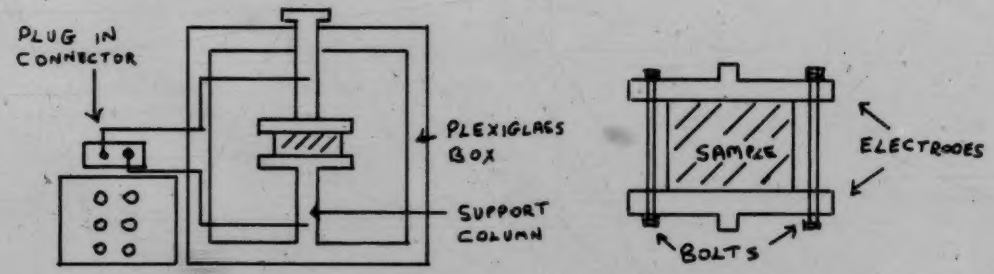

Figure(3.1) Test Cell Holder

3.2.2 Electrode Preparation

Initially, the author felt that the measurements would be straightforward and would proceed rapidly. The results were questionable due to the possibility of contact and polarization errors.

Chapter Two described the low frequency dispersion which was likely to result from either contact or polarization errors. Preliminary measurements showed that the permittivity was strongly dependent on frequency and was not independent of electrode spacing. However, mechanisms such as membrane polarization within a sample can account for large dielectric permittivities. In order to ascertain whether measured results were indicative of sample properties or electrode errors, measurements were required at various sample thicknesses. If, as mentioned in Chapter Two, the results are dependent on electrode spacing, errors due to contact and/or polarization effects are influencing the measurements. Electrode polarization errors are generally considered to be a problem below 1kHz. Above this frequency ions do not accelerate quickly enough under the influence of the alternating electric field to exchange across the interface. The drift of the ions, though not across the interface,does influence the bulk sample by its capacitive effect. Electrode contact errors are considered a problem up to high frequencies until the impedance of the air gap is negligible compared to the sample. In order to determine whether the results were influenced by contact and/or polarization errors, a variety of electrode techniques and materials were tested.

The first attempt to reduce contact errors was to place blotters soaked in a sodium hydroxide salt solution between each aluminum electrode and the sample. It was felt that these blotters would provide intimate contact between the sample and electrode. The salt solution was added to the blotter to ensure that the blotter impedance remained very small. Above 20kHz, measurements made on two different sample spacings showed little polarization or contact problems. As the frequency was lowered the results agreed less and less, indicating that polarization errors were present. In an attempt to lessen the polarization error the blotters were soaked in an electrolyte obtained from a tar sand and water slurry. The author felt that this slurry contained the same charge carriers which were responsible for electrical conduction in the tar sand. Thus polarization at the blotter tar sand interface would be minimized. However, the electrode blotter interface was not given sufficient consideration and this procedure was discontinued after several sets of poor data were obtained.

The next attempt to alleviate contact problems involved the use of thin metal foil. As discussed in

Chapter Two metal foil has proven very successful in rock measurements. Thin aluminum foil was applied under finger pressure to both sides of a previously formed tar sand 'disc' sample. Electrodes were then clamped on both sides of this sample. This technique yielded good results above 10kHz. Below this frequency, measurement problems became evident as shown by permittivity dependence on electrode spacing.

A technique similar to the above, employing mercury electrodes, was also tested. The tar sand sample was moulded into a disc and floated on top of a mercury covered electrode. Additional mercury was poured on top of the floating sample so as to cover it entirely. This mercury was restrained by the plexiglass ring containing the sample. The second electrode consisted of a wire inserted into the top mercury pool. Because of the high surface tension of the mercury, voids existed between the sample and the mercury, thereby diminishing electrode contact. However, Alvarez** reported success using a mercury indium amalgam on rock samples. This amalgam consisted of a liquid metal phase, similar to mercury, with much reduced surface tension. An attempt was made to apply this method to tar sand measurements and various supplies of amalgam were prepared. The surface tension was reduced so much that the desired phase coated the inside of the mixing beaker and could not easily be removed. Once the amalgam was placed on the sample it could not be spread evenly. Any attempt to coat the sample resulted in a slurry of amalgam and tar sand being formed. There was difficulty in collecting enough of the desired metal to cover a sample and once applied, the metal could not be regained in an uncontaminated form. In view of the expense of the indium and the care required to prepare the amalgam this technique was rejected.

At this point an attempt was made to eliminate polarization error. The conductive current path between the electrodes was removed, thus producing "blocking" electrodes. As described in Chapter Two the measuring current would be capacitive only, eliminating errors associated with the Faradaic impedance. Initially, very thin sheets of mylar were placed on each face of the sample and the sample was inserted between the electrodes. The two-electrode cell with a tar sand sample inserted was primarily resistive with a small series reactance. However, the series reactance of the mylar was much greater than that of the tar sand and dominated the measured reactance. Therefore, the series tar sand reactance could not be isolated from the measured impedance with any degree of accuracy. In order to produce a "blocking" electrode with lower series reactance a much thinner insulating layer had to be placed between the sample and each electrode. Aluminum oxide (alumina) has been successfully used on aluminum electrodes to produce a "blocking" electrode.[45] The alumina is formed on the electrode by suspending two electrodes in a sulphuric acid solution and passing a $1.5 mA/cm^2$ current through the electrodes. The current is controlled by a ballast resistor. As the oxide layer builds up, the resistor must be adjusted in order to maintain the current density. An important feature of this anodizing process is that the insulating layer thickness and thus the series reactance of the electrode is governed by the forming voltage. Young, quoted in Ferris[46], showed that the oxide thickness, t, in angstroms is given empirically by:

$$T = 17.5 V_f \tag{3.1}$$

where V_f is the voltage across the electrodes. In order to provide a "blocking" electrode, the alumina had to withstand the signal impressed across the electrodes. In turn, the insulating coating had to be made thicker which increased its series reactance to greater than that of the tar sand sample. Again the tar sand reactance could not be isolated from the measured series reactance.

The sulphuric acid anodizing technique is considered a "soft" anodizing process because the oxide layer is quite porous. In order to provide a more effective "blocking" electrode a so called "hard" anodizing technique which used an oxalic acid bath was also attempted. In order to avoid dielectric breakdown, this coating was also thicker than could be allowed in terms of series reactance.

Finally, in order to reduce both the contact and polarization errors to an acceptable level, an attempt was made to devise a reversible electrode system. As described in Chapter Two this system consists of a metal electrode in contact with an electrolyte of a metal salt. For solid sample measurements the electrolyte is present in soaked blotting paper between the electrode and the sample. In order to discover an electrode system suited to the measurement of solid samples, Scott et al.[47] tested seven different samples. The samples ranged from little water content (low conductivity) to moderate water content (high conductivity). The measurements were taken at 100Hz, a frequency low enough to indicate any polarization effects. Scott tested for polarization by ensuring that the permittivity and conductivity remained independent of electrode spacing. This procedure is equivalent to the polarization test described in section 2.4.

Scott's sample was a layered arrangement: an electrode, a soaked blotter, the dielectric sample, another blotter and finally the second electrode. His work indicated that platinized platinum electrodes, complete with blotters soaked in a suspension of silver and silver chloride, have the lowest polarization of the tested electrodes. Silver electrodes with the above electrolyte followed and then copper electrodes with a copper sulphate electrolyte. As mentioned in Chapter Two the cost and fragile nature of the platinum electrodes precludes their use for tar sand measurements.

The two remaining electrode systems mentioned above both showed low polarization errors for samples containing 10% water or less. Since polarization errors exert less influence on sample impedance with decreasing water content (conductivity) and since tar sand generally contains less than 5% water, the author felt polarization error due to either electrode system would be small.

Two sets of copper electrodes for the test cell of figure 3.1 were machined. One set was silver plated and used in conjunction with blotters soaked in silver chloride solution. The remaining copper electrode set was tested with copper sulphate electrolyte. Both electrode systems were used to measure fairly conductive samples of tar sand versus frequency. The measurements were taken first at one spacing then at one half this spacing to monitor polarization or contact errors. The low frequency limit for both types of electrodes was around 100Hz for low conductivity samples. For samples with higher conductivity the limit was somewhat higher due to erratic readings at low frequencies. These results will be illustrated in Chapter Four. The upper measurement frequency was determined by the residual inductance of the measuring circuit. At frequencies above 20kHz polarization effects were expected to be minimal but the continued use of the blotters ensured contact problems were minimized. Since no discernible change could be seen between the copper or silver systems, the author chose the copper- copper sulphate system for its greater durability.

3.2.3 Sample Preparation

Prior to each measurement a dish of tar sand was removed from the moist room. Any stones present were removed and large lumps were broken down. Laboratory results by Clark[48] and by Blair[49] indicate an average tar sand density between 1.9 and 1.96gms/cm^3. Shell Oil (quoted in Blair) recorded a slightly higher range between 1.98 - 2.08gms/cm^3, using a formation density log in situ. Since the measurement cell volume was slightly over 130cm^3 for a 1/2inch spacing, a 250gm sample was required. Sample measurements at the 1 inch spacing required a 500gm sample. These masses provided a sample whose density fell within the range of in situ densities shown above. The correct amount of tar sand was weighed out using a triple beam balance, placed inside one of the plexiglass rings and moulded into a 'disc'. Because of the pliable nature of the tar sand it was possible to form nearly plane surfaces on the 'disc' by rolling the sample carefully with a glass rod.

To facilitate rapid measurements at two spacings, certain trials were made using two 1/2 inch 'discs' joined together to make a 1 inch sample. Measurements were taken on this joint sample; the sample was then pulled apart and one of the 1/2 inch samples was measured. This procedure reduced the parameter variations, due to drying, between the measurements at different spacings.

The copper electrodes were cleaned in a weak nitric acid solution and rinsed with distilled water. Allowing the blotters to soak in the electrolyte for at least five minutes helped ensure consistent electrode impedances. These blotters were then applied to the electrodes. The electrolyte strength was 0.1M (1mole of copper sulphate to 10 litres of distilled water). The excess electrolyte was squeezed off each electrode by rolling a hard rubber roller over the blotter. Periodically, the electrode impedance was checked by placing two soaked blotters between the electrodes and measuring the impedance. Typically, the series resistance was less than 2 ohms and the series capacitance was over several hundred microfarads. Thus, measurements could be taken to a lower frequency limit of approximately 100Hz before the electrode impedance influenced the measured results, as discussed in section 2.3.

In addition to the regular batch tests using fresh tar sand, a drying test was carried out. The purpose of this test was to determine changes in the electrical properties as the moisture content of the tar sand varied. The test consisted of spreading a large amount of tar sand over a wide area to dry in the air. At regular time intervals, samples at 1 and 1/2 inch spacings were pressed into discs and measured in the test cell. Great care was taken to ensure the blotter did not introduce extraneous moisture into the dried tar sand. This care included drying the rinsed electrodes with compressed air, removing all excess electrolyte from the blotters and allowing the blotters to air dry for a short interval. Measurements were undertaken as rapidly as possible to avoid any possibility of electrolyte penetration into the sample. A portion of each sample was analysed in the physical extraction unit (which is described later) and the bitumen and water contents were recorded.

At the end of the drying test, when no more water could be extracted from the dried tar sand, an attempt was made to remoisten the tar sand. The tar sand was placed inside a wire mesh pan over a steam generator. Cold air was blown above the sample to ensure condensation within the sand. The electrical parameters of this remoistened sand were measured. This test was undertaken to determine the feasibility of increasing the conductivity of in situ tar sand to facilitate low frequency heating. Samples of water free bitumen obtained from both the tar sand analysis unit and the Syncrude laboratory were also measured.

Chapter Four will present graphically the results of each measurement. In addition to ε_r and σ versus frequency for various tar sand batchs, graphs of ε_r and σ versus time, obtained from the drying test described above, will be presented.

3.2.4 Measuring Instruments

Initial measurements were undertaken using a Hewlett Packard model 4800A vector impedance meter. This instrument measures the series impedance of the circuit between the measuring terminals and displays the polar components of magnitude and phase. It can measure any impedance to 10M and any phase angle between ±90° over a frequency range from 5Hz to 500kHz. The impedance accuracy is ±5% while the phase accuracy is ±6°. Digital voltmeters were connected to the outputs on the rear of the instrument. These outputs provide an analog voltage proportional to the magnitude and phase of the unknown impedance being measured. The digital instruments ~~increased~~ the overall accuracy and readability of the impedance meter.

In order to calibrate the digital instruments, adjustable potentiometers are provided on the rear of the vector impedance meter. A precision 1kΩ resistor is used to calibrate the magnitude scale and to zero the phase scale. Then, a high quality capacitor is used to calibrate the -90° point and check the magnitude calibration at this angle. The author felt that operation of the impedance meter with the digital presentation increased the overall accuracy to ±2%. This greater accuracy resulted from the increased resolution in phase angle measurement.

As described in Chapter One, the extraneous capacitances associated with the cell overhang and leads must be removed from the measured impedance value, yielding the sample parameters. Since the vector impedance meter measured the series impedance of the sample, the measured reading was converted to a parallel equivalent form at each frequency. The impedance of the empty cell was then measured, converted to its parallel equivalent form and subtracted from the full cell reading. Thus the extraneous capacitances were removed and the sample parameters could be obtained. A block diagram of the measuring arrangement is shown below.

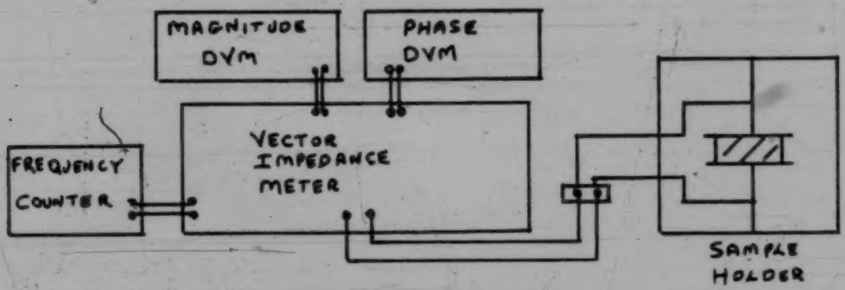

Figure(3.2) Mid-range Measurements

Initial measurements showed the tar sand to be mainly resistive with a small series reactive component; the series impedance had a phase angle close to zero. Reading this small phase angle led to large errors since a change of a few degrees could result in greater than 100% error in the series capacitance determination.

Since the vector impedance meter was not capable of measuring these small angles accurately, a General Radio 1608A bridge was purchased. This instrument contains six bridge circuits that enable it to measure the passive half of the complex impedance plane. For tar sand measurements, the parallel conductance bridge was selected. This bridge measures the parallel conductance (Gp) and the capacitive Q (ωRpCp), where Rp is the parallel resistance, Cp is the parallel capacitance, and ω the angular frequency. The basic accuracy of this bridge was ±.05% of the reading for the conductance component and ±2% for the determination of Q. A frequency dependent error term must also be included in the conductance bridge due to the network which compensates for stray capacitance. This term adds an additional error of approximately .8% at 20kHz.

The General Radio bridge is supplied with a 1kHz internal oscillator to drive the bridge. An internal detector with a narrow bandpass filter is centered on the oscillator frequency to observe the null point. The frequency range of this bridge could be extended through the use of an external oscillator from 20Hz to 20kHz. In this case, the internal bandpass filter must be removed from the circuit. When measuring resistive samples with a low Q, the bridge balance point becomes shallow and a null is difficult to obtain. To obtain a satisfactory null in the presence of harmonic distortion and noise, a Hewlett Packard wave analyser,model 302A, was inserted between the bridge and oscilloscope. This instrument, consisting of a sharp tunable bandpass filter and amplifier, functioned as a detector. The additional gain of the wave meter assisted in detecting the shallow null.

In operation, the bridge was balanced by adjusting the internal capacitors and resistors to equal the sample parameters so that a null was obtained. The internal components then indicated the sample parameter values on the instrument's digital display. Both the parallel conductance and the Q dials had a coarse and a fine adjustment in order to achieve a suitable null. For tar sand samples at high frequencies, the Q value was very small, less than the first division adjustment on the fine scale. A slight external modification, consisting of the addition of a parallel resistor between the bridge arm responsible for Q measurement and ground was required. This increased the Q magnitude by a factor of almost 70, shifting the scale to midrange for improved readability. The Q reading was then obtained to three figure accuracy and converted back to the proper reading. The low frequency bridge gave satisfactory results between 100Hz and 20kHz. Readings could be taken up to 50kHz with slightly lower accuracy. A block diagram of the low frequency measuring arrangement is shown in figure(3.3) while the photograph on the following page illustrates the measurement arrangements.

PLATE 2 INSTRUMENT ARRANGEMENT FOR MEASUREMENTS

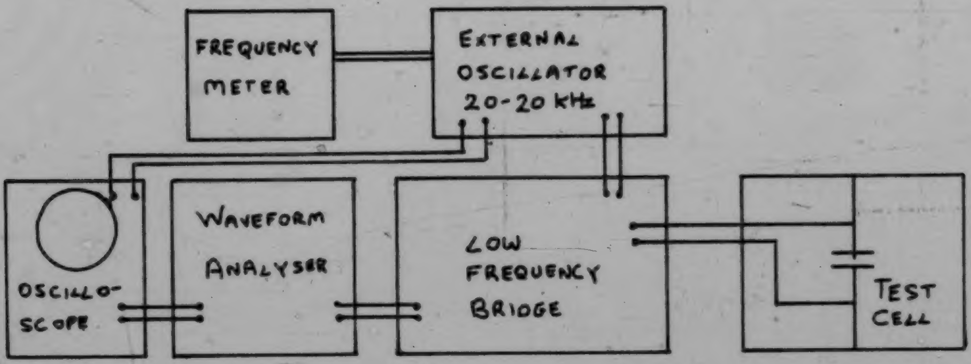
FREQUENCY METER
EXTERNAL OSCILLATOR 20-20 kHz
OSCILLO-SCOPE
WAVEFORM ANALYSER
LOW FREQUENCY BRIDGE
TEST CELL

Figure (3.3) Low Frequency Measurement Arrangement

The low frequency vector impedance meter described earlier was used to take measurements between 10kHz and 500kHz. A high frequency vector impedance meter extended the measurement range further to 10MHz. This instrument, a Hewlett Packard model 4815A, measures any complex impedance up to 100k between 500kHz and 108MHz. The impedance accuracy is ±4% of the full scale reading while the phase accuracy is ±3°. The addition of the digital voltmeters to record the analog voltages once again improved the readability and accuracy. The measuring configuration at high frequencies is identical to that shown in figure 3.2 except that the high frequency meter is substituted for the low frequency meter.

As mentioned previously, the connections for each bridge were brought out to a terminal board near the measurement cell to facilitate rapid testing. Since each measurement instrument had different lead connector configurations the empty capacitance (Cempty) shown in figure 1.2 had to be determined separately for each bridge.

3.3 COAXIAL MEASUREMENT CELL

Tar sand samples were measured over the frequency range of 100kHz to 100MHz by a summer student assistant using a coaxial transmission line cell. The cell was made up of sections of threaded brass pipe through which a brass center conductor could be inserted. Additional lengths could be added onto both the inner and outer conductors to vary the transmission line length. A tapered section formed the transformation between the coaxial cell and the connector on the measurement bridge, a Wayne Kerr SR 268/B801 impedance bridge. The tar sand samples were obtained from the same sealed drum as the two electrode cell samples. A sample was prepared by forcing the tar sand between the inner and outer conductors with a specially designed plunger. This plunger allowed the sample to be packed to the correct density while maintaining the center conductor in its proper position. The coaxial cell is illustrated in the photograph on the following page.

PLATE 3 COAXIAL MEASUREMENT CELL

As described in Chapter One (equations 1.21 to 1.27 inclusive) measurements of the parallel conductance and capacitance plus a knowledge of the empty line parameters yield the conductivity and permittivity of the sample within the transmission line.

3.4 Tar Sand Sample Analysis

Tar sand samples were analysed by extraction of the bitumen with toluene. The extraction assembly consisted of a permeable thimble containing a known weight of tar sand over a flask of toluene. Above the thimble, but offset slightly, was a condensation coil equipped with a trap to retain any water condensed. The photograph on the following page illustrates this arrangement. The heater beneath the flask vaporized the toluene causing it to rise and condense on the water cooled coil. The liquid toluene fell, filling the trap and also the tar thimble. Once the thimble was full, the toluene, now containing bitumen and some moisture, was siphoned back into the flask. Here it was revaporized taking the water with it but leaving the bitumen behind in the flask. Upon condensation the liquid toluene and water fell into the trap. The water, having a higher density, would displace the toluene and remain in the trap.

PLATE 4 TAR SAND ANALYSIS UNIT

The thimble would be refilled with toluene and the cycle would begin again. The procedure was continued until no sign of bitumen showed in the toluene draining from the thimble.

The sand and mineral matter remaining in the thimble was oven dried and weighed. From this weight and the weight of water collected from the trap, the percentage of each component could be obtained.

Pure bitumen was obtained by heating the mixture remaining in the distillation flask until the temperature rose sharply. This temperature rise indicated all the toluene had been distilled. However, in order to drive off all the toluene, some of the lighter fractions of the bitumen were probably lost. Thus the bitumen obtained was presumably a slightly cracked product and not a true representation of the in situ bitumen.

CHAPTER FOUR

EXPERIMENTAL RESULTS

4.1 GENERAL

This chapter presents the results of the various tar sand measurements in graphical form. Each figure is composed of two plots; the first showing conductivity versus frequency, the second showing permittivity versus frequency. Generally each plot includes measurements taken on both 1 inch and 1/2 inch samples. As mentioned in Chapter Three, measurements at two spacings enable electrode polarization or contact errors to be detected. The chapter includes graphs showing the permittivity and conductivity of bitumen samples and a composite plot of tar sand samples dried over several days. In addition, measurements taken over a higher frequency range with a coaxial cell are presented in section 4.3.

4.2 CAPACITIVE CELL RESULTS

Although a variety of measurement techniques and electrode materials were tried, a major portion of the results presented in this thesis were obtained using the copper copper-sulphate arrangement described in Chapter Three. Results obtained from the other electrode arrangements were inconsistent and have not been included.

The conductivity is displayed on a linear scale versus log frequency. Because the permittivity changed by several orders of magnitude over the frequency range of interest, it is plotted on a log scale versus log frequency.

The various samples are identified by a unique name composed of literal and numeric characters which describe the day and week in which the measurement took place and the thickness of the sample. For example, the sample labelled 4W1 was measured on Wednesday of the fourth week and was 1 inch thick. The sample 5T1a was measured on Tuesday of the fifth week and was 1/2 inch thick. The sample label is included in the title of each group but the graphs will be referred to by figure number.

Figures 4.1 to 4.4 inclusive are measurements on a tar sand batch with an average bitumen content of 11.25% by weight and an average water content of 3.8% by weight. The water and bitumen contents were obtained from the distillation apparatus described in section 3.4. Figures 4.1, 4.3 and 4.4 compare 1 inch samples with 1/2 inch samples. Each figure shows that the conductivity is relatively independent of frequency while the permittivity increases steadily with decreasing frequency. The conductivity and permittivity remain constant, within experimental error, between the 1 inch and the 1/2 inch samples thus showing negligible electrode polarization errors. Figure 4.2 shows two 1 inch samples prepared at the same time but measured approximately thirty minutes apart. Sample 4M3 was exposed to the air for the longer period and shows a decrease in conductivity due to moisture loss when compared to sample 4M1. Figure 4.5 is a composite graph showing the measurement repeatability between the samples taken from the same tar sand batch.

The next fourteen graphs, figures 4.6 to 4.19 inclusive, illustrate samples with an average bitumen content of 11.5% by weight and a water content between 1.6% and 2.2% by weight. Each figure with the exception of figures 4.12 and 4.13 is a plot of measurements on both a 1 and a 1/2 inch sample. Figure 4.12 is a plot of two 1 inch samples prepared at the same time with sample 5W3 being measured slightly later than sample 5W1. Again, the sample exposed longer had a lower conductivity resulting from moisture loss to the air. Figure 4.13 is a graph of sample 5W2, consisting of two 1/2 inch samples pressed together, and sample 5W3 consisting of a solid 1 inch sample. This figure indicates that the 1 inch samples, actually made up of 1/2 inch samples, are equivalent to solid 1 inch samples. Once again, Figure 4.20 is a composite graph of all the samples in the second batch showing the close agreement between the conductivity and permittivity of samples taken from the same tar sand batch.

When comparing the second set of figures (4.6 to

4.19) to the first set (4.1 to 4.4), two points are noted. First, due to the lower water content, the conductivity of the second set is significantly lower than that of the first set. Second, the permittivity of the second set is generally 1000 or less at the lowest indicated frequency compared to an average permittivity of 5000 or greater for the first batch. This greater permittivity with more conductive samples is the same phenomenon discussed in recent literature (see Chapter Two). Measurements on samples of the second batch taken at two electrode spacings display the same conductivity and permittivity, indicating polarization errors were very small.

The next six graphs, figures 4.21 to 4.26 inclusive, consist of measurements made on a tar sand batch with an average bitumen content of 12% by weight and an average water content of 4.5% by weight. Figure 4.23 shows two solid 1 inch samples. The conductivity of 6F2 is about 20% lower than that of 6F1, showing how rapidly the tar sand moisture is lost. Also the low frequency permittivity is slightly less than that of 6F1 as is expected from the lower conductivity.

The conductivity of the 1 inch sample is higher than that of the 1/2 inch sample in both figures 4.21 and 4.22. Generally, the reverse is true as any contact or polarization errors are more visible in the 1/2 inch measurements. This disparity is probably due to poor preparation of the sample. For instance, insufficient saturation of the blotters with the copper solution could yield the above results. Since the permittivity curves agree quite closely, polarization errors are not influencing results. Figure 4.27 combines the results of the third batch samples on one plot to show conductivity and permittivity agreement between samples.

Figure 4.28 is a graph of four tar sand samples measured consecutively twenty-four hours apart. A large amount of tar sand was spread in the open air to dry. Every twenty-four hours a sample was prepared from the drying tar sand. The first sample, 7R1, was measured immediately. Physical analysis showed a water content of 1.75% and a bitumen content of 12.1%. The second sample, 7F2, measured twenty-four hours after 7R1, had a water content of 0.4% while the bitumen content was virtually unchanged. The third and fourth samples, 7S1 and 7Su1 respectively, showed insufficient water to be measured. Since the conductivity varied over such a wide range, it was plotted on a logarithmic scale. Figure 4.28 clearly illustrates the dependence conductivity has on the water content of tar sand. In addition, as the sample dried and the conductivity decreased the permittivity became small and the frequency dependence lessened.

Figure 4.29 is a plot of two samples of pure bitumen, one obtained from the distillation process described in section 3.4, the other obtained from the Syncrude research laboratory in Edmonton. There is quite close agreement between the two samples. Comparing the conductivity plot of figure 4.29 to that of figure 4.28, one sees that even after drying over seventy hours some moisture remains in the dried sample as shown by the higher conductivity of the dried tar sand. Finally, figure 4.42 shows the upper and lower limits for the permittivity and conductivity based on the samples measured. For tar sand samples with a water content of less than 5% and a bitumen content less than 15%, the conductivity and permittivity should remain within the limits of figure 4.42.

4.3 COAXIAL CELL RESULTS

The coaxial cell measurements were carried out over the frequency range of 100kHz to 100MHz by a summer assistant. Unfortunately, difficulties were experienced in accounting for the effect of the tapered section which connected the coaxial cell to the measuring instrument. The results of conductivity and permittivity are valid only up to 25MHz. The tests carried out include measurements of different sample lengths and drying tests conducted in much the same manner as for the two-electrode capacitive cell. Measurements on two different lengths of transmission line are analogous to measurements at different plate separations of the two-electrode cell. If one section of transmission line is exactly twice the length of the other, the sample parameters may be easily obtained. In these measurements, tests were carried out using 10 and 20cm lengths of coaxial transmission line. The nomenclature for the high frequency results differs from that of the capacitive cell measurements. However, since the graphs are referred to by their figure numbers, no ambiguity should result. Figure 4.30 shows a sample with high conductivity indicating a relatively large water content. The permittivity is quite large at the lowest frequency and decreases as the frequency is raised. Figures 4.31 to 4.34 inclusive are plots of a batch of tar sand with an average water content of 1.15% and a bitumen content of 14.7%. The conductivity is low as is expected from the low water content. The dielectric permittivity is also low and shows little frequency dispersion. Figure 4.35 is a composite graph of figures 4.31 to 4.34 inclusive, showing the agreement in conductivity and permittivity within samples taken from the same batch. Figures 4.36, 4.37 and 4.38 are results from a batch of tar sand with much higher conductivity. As is expected from the higher conductivity, the permittivity is high but decreases as the frequency increases. Figure 4.39 is a composite graph of the above three figures.

Figures 4.40 and 4.41 are graphs of drying tests conducted in a similar manner to the low frequency test shown in figure 4.28. A large amount of tar sand was spread to dry in the air. The first sample was measured immediately, then every twenty-four hours a new sample was prepared and measured. Once again the conductivity decreases rapidly as the sample moisture decreases, showing the dependence of conductivity on water content.

4.4 DISCUSSION OF RESULTS

The results presented in this chapter indicate that permittivity is strongly dependent on frequency, falling from a value of several thousand below 500Hz to around twenty at 10MHz. The high frequency results, obtained from the coaxial cell measurements, confirm that the permittivity continues to decrease as the frequency rises. In addition, the higher the conductivity of the sample, the higher the low frequency permittivity is likely to be. Insufficient data were collected to indicate the effect that bitumen saturation has on the overall tar sand permittivity. Since the bitumen component has low ohmic conductivity and small permittivity, very little change in overall permittivity should result with changes in bitumen content.

The conductivity remained relatively constant as the frequency increased. At about 1MHz it began to rise as the frequency was raised. The conductivity was dependent upon tar sand moisture content as the figures of drying tests showed.

Precautions were taken to ensure that the results presented accurately reflect the electrical properties of the tar sand samples. Measurement errors were examined and minimized. As mentioned in Chapter Two, the low frequency results are difficult to explain in terms of the polarization effects present in homogeneous materials. Several explanations have been presented by researchers who have noticed similarly high permittivities.

Alvarez[50] explained the dispersion in permittivity for lossy rocks in terms of the Maxwell-Wagner effect. This effect deals with charge accumulation at interfaces between materials which differ in conductivity or dielectric permittivity. Alvarez extended the Maxwell-Wagner effect to include the general case where the conductivity and/or permittivity are functions of position within the sample and there is no strict division between the various media making up the sample. He found that in order to satisfy the continuity of charge equation, a charge must accumulate within the sample. If there is no variation of conductivity or permittivity within the sample,(i.e. A homogeneous sample), no excess charge must accumulate. Within a heterogeneous sample, charges must accumulate among materials whose electrical parameters differ. This charge accumulation appears as a polarization and contributes to the sample permittivity.

Keller and Licastro[51] pointed out that the Maxwell-Wagner effect required large water contents to account for high values of permittivity found at low frequencies. They plotted results obtained from a hypothetical rock made up of layers of quartz and water. To explain a dielectric permittivity greater than 1000 in terms of the Maxwell-Wagner effect, the rock must contain in excess of 60% water. Since the water content of tar sand seldom rises above 10%, the Maxwell-Wagner effect cannot be the sole contributing factor to the excess permittivity.

This effect assumes that the movement of charge carriers through the tar sand is not impeded. The tar sand consists of solid particles of sand and clay connected by channels or pores containing ions in water. These ions are responsible for charge transport within tar sand. Any region where the ionic mobility changes will experience a charge pile up and additional polarization which contributes to the overall permittivity.

Keller and Frischknecht[52] described two mechanisms which decrease ionic mobility. Along any pore wall, layers of water molecules are loosely held. As an ion drifts through a fine pore or channel, the forces holding the water molecules near the wall will increase the viscosity and decrease the mobility of the ions. There is a tendency for positive ions to pile up on one side of the pore and negative ions on the other. The second mechanism described by Keller deals with selectively permeable membranes. These membranes result from minerals which are fixed within the sample framework and can be ionized. When the ion goes into solution, a charged mineral particle (usually clay) is left behind. This charged particle blocks free ion movement through the pore. The particle acts like an ion sieve allowing positive ions to drift along the pore but blocking the negative ones by repulsion. The resulting charge separation increases the sample polarization.

Fuller and Ward[53] interpreted the high dielectric permittivities measured on earth-type materials in terms of electrical parameters which can have both in-phase and quadrature phase components. The classical description of conduction current is a current in phase with the applied electric field. Similarly, displacement current is a current in quadrature with the applied electric field. Conduction current is due to the drift of free charges while displacement current is due to realignment of bound charges. Conduction in most soil materials takes place by ionic drift through pore liquids. Factors such as viscosity of the pore liquid or restraining forces set up by local polarizations within the sample framework may cause the ion drift to slow. The result will be a conduction current out of phase with the applied electric field. Fuller and Ward postulated that the out of phase component of the conduction current will contribute to the displacement current. The resulting greater displacement current accounts for the large permittivities measured at low frequencies. However, there is some doubt regarding the validity of this explanation, since displacement current leads the conduction current by +90°. The conduction component out of phase due to slow ionic drift will lag the in-phase conduction current, and subtract from the displacement current. Thus a lower dielectric permittivity will be measured.

4.5 CONCLUSIONS

This thesis examined the conductivity and permittivity of tar sand samples as a function of frequency. The main emphasis was on low frequency measurements taken with a two-electrode capacitive cell. Measurements taken with a coaxial cell extended the results up to 25MHz. The tar sand samples ranged from 1% to 5% water content by weight, while the bitumen saturation varied between 10% and 15% by weight. Measurements were taken on two sample lengths to ensure that contact and polarization errors remained small.

The tar sand conductivity depends strongly on moisture content. The conductivity displays very little change with frequency, remaining constant as the frequency is increased to 1MHz. As the frequency is further increased, the conductivity slowly rises. No correlation could be determined between the bitumen content and the conductivity, since small changes in moisture content overshadowed the conductivity variation expected from the bitumen variation. The permittivity is very strongly dependent on frequency. At low frequencies the permittivity is very large, decreasing rapidly as the frequency increases to 10MHz. At this frequency and above, the measured values are comparable to those found for homogeneous samples. The permittivity also depends on the conductivity of the sample, increasing as the conductivity increases. This dependence on conductivity is especially noticeable at low frequencies.

This thesis laid the basic framework for low frequency tar sand measurements. The graphical results presented in this chapter indicate values expected for typical tar sand samples. There is a need for future research into the dependence of the tar sand parameters on temperature. To ensure that the laboratory results truly represent in situ tar sand, careful handling of the tar sand batch is required. Once a batch has been removed from the ground it should be stored in a frozen state to minimize moisture losses before measurements are taken.

The electrical parameters of tar sand will be used in the design of in situ electrical heating systems. The permittivity and conductivity will indicate suitable frequency ranges and electrode configurations for coupling electromagnetic energy into the tar sand. Information regarding the temperature dependence of permittivity and conductivity will be used to design systems which can adapt as the electrical parameters change due to heating. The electrical parameters will indicate the most efficient and practical in situ electrical heating schemes and thereby contribute to the development of economical methods for recovering bitumen from tar sand deposits which might otherwise not be exploited.

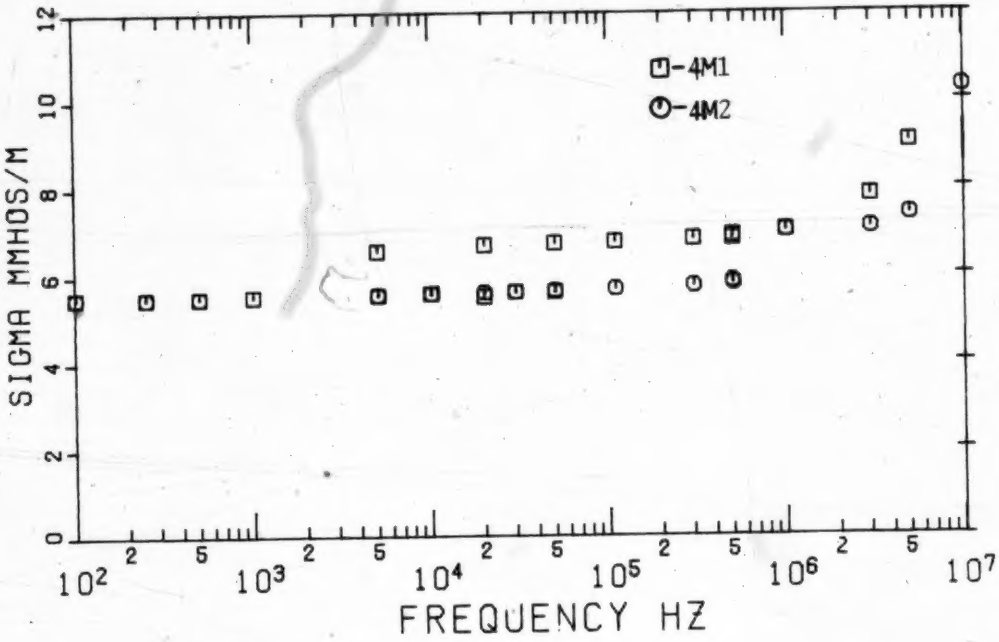

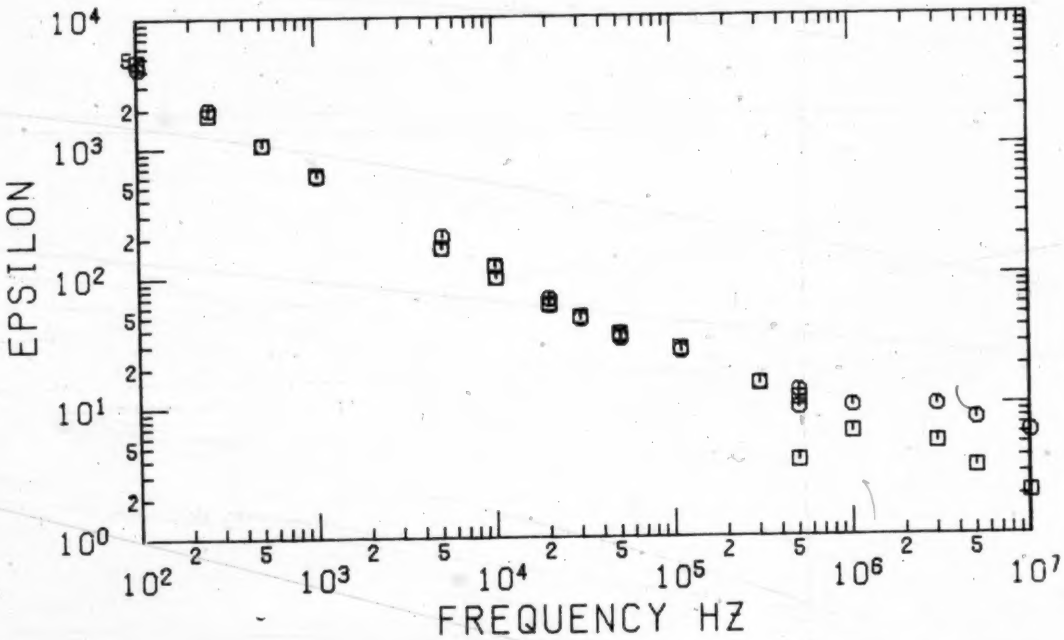

FIGURE (4.1) TAR SAND SAMPLES 4M1 4M2
Water Content 4M1-3.6% 4M2-3.6%
Bitumen Content 4M1-10.9% 4M2-10.9%

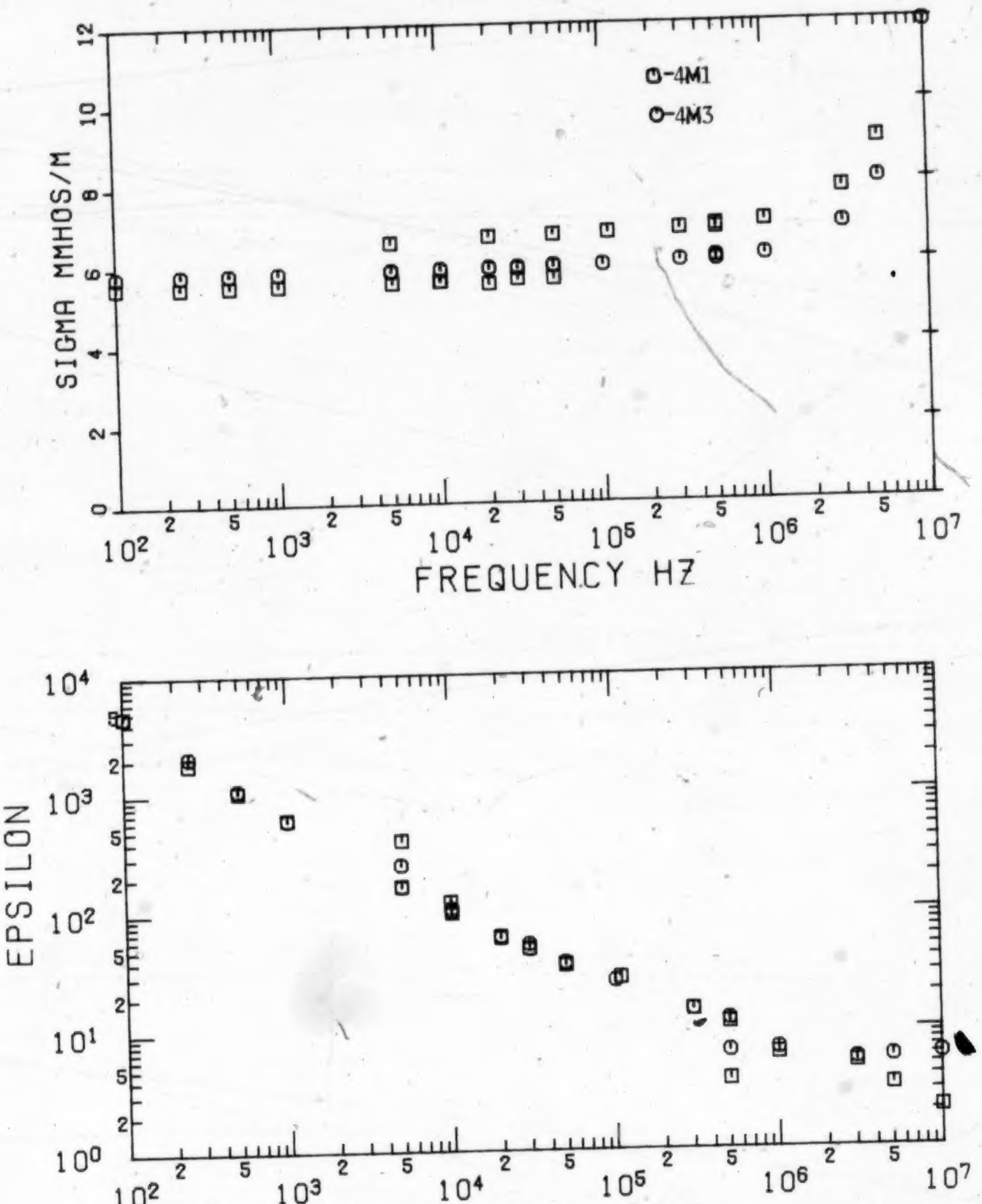

FIGURE (4.2) TAR SAND SAMPLES 4M1 4M3
Water Content 4M1-3.6% 4M3-3.6%
Bitumen Content 4M1-10.9% 4M3-10.9%

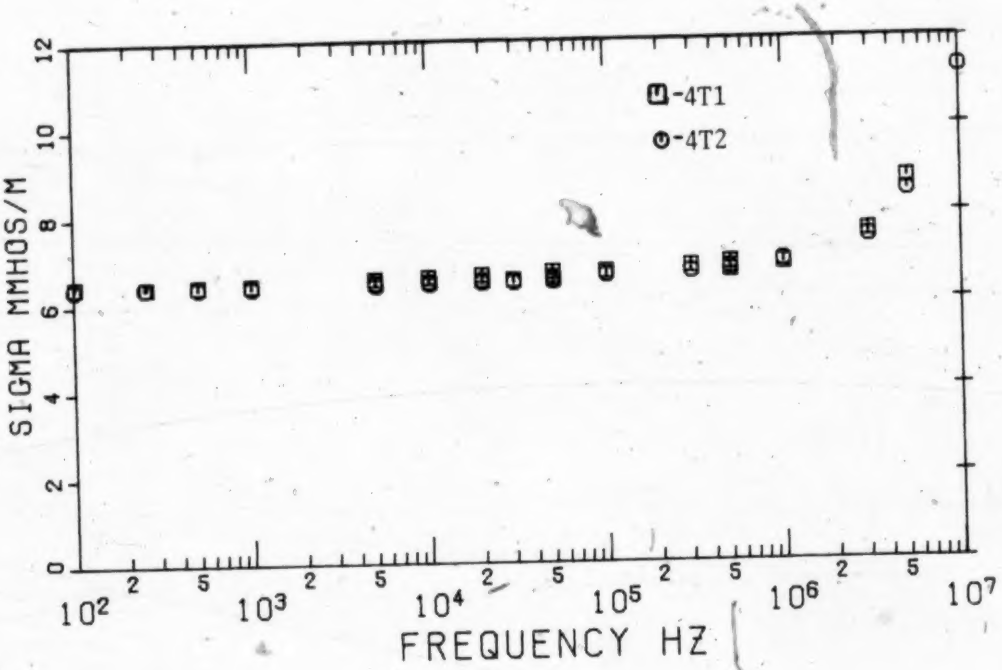

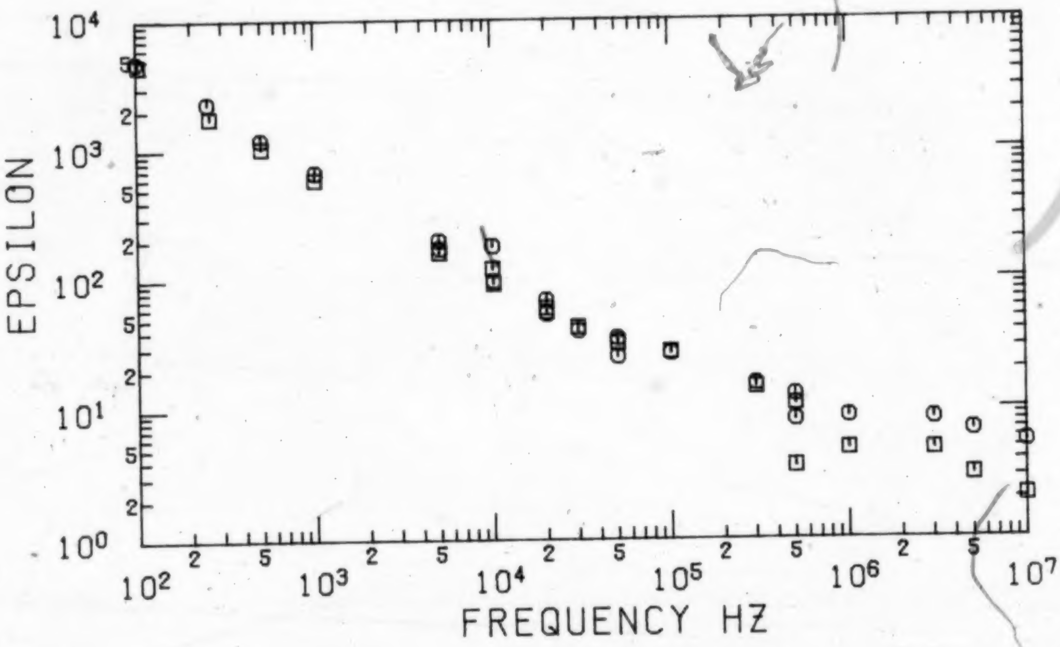

FIGURE (4.3) TAR SAND SAMPLES 4T1 4T2
Water Content 4T1-3.8% 4T2-3.7%
Bitumen Content 4T1-11.2% 4T2-11.6%

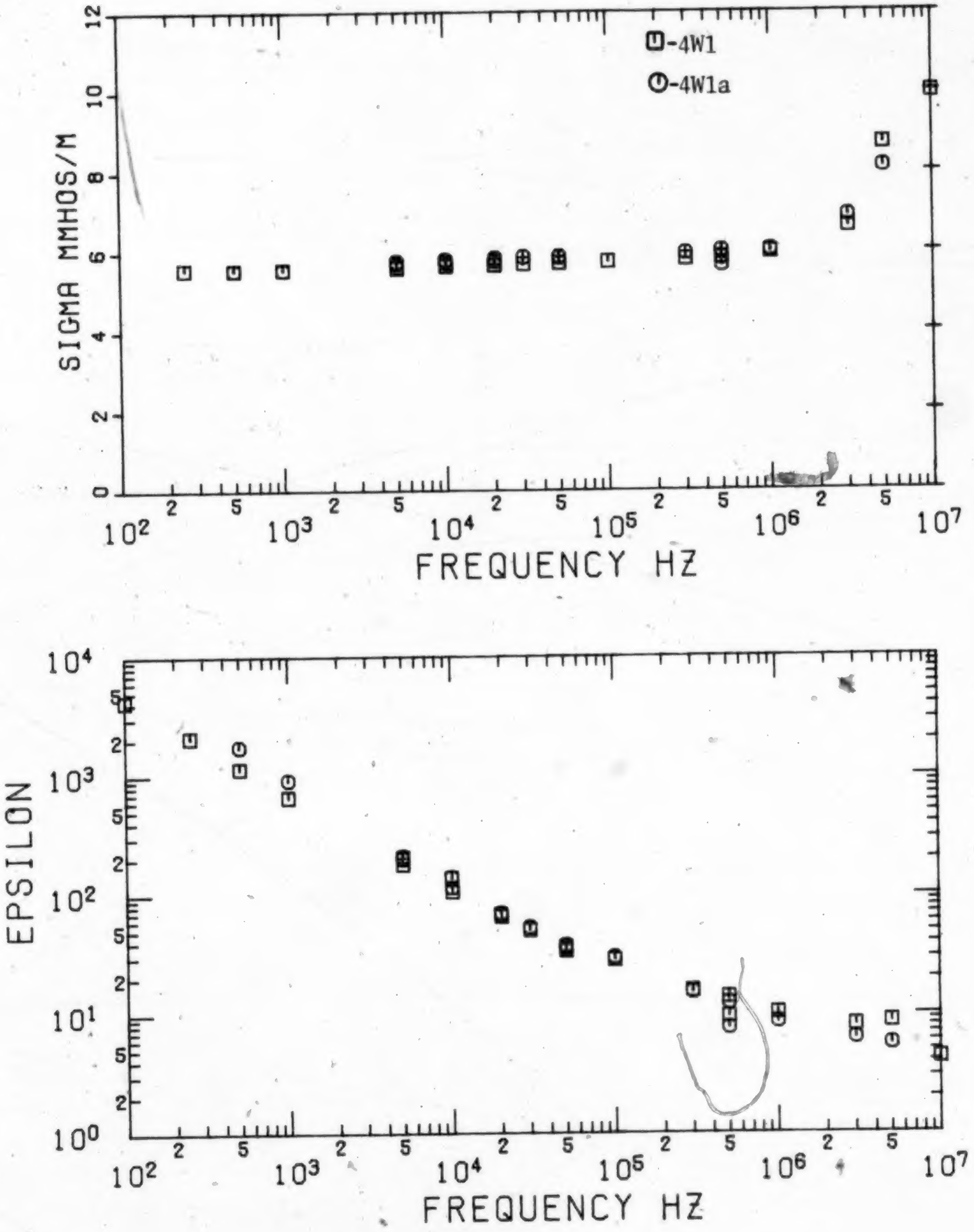

FIGURE(4.4) TAR SAND SAMPLES 4W1 4W1a
Water Content 4W1-3.8% 4W1a-3.8%
Bitumen Content 4W1-11.6% 4W1a-11.6%

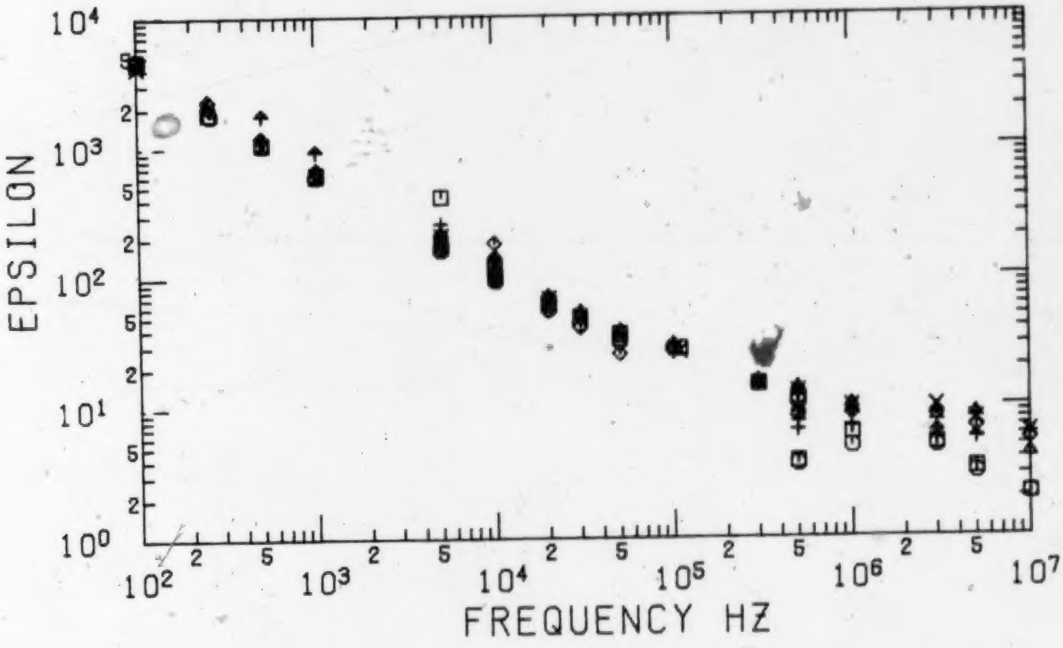

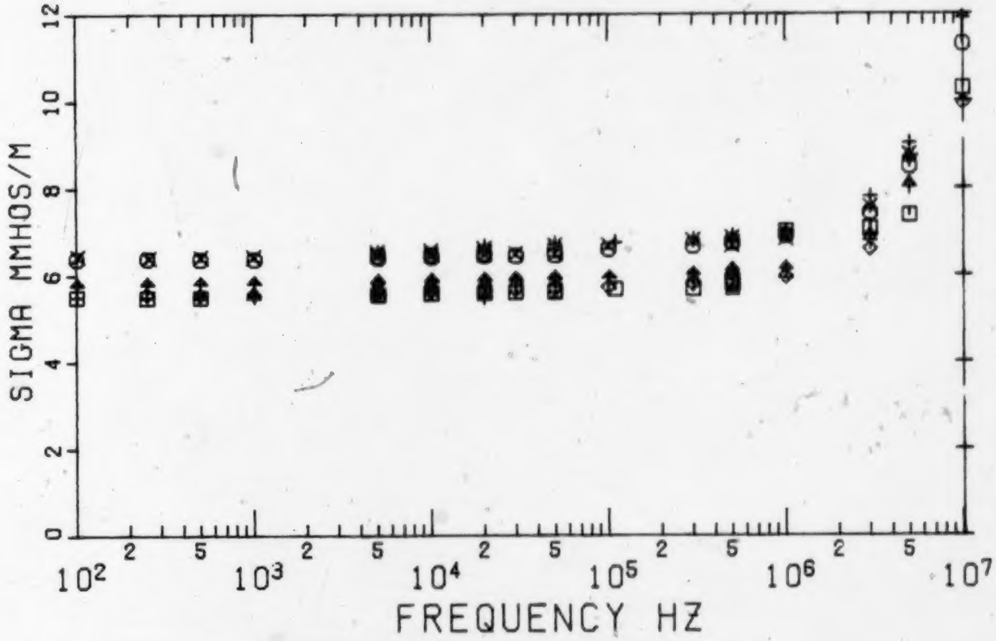

FIGURE(4.5) COMPOSITE GRAPH OF BATCH 1
Average Water Content 3.7%
Average Bitumen Content 11.3%

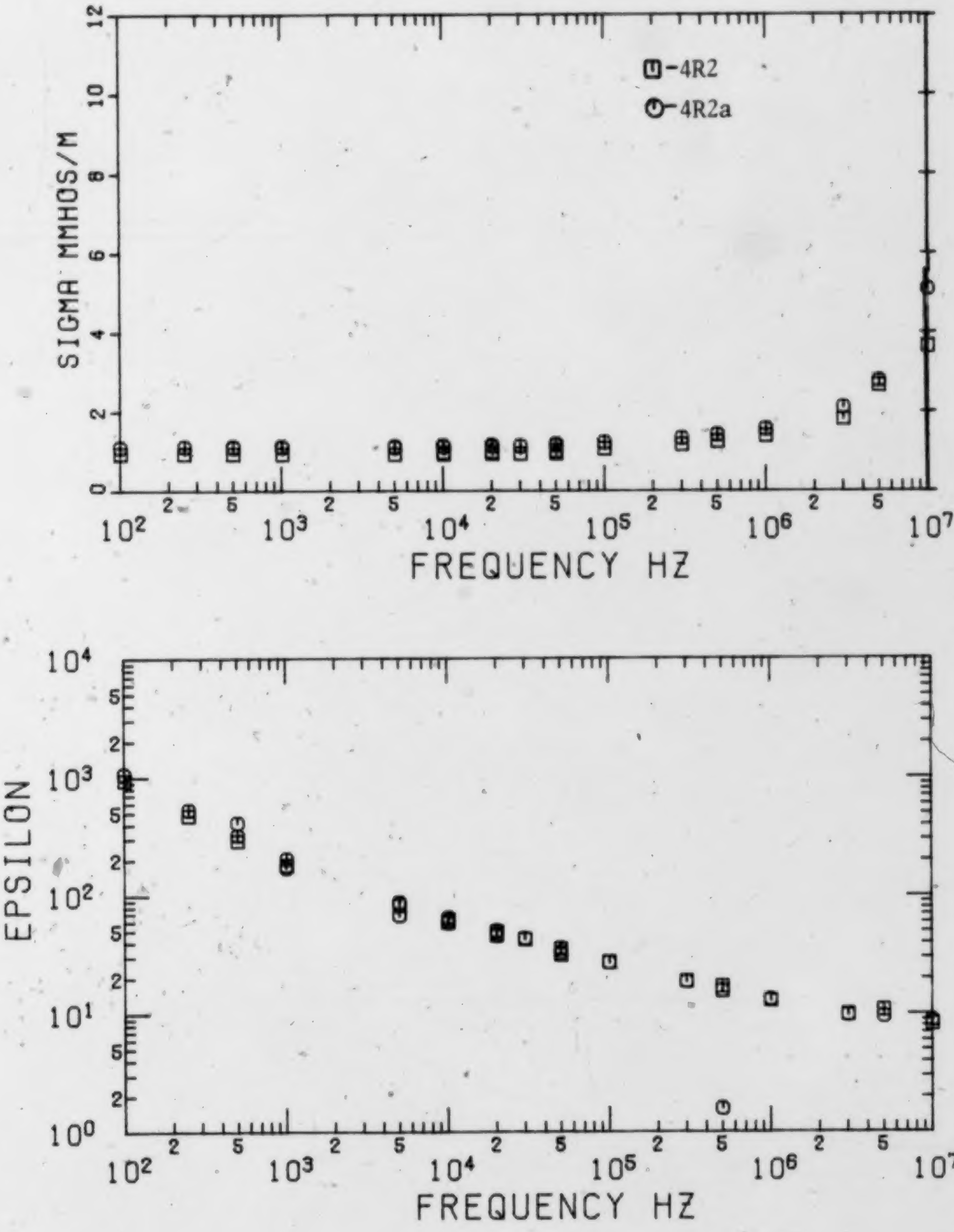

FIGURE(4.6) TAR SAND SAMPLES 4R2 4R2a
Water Content 4R2-2.4% 4R2a-2.4%
Bitumen Content 4R2-11.1% 4R2a-11.1%

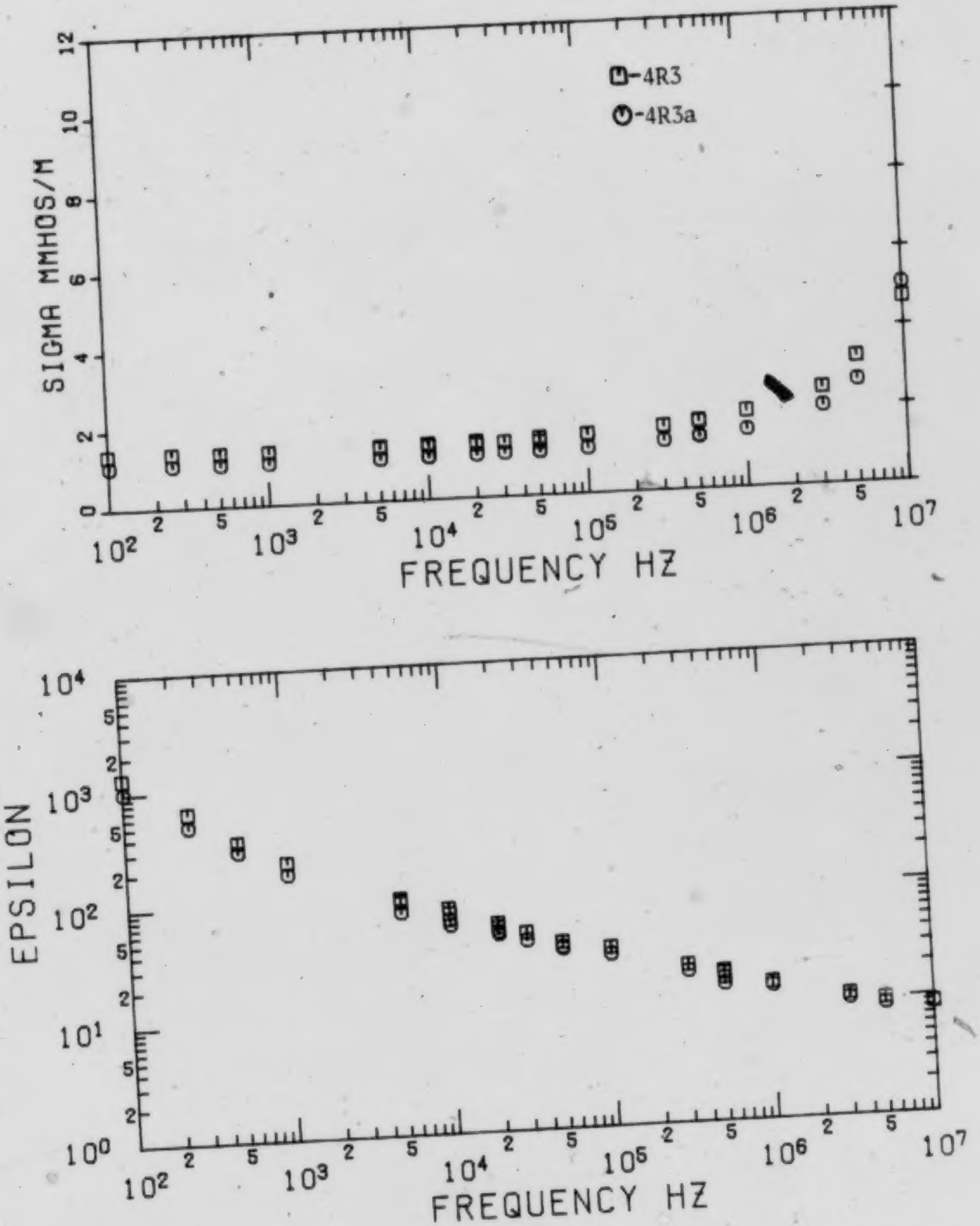

FIGURE(4.7) TAR SAND SAMPLES 4R3 4R3a
Water Content 4R3-2.4% 4R3a-2.4%
Bitumen Content 4R3-11.1% 4R3a-11.1%

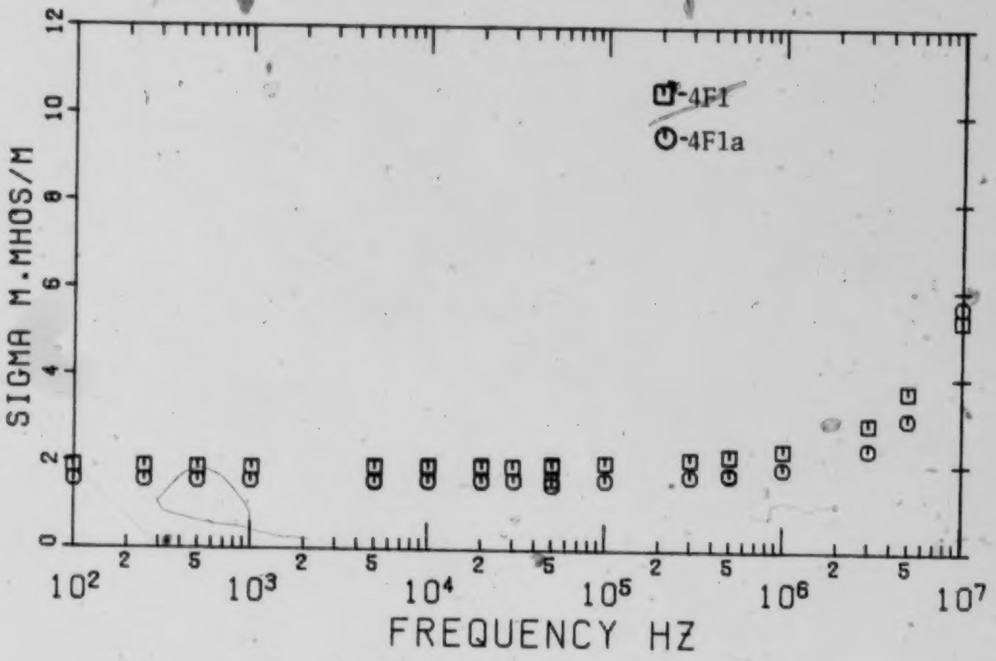

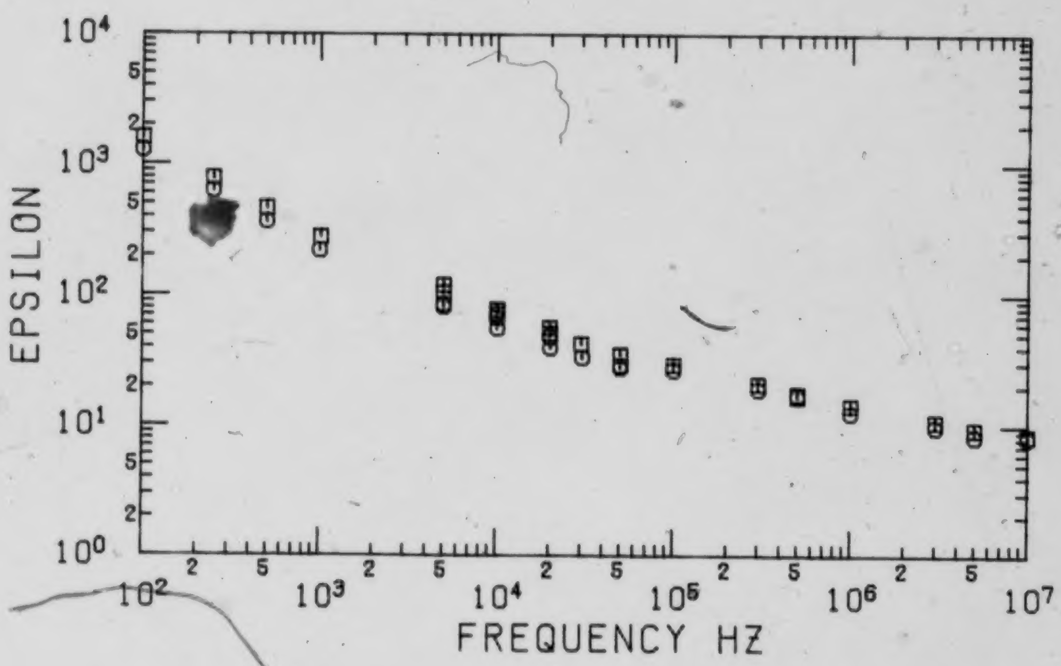

FIGURE (4.8) TAR SAND SAMPLES 4F1 4F1a
Water Content 4F1-1.7% 4F1a-1.7%
Bitumen Content 4F1-12.1% 4F1a-12.1%

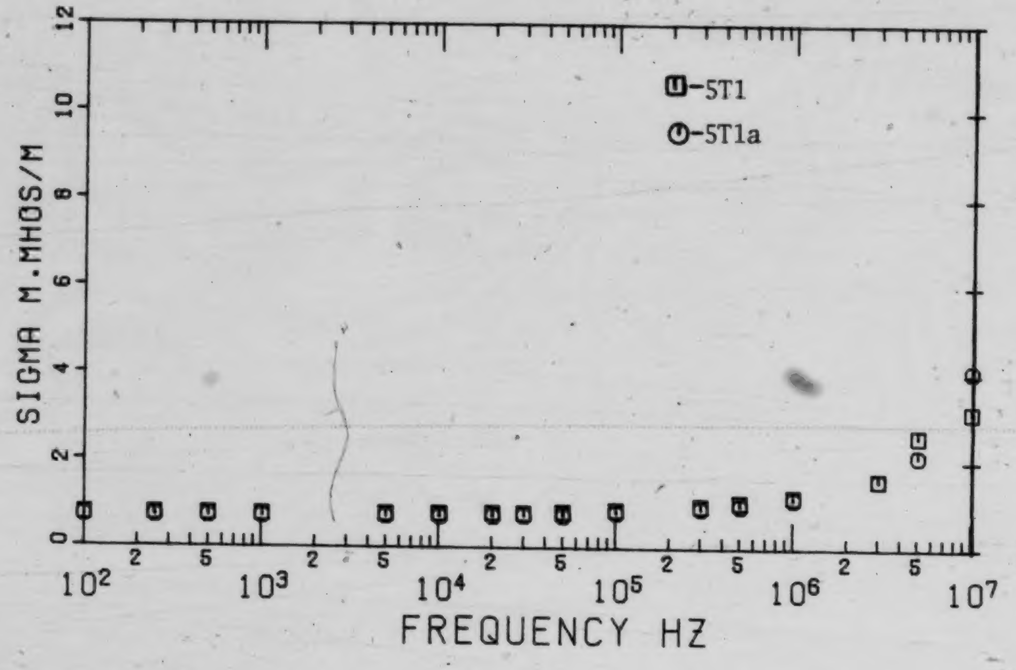

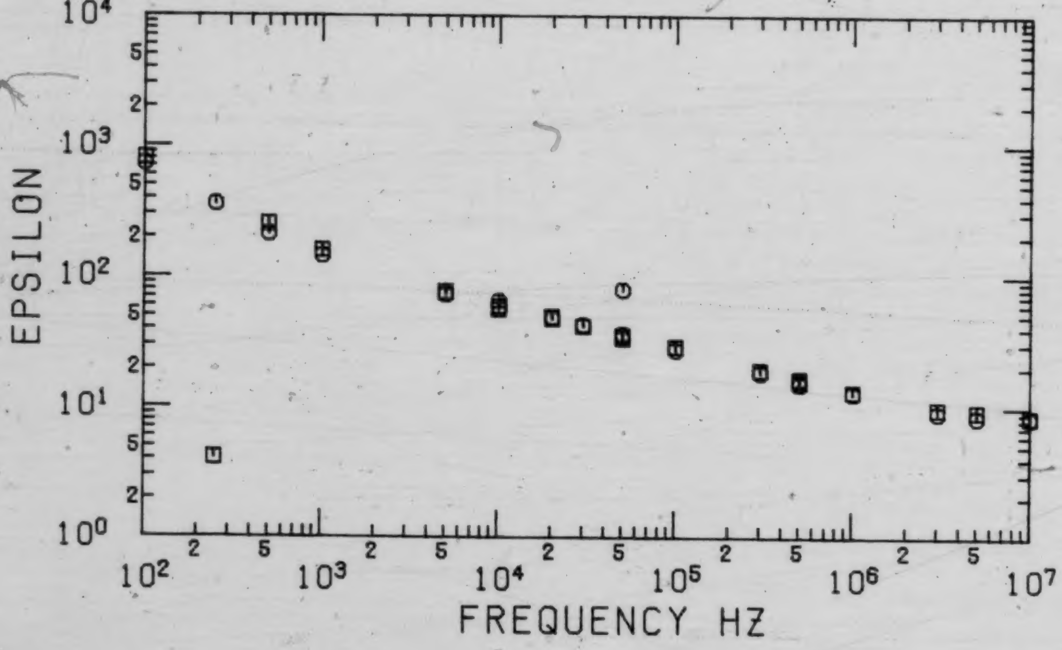

FIGURE(4.9) TAR SAND SAMPLES 5T1 5T1a
Water Content 5T1-1.7% 5T1a-1.7%
Bitumen Content 5T1-11.4% 5T1a-11.4%

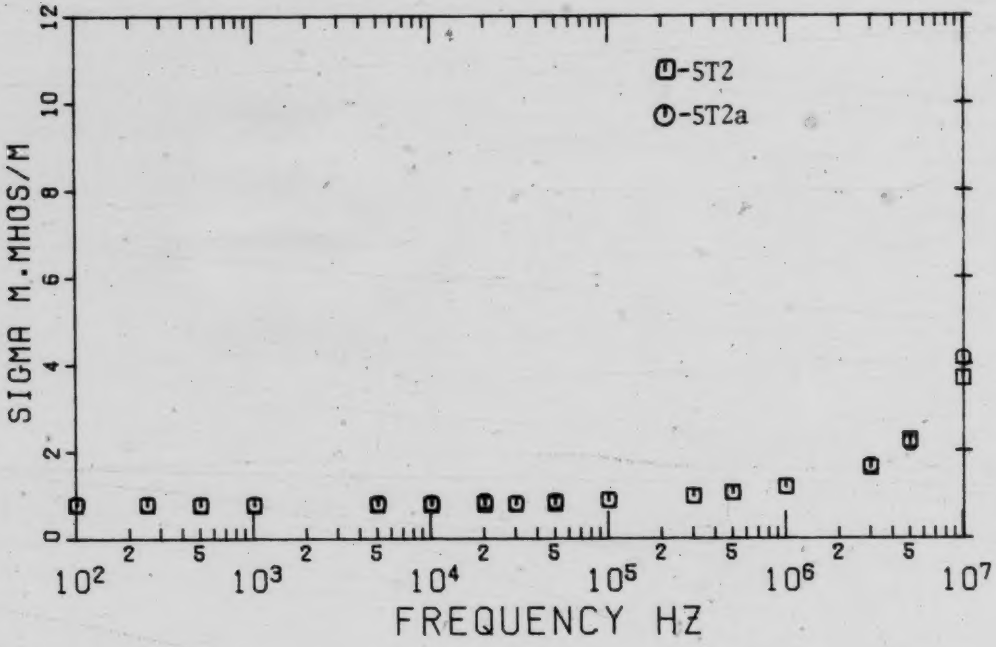

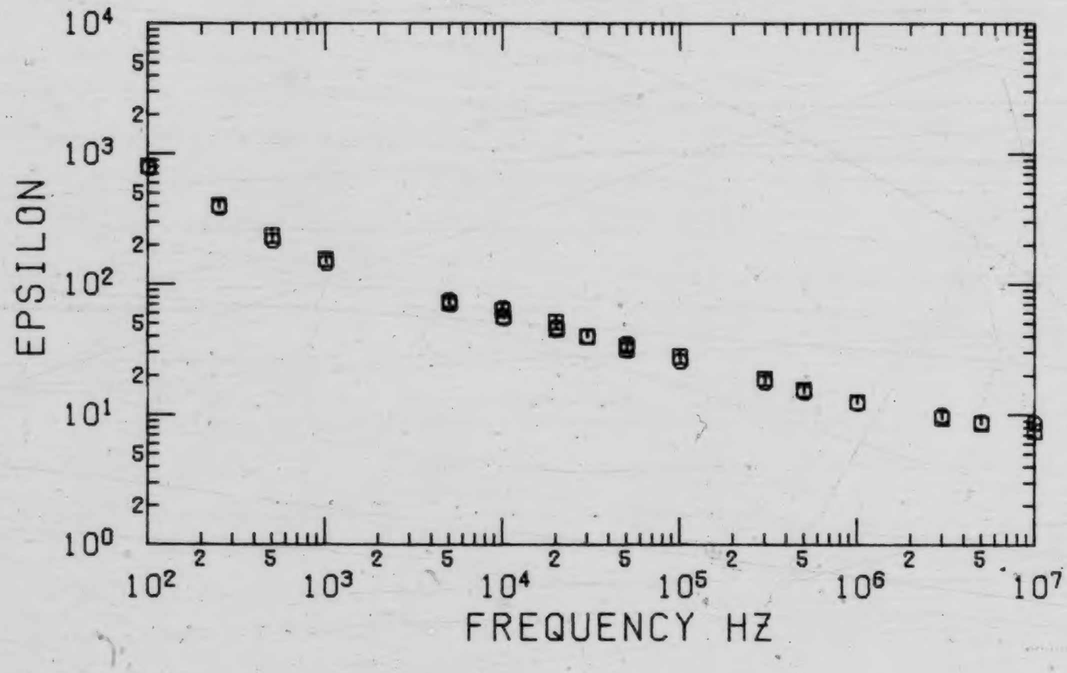

FIGURE(4.10) TAR SAND SAMPLES 5T2 5T2a
Water Content 5T2-1.7% 5T2a-1.7%
Bitumen Content 5T2-11.41% 5T2a-11.41%

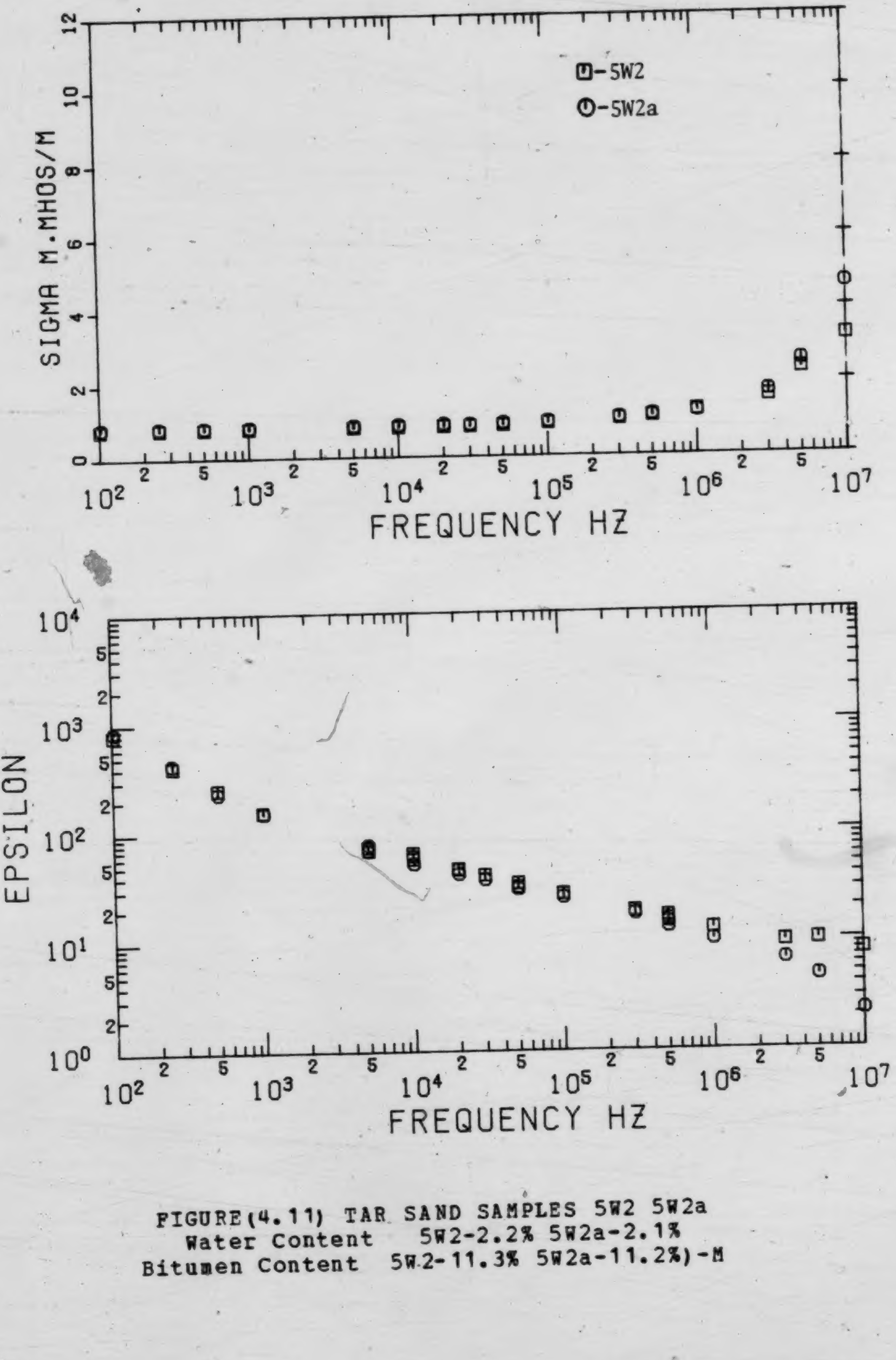

FIGURE(4.11) TAR SAND SAMPLES 5W2 5W2a
Water Content 5W2-2.2% 5W2a-2.1%
Bitumen Content 5W2-11.3% 5W2a-11.2%)-M

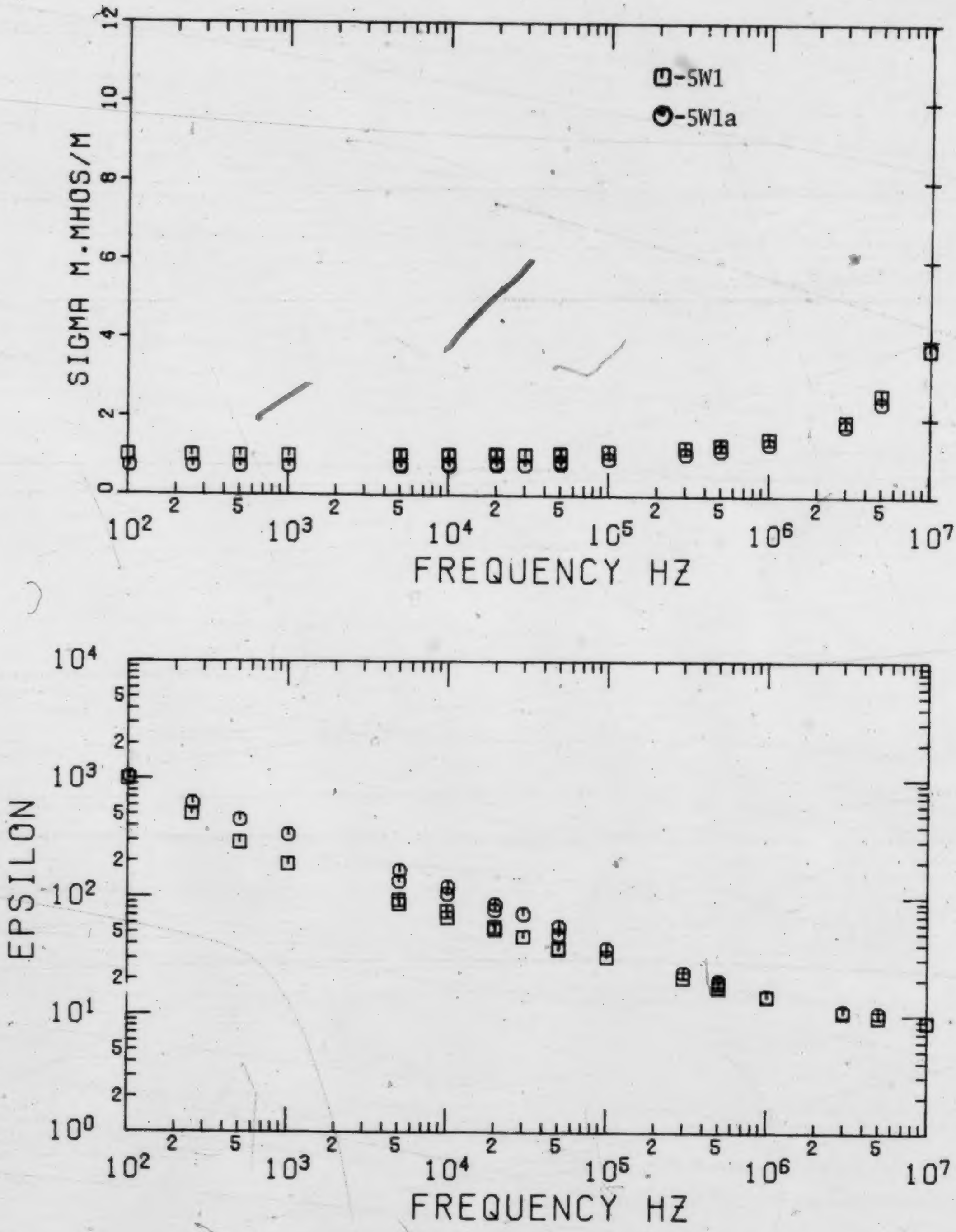

FIGURE(4.12) TAR SAND SAMPLES 5W1 5W3
Water Content 5W1-2.1% 5W3-2.1%
Bitumen Content 5W1-11.2% 5W3-11.2%

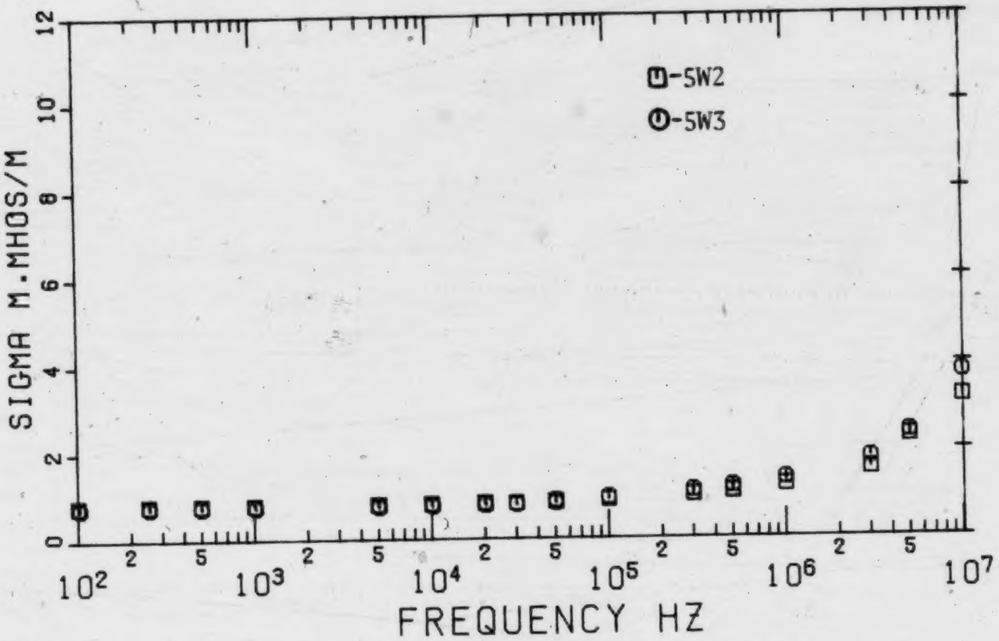

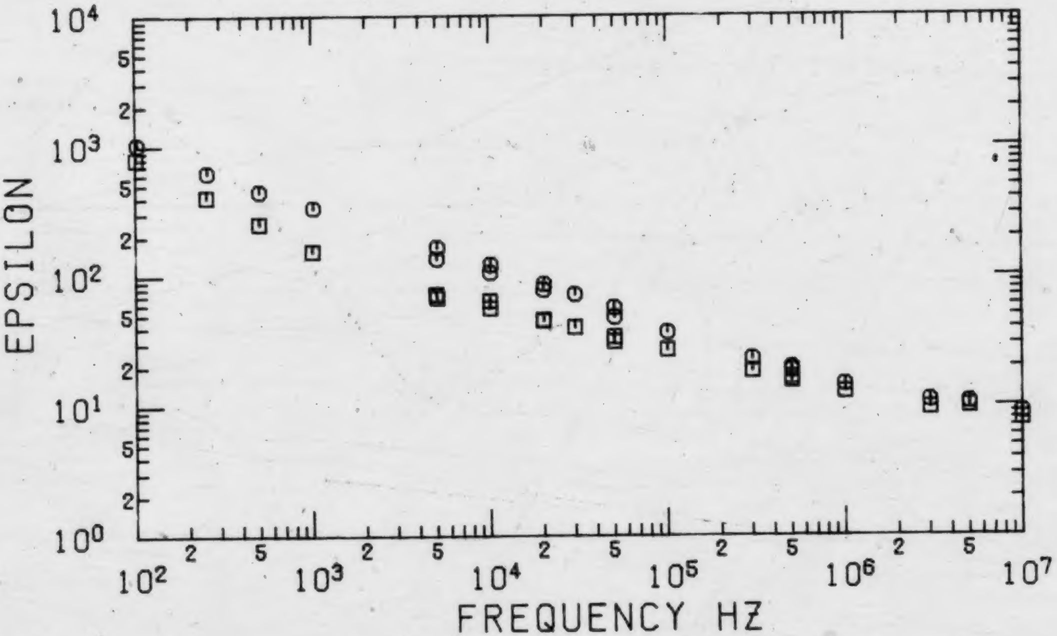

FIGURE(4.13) TAR SAND SAMPLES 5W2 5W3
Water Content 5W2-2.2% 5W3-2.1%
Bitumen Content 5W2-11.3% 5W3-11.2%)-M

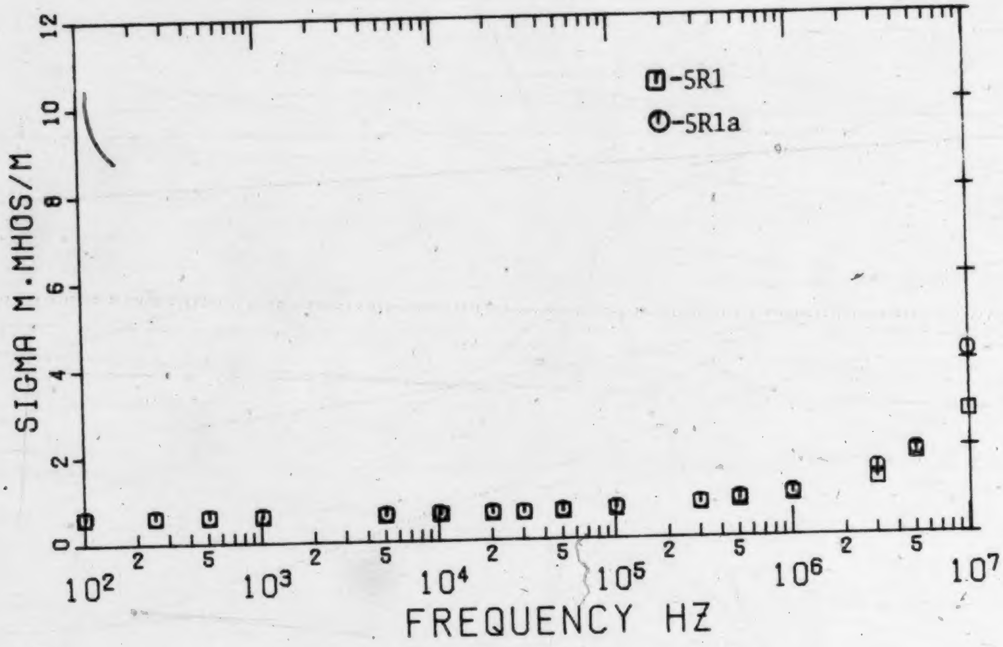

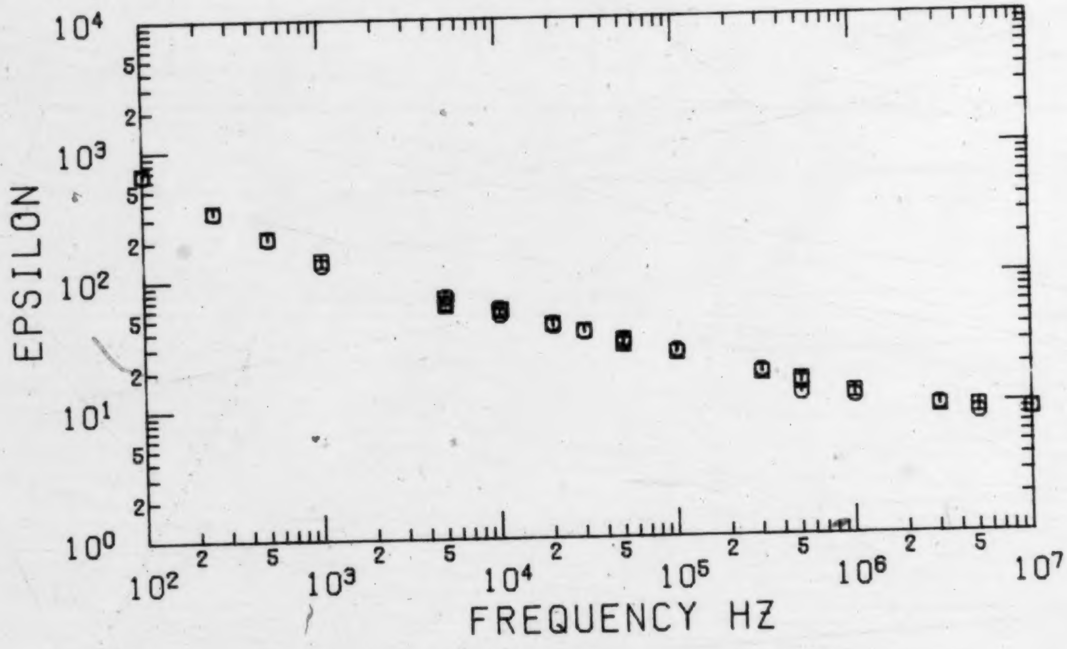

FIGURE(4.14) TAR SAND SAMPLES 5R1 5R1a
Water Content 5R1-1.9% 5R1a-1.9%
Bitumen Content 5R1-11.5% 5R1a-11.5%

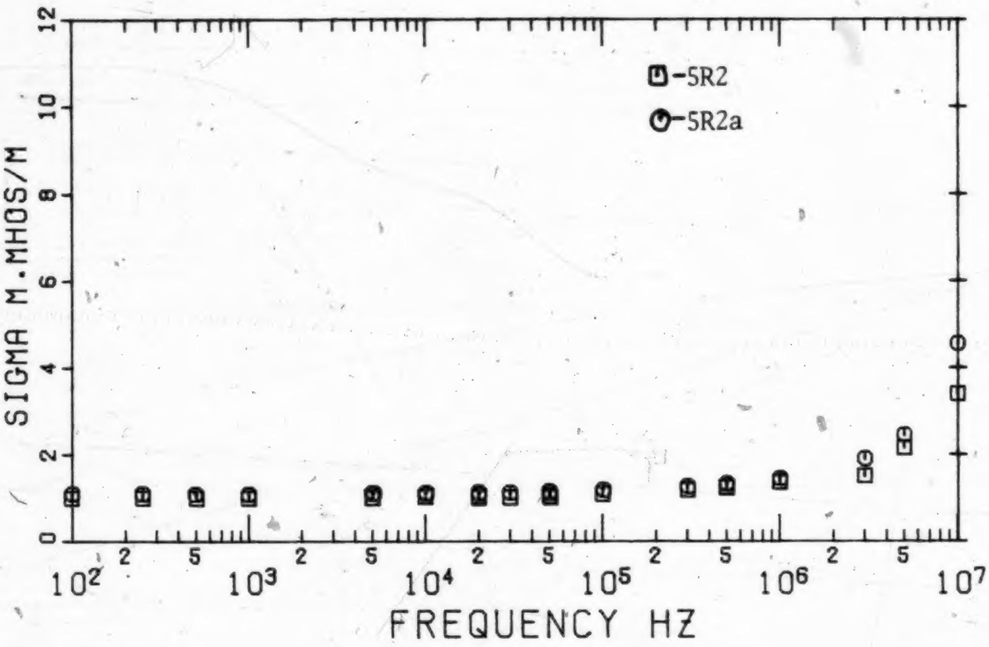

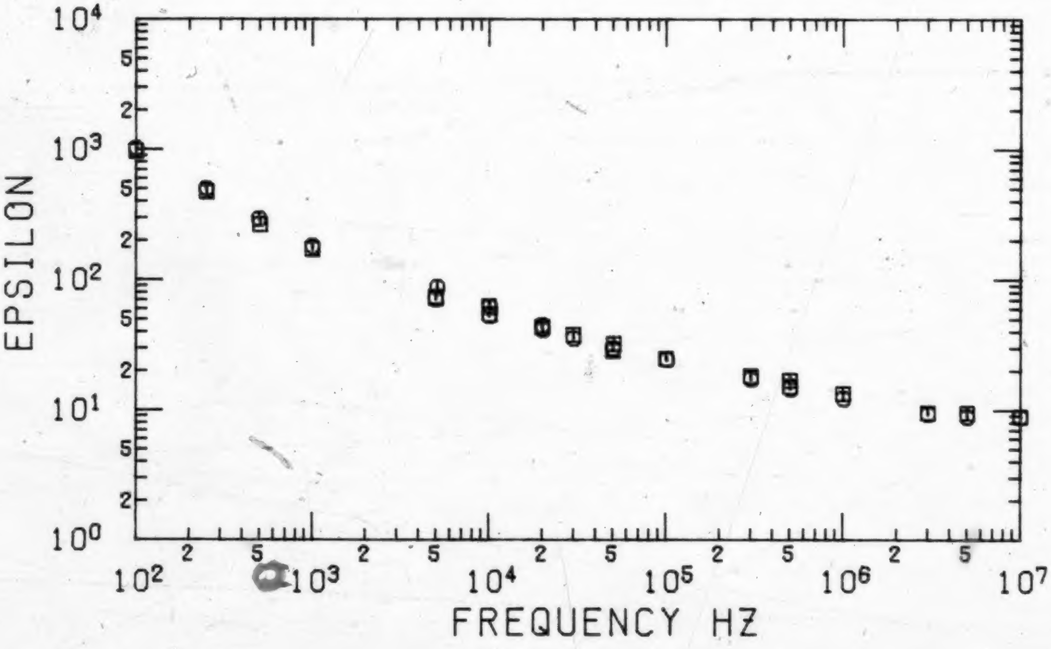

FIGURE(4.15) TAR SAND SAMPLES 5R2 5R2a
Water Content 5R2-1.9% 5R2a-1.4%
Bitumen Content 5R2-11.5% 5R2a-11.8%

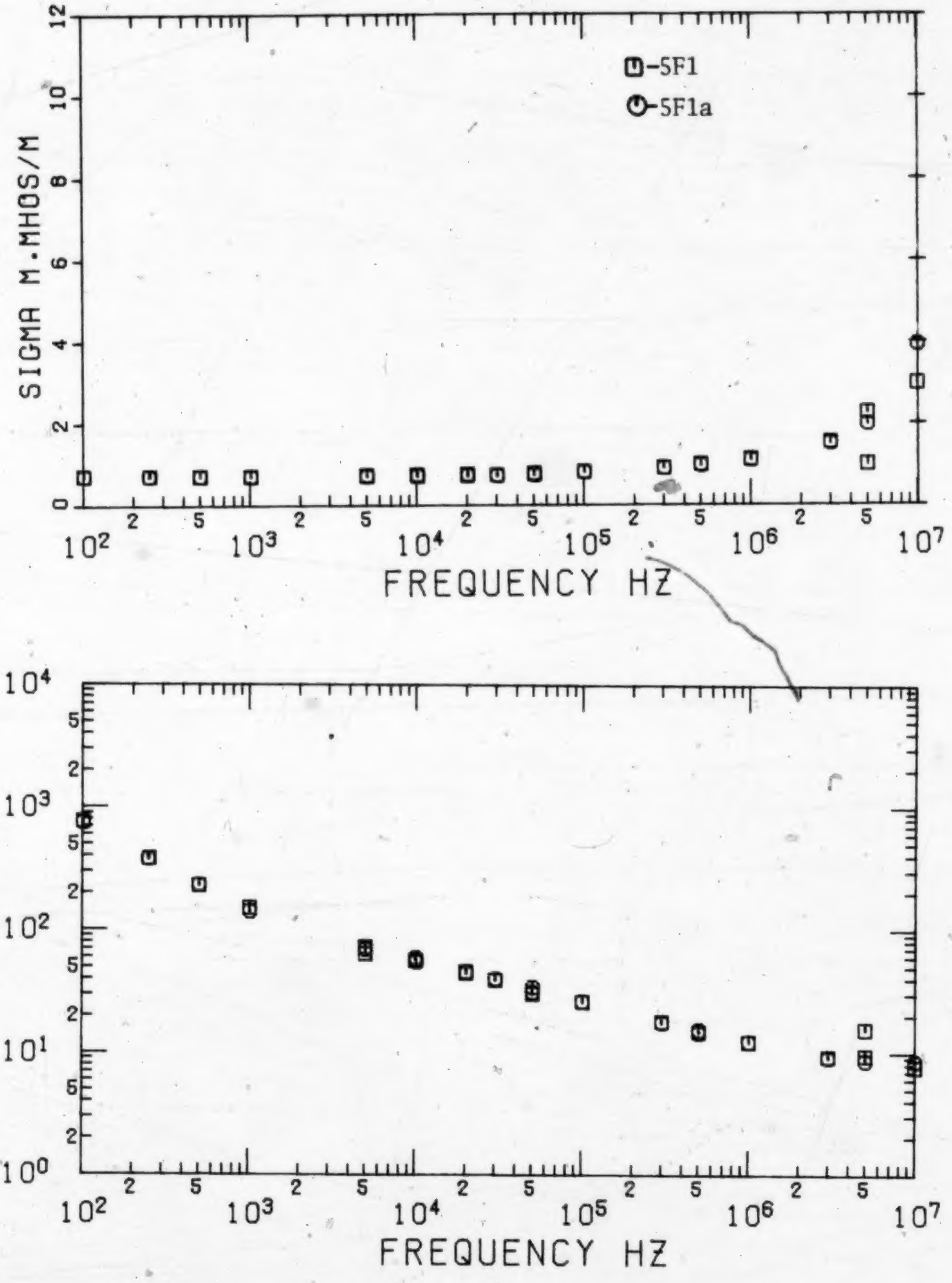

FIGURE(4.16) TAR SAND SAMPLES 5F1 5F1a
Water Content 5F1-1.9% 5F1a-1.9%
Bitumen Content 5F1-11.4% 5F1a-11.4%

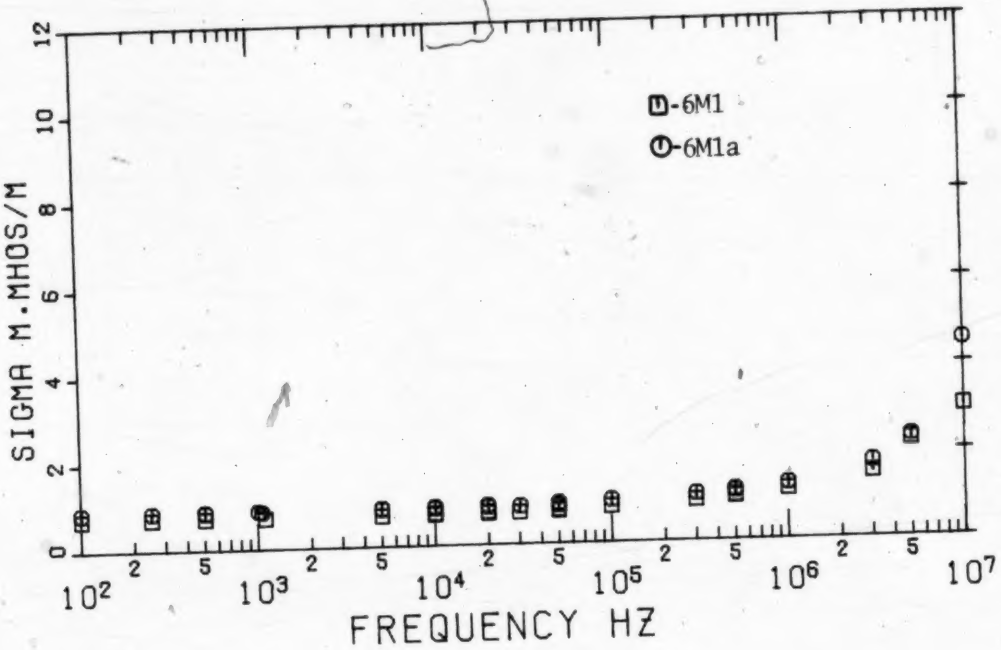

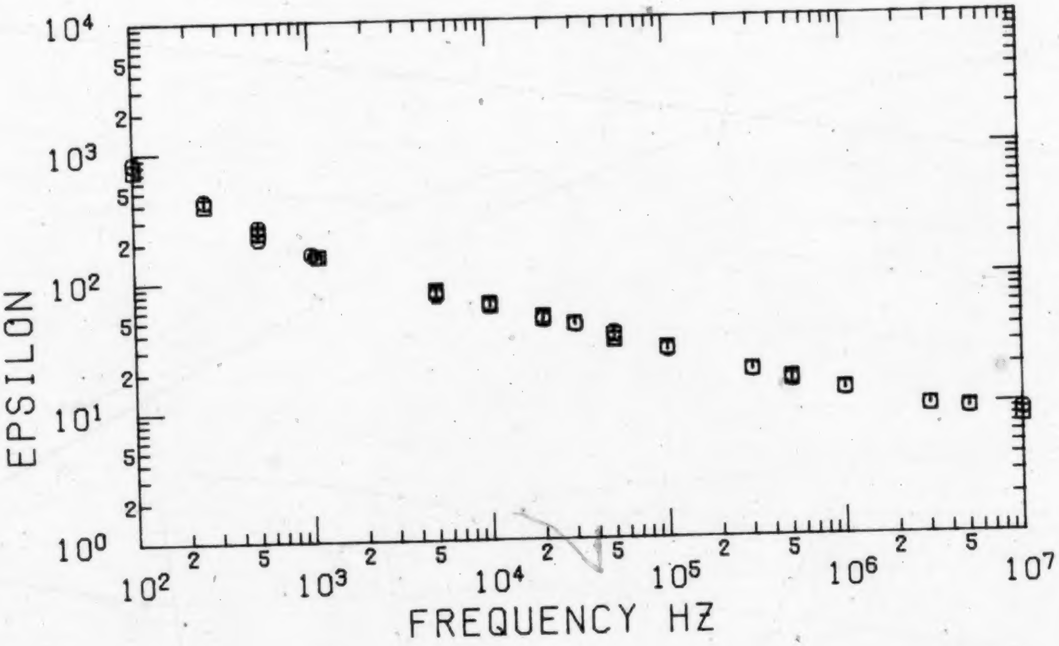

FIGURE(4.17) TAR SAND SAMPLES 6M1 6M1a
Water Content 6M1-1.7% 6M1a-1.7%
Bitumen Content 6M1-11.5% 6M1a-11.5%

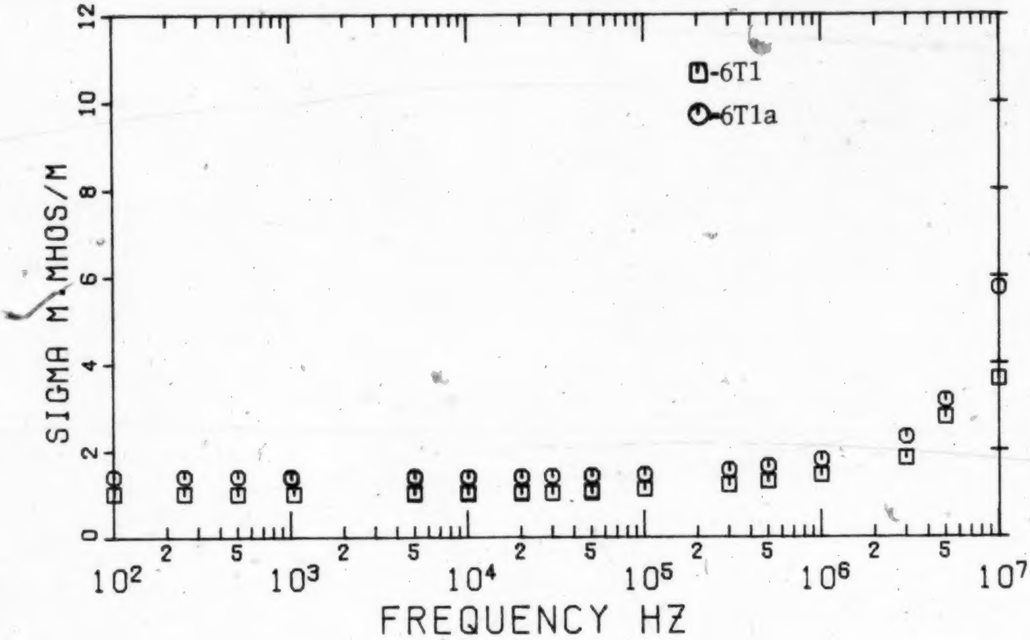

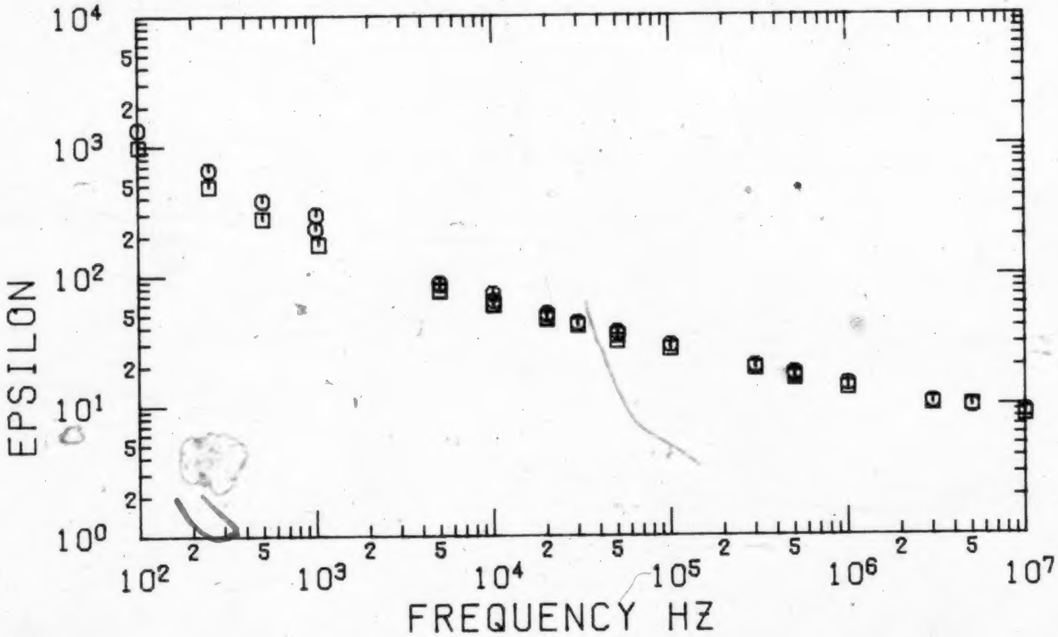

FIGURE(4.18) TAR SAND SAMPLES 6T1 6T1a
Water Content 6T1-2.0% 6T1a-2.0%
Bitumen Content 6T1-11.3% 6T1a-11.3%

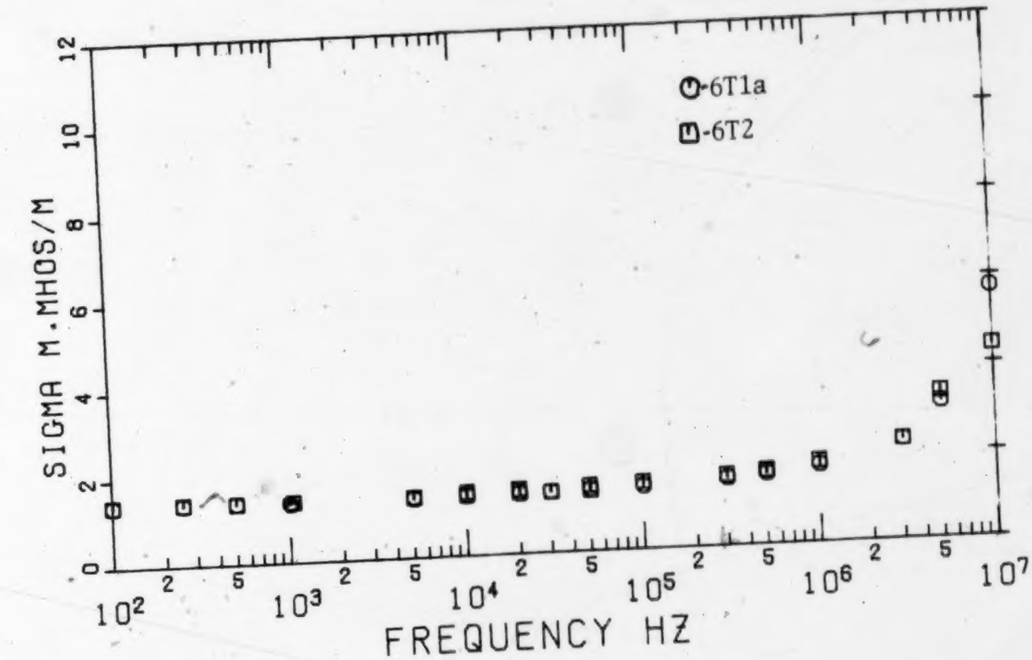

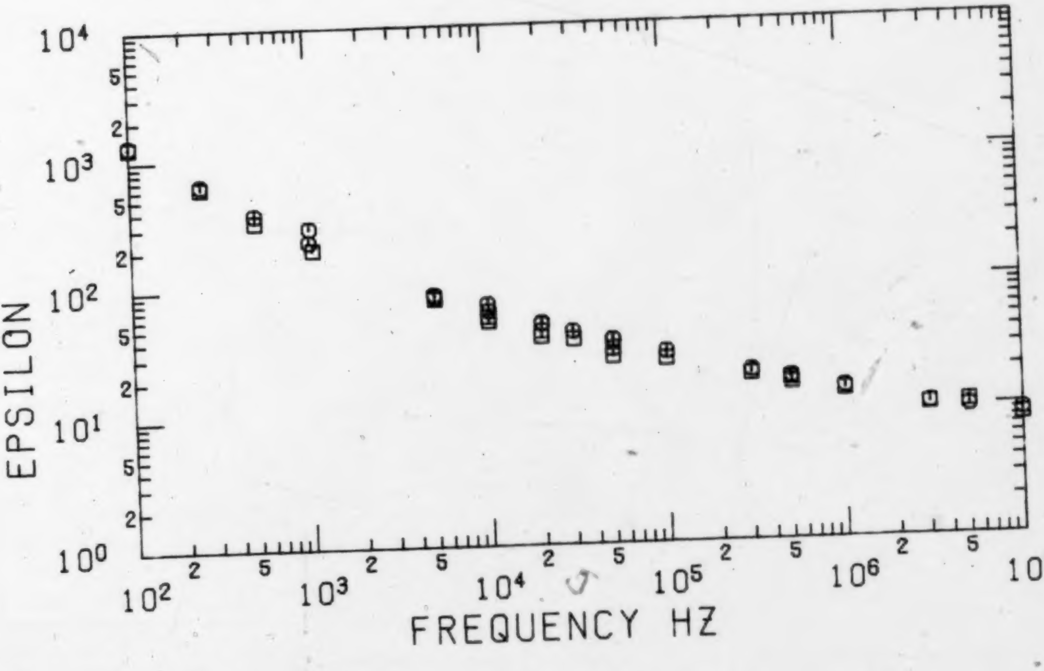

FIGURE(4,19) TAR SAND SAMPLES 6T1a 6T2
Water Content 6T1a-2.0% 6T2-2.0%
Bitumen Content 6T1a-11.3% 6T2-11.3%

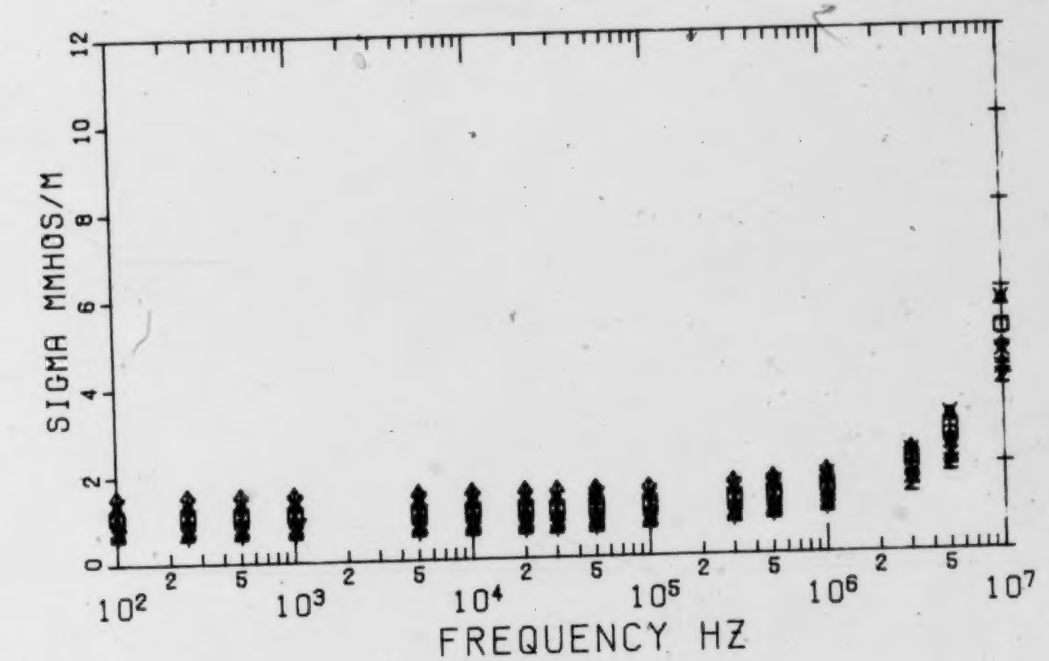

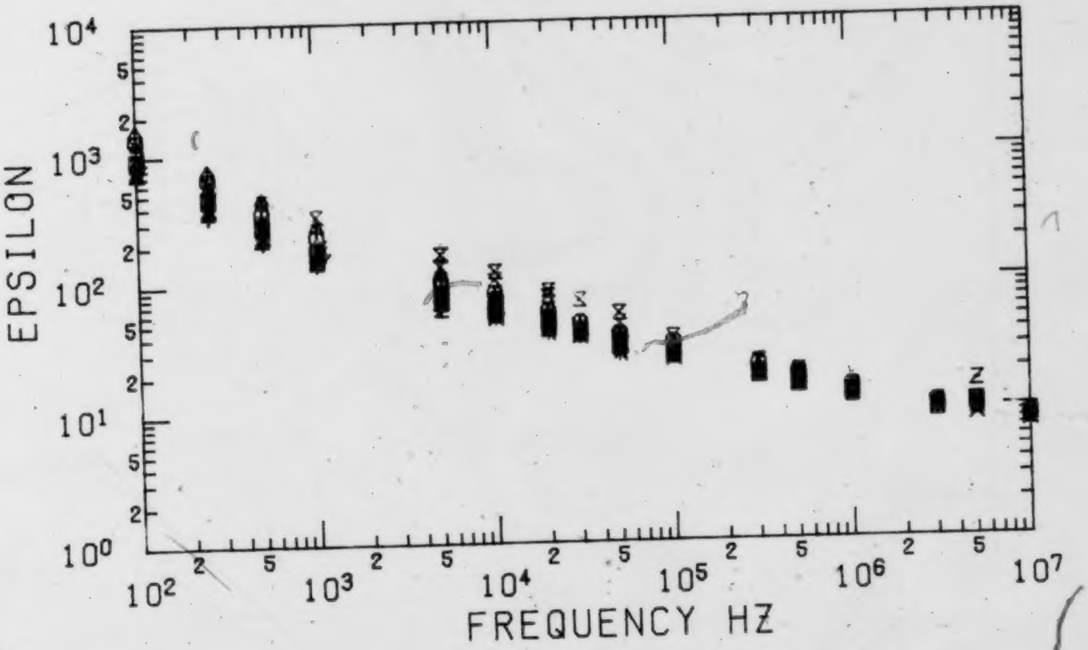

FIGURE(4.20) COMPOSITE GRAPH OF BATCH 2
Average Water Content 1.9%
Average Bitumen Content 11.4%

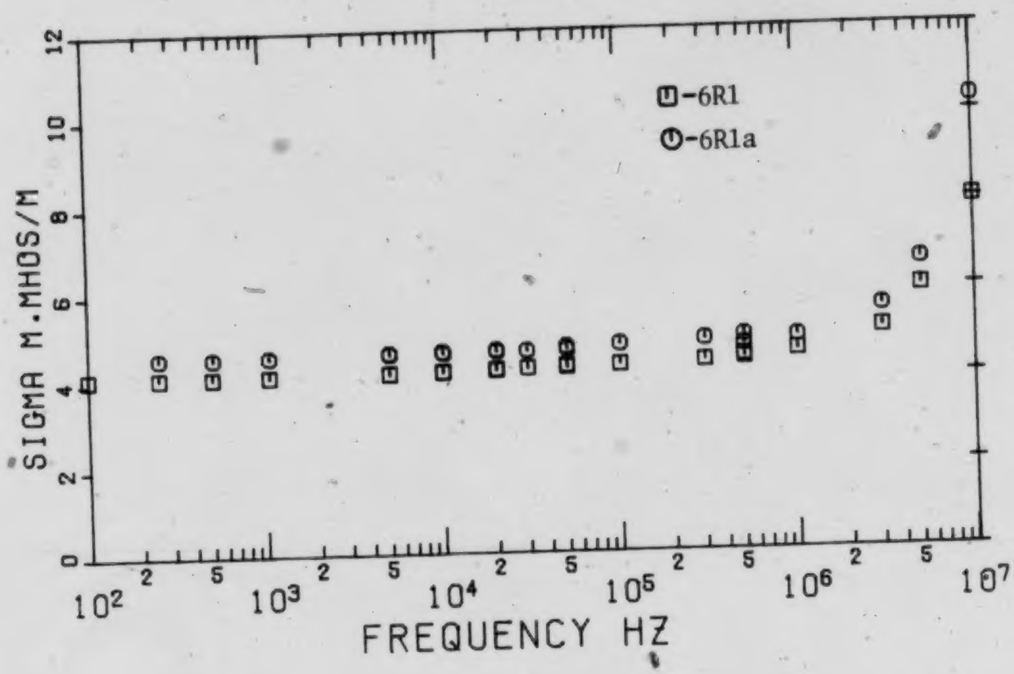

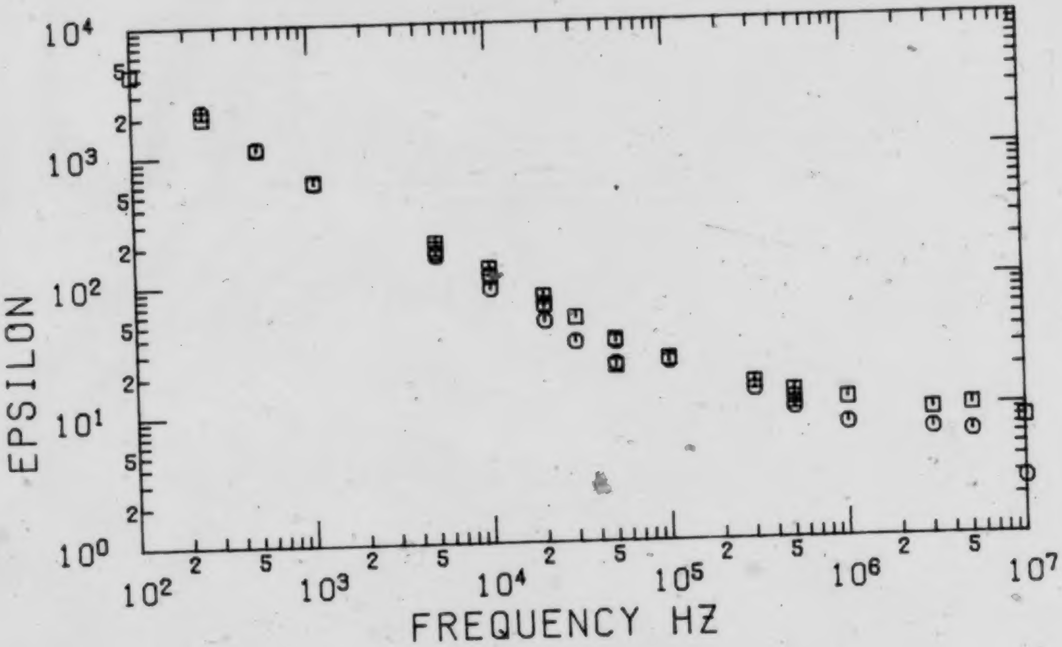

FIGURE(4.21) TAR SAND SAMPLES 6R1 6R1a
Water Content 6R1-4.9% 6R1a-5.8%
Bitumen Content 6R1-12.7% 6R1a-11.7%

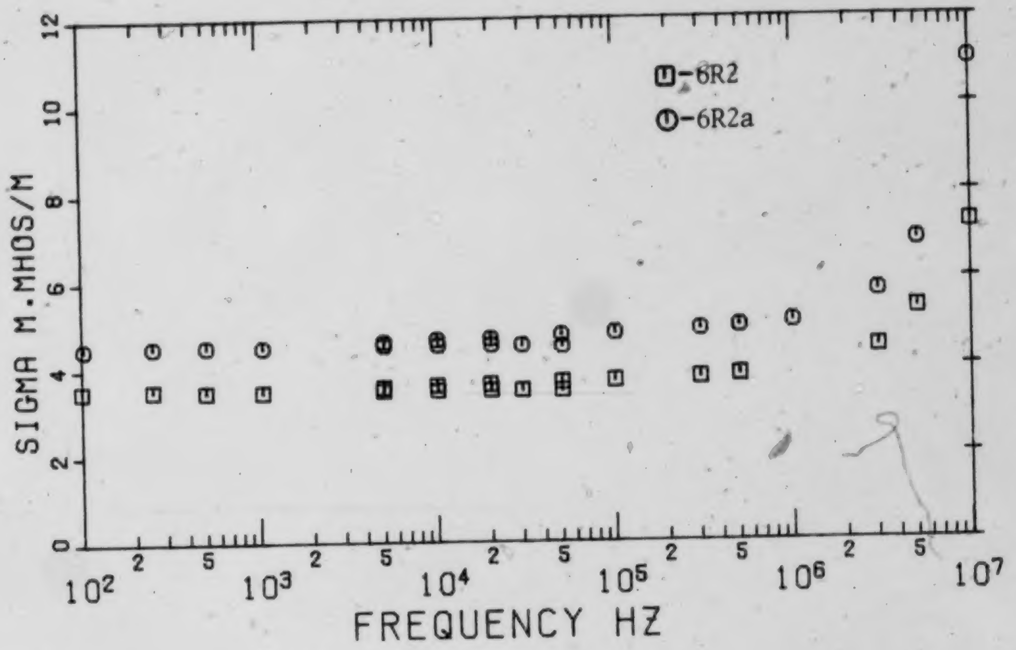

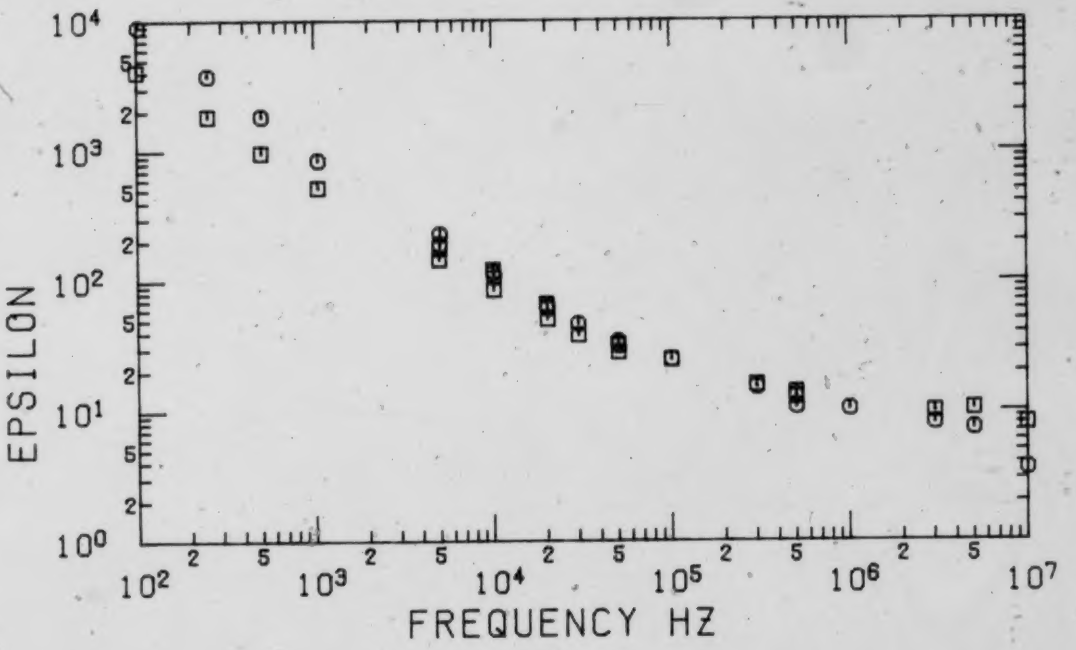

FIGURE(4.22) TAR SAND SAMPLES 6R2 6R2a
Water Content 6R2-4.9% 6R2a-4.9%
Bitumen Content 6R2-12.7% 6R2a-12.7%

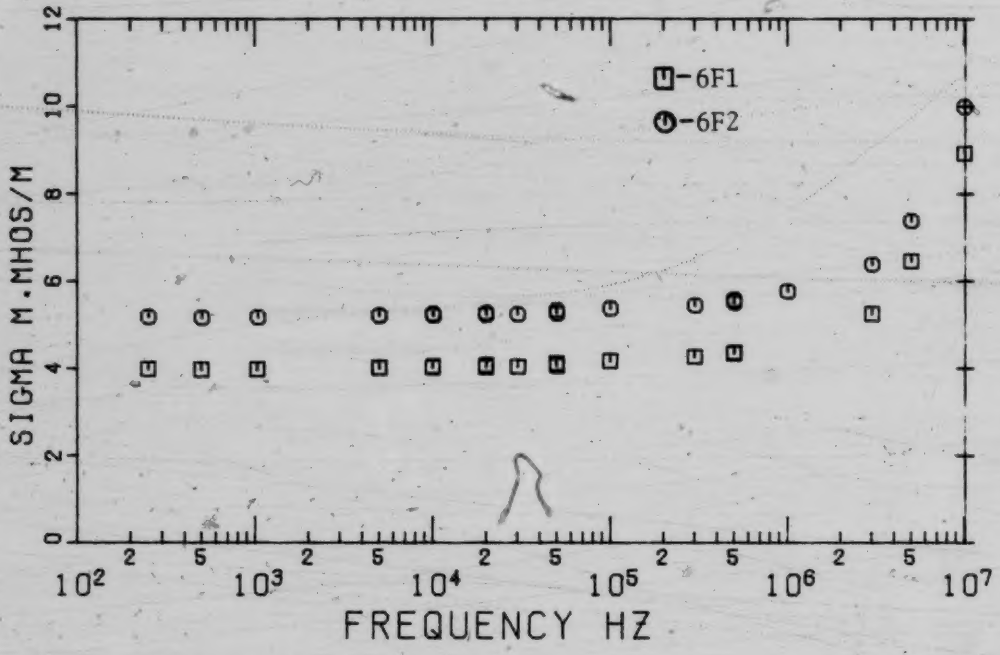

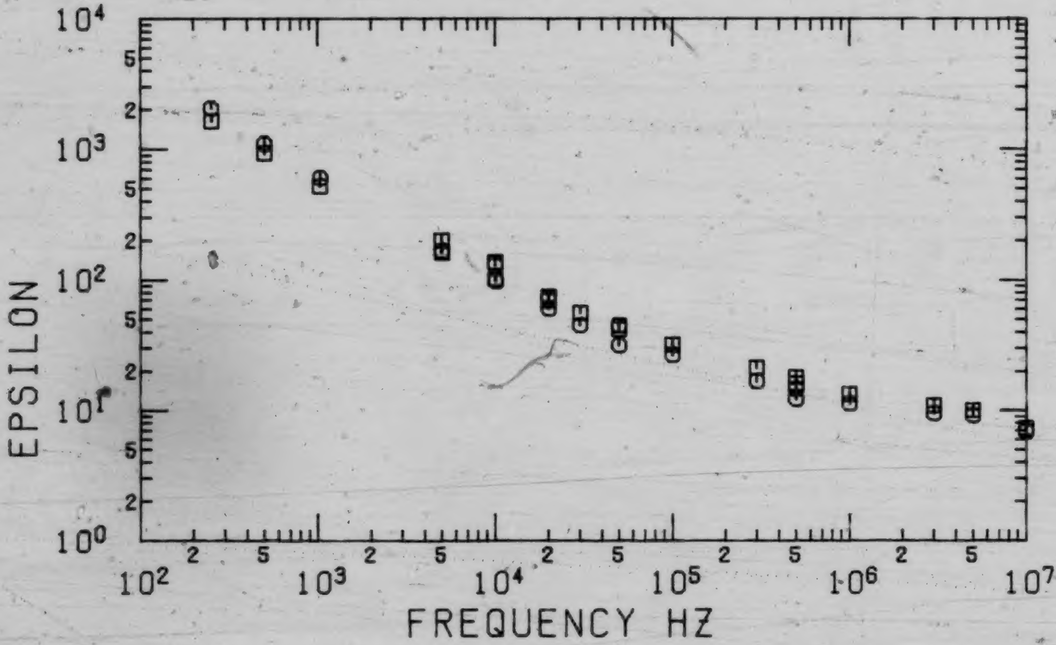

FIGURE(4.23) TAR SAND SAMPLES 6F1 6F2
Water Content 6F1-3.8% 6F2-3.8%
Bitumen Content 6f1-12.8% 6F2-12.8%

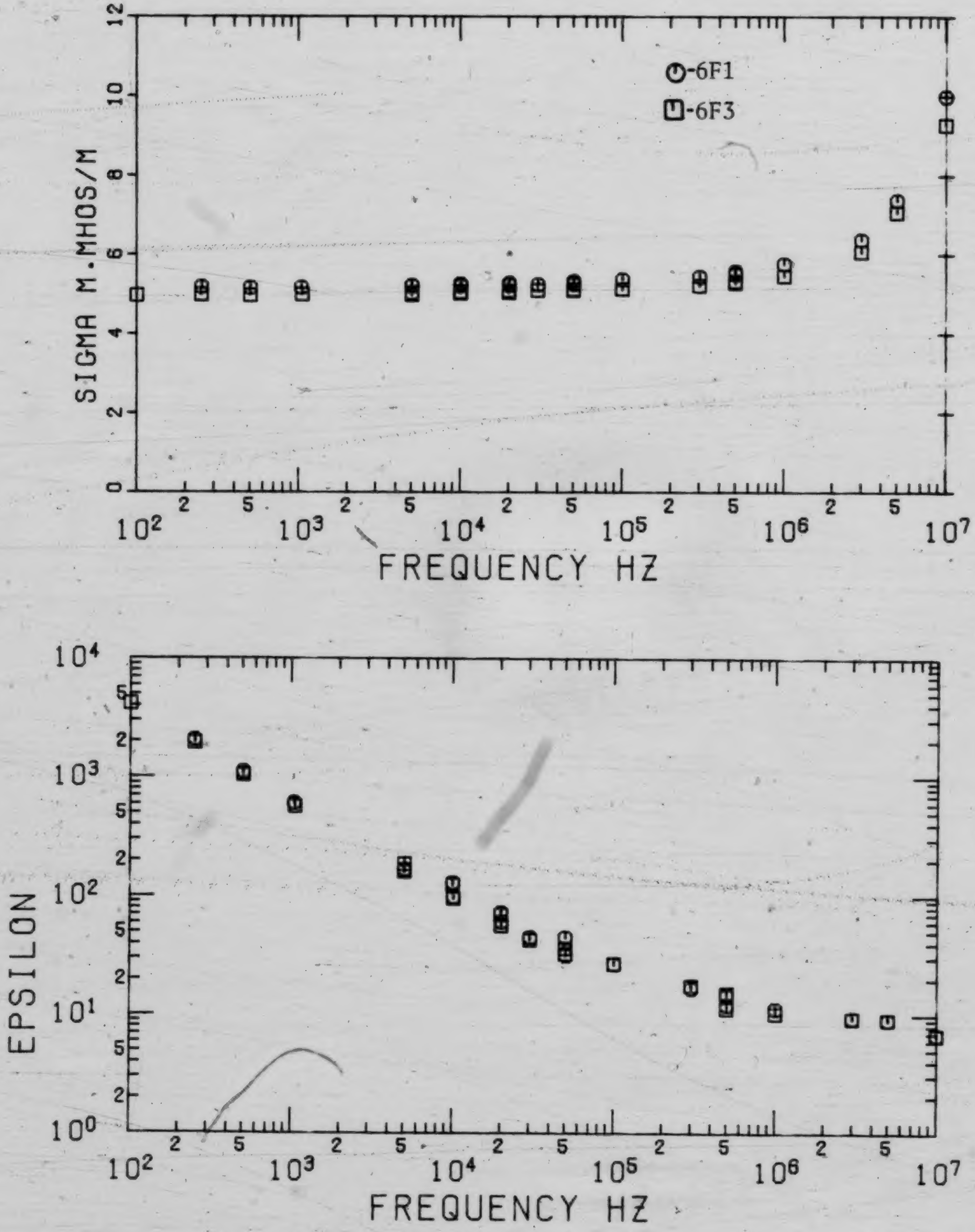

FIGURE(4.24) TAR SAND SAMPLES 6F1 6F3
Water Content 6F1-3.8% 6F3-3.8%
Bitumen Content 6F1-12.8% 6F3-12.8%

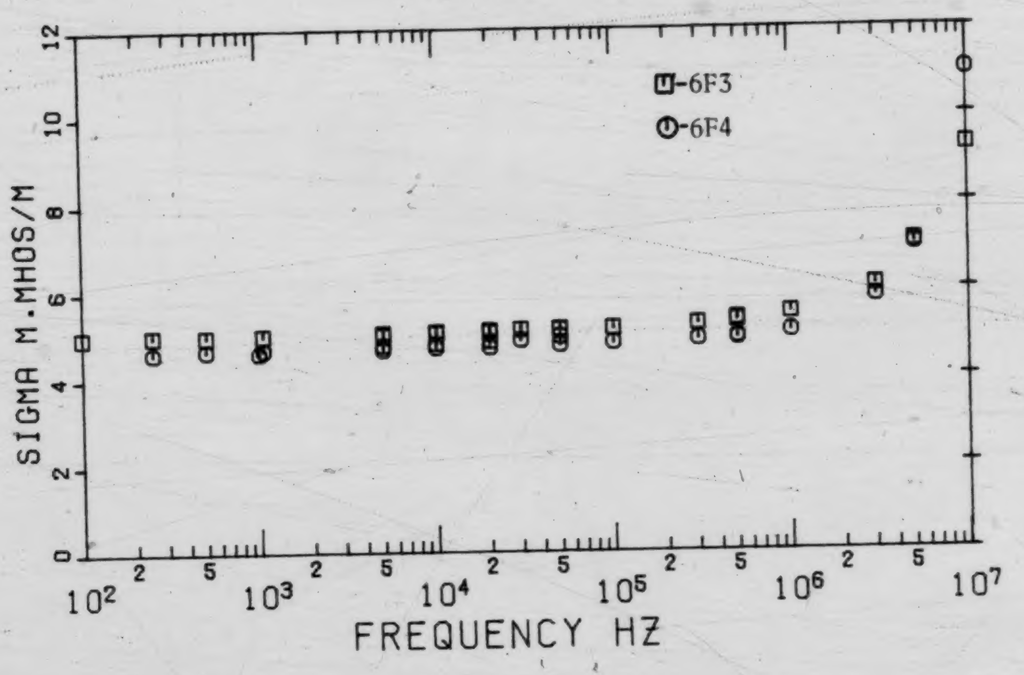

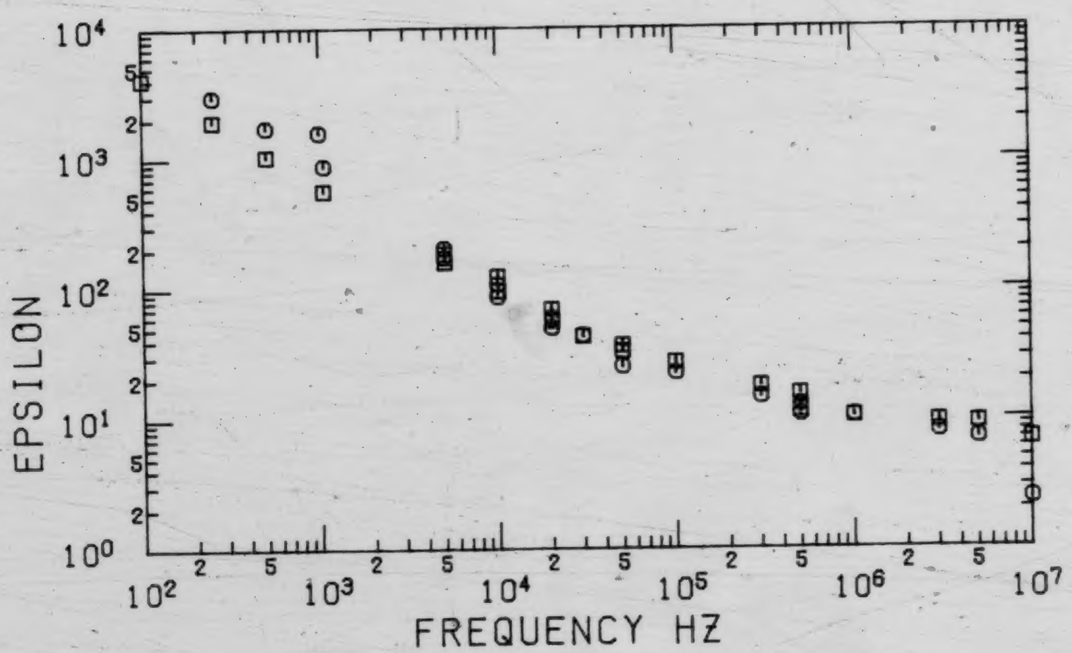

FIGURE(4.25) TAR SAND SAMPLES 6F3 6F4
Water Content 6F3-3.8% 6F4-3.8%
Bitumen Content 6F3-12.8% 6F4-12.8%

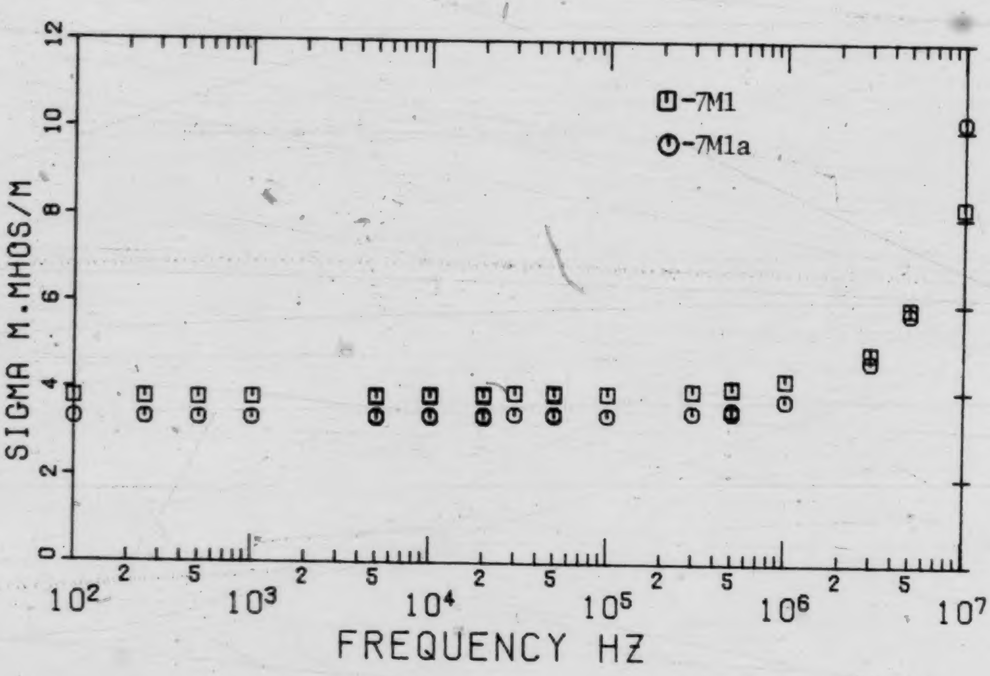

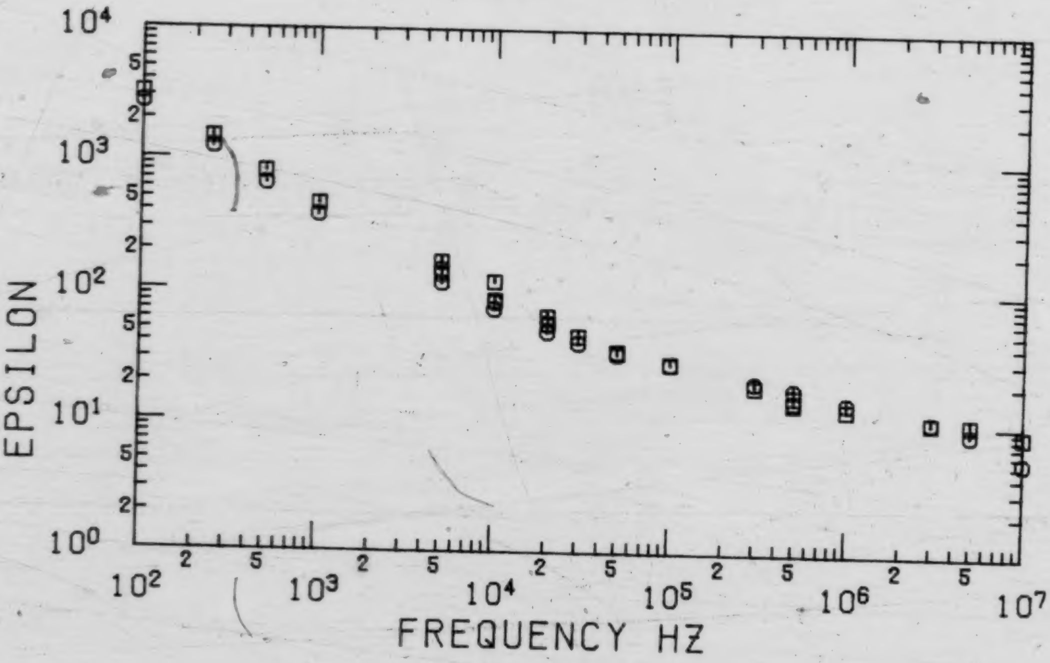

FIGURE(4.26) TAR SAND SAMPLES 7M1 7M1a
Water Content 7M1-2.7% 7M1a-3.6%
Bitumen Content 7M1-11.1% 7M1a-11.5%

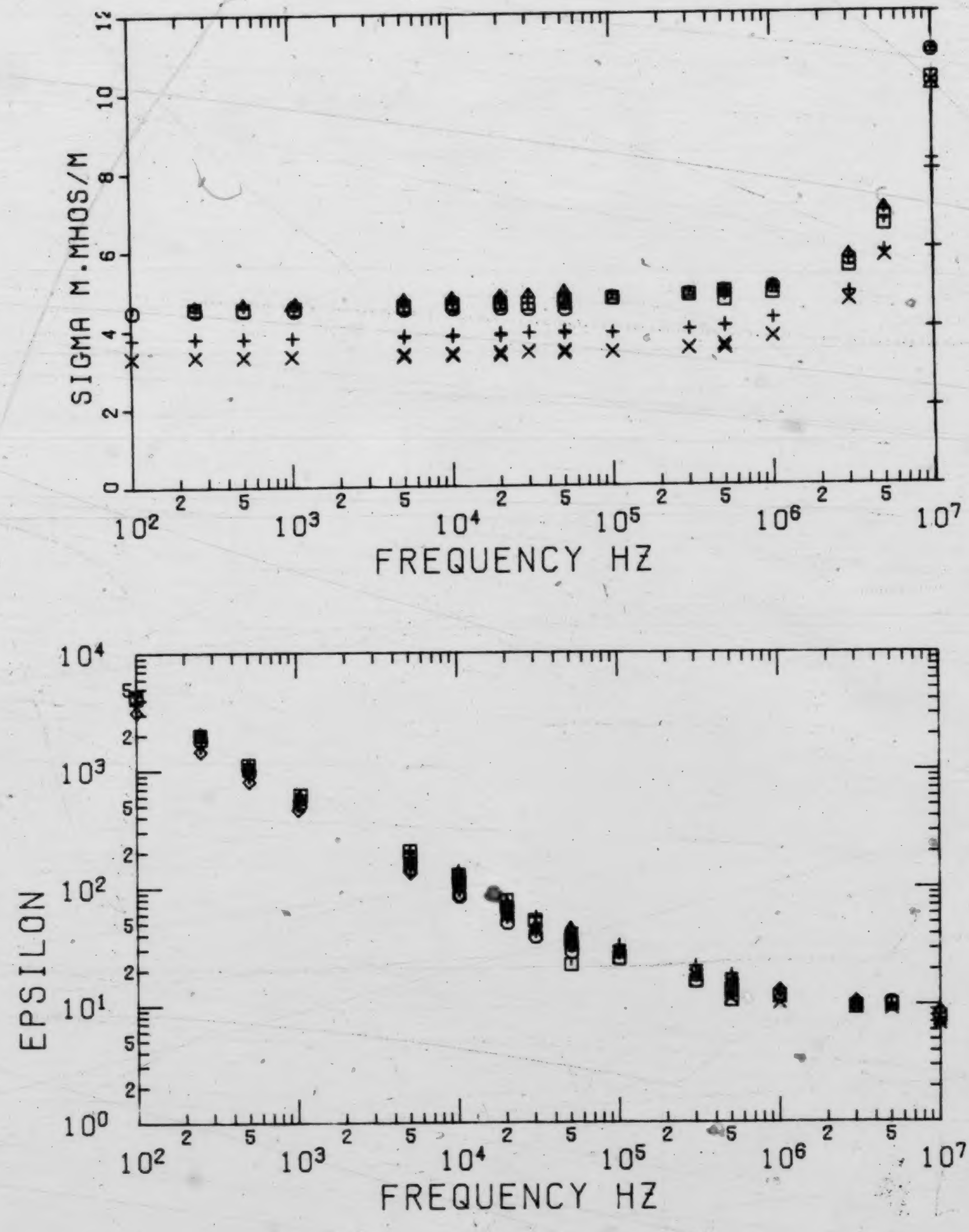

FIGURE(4.27) COMPOSITE GRAPH OF BATCH 3
Average Water Content 4.1%
Average Bitumen Content 12.4%

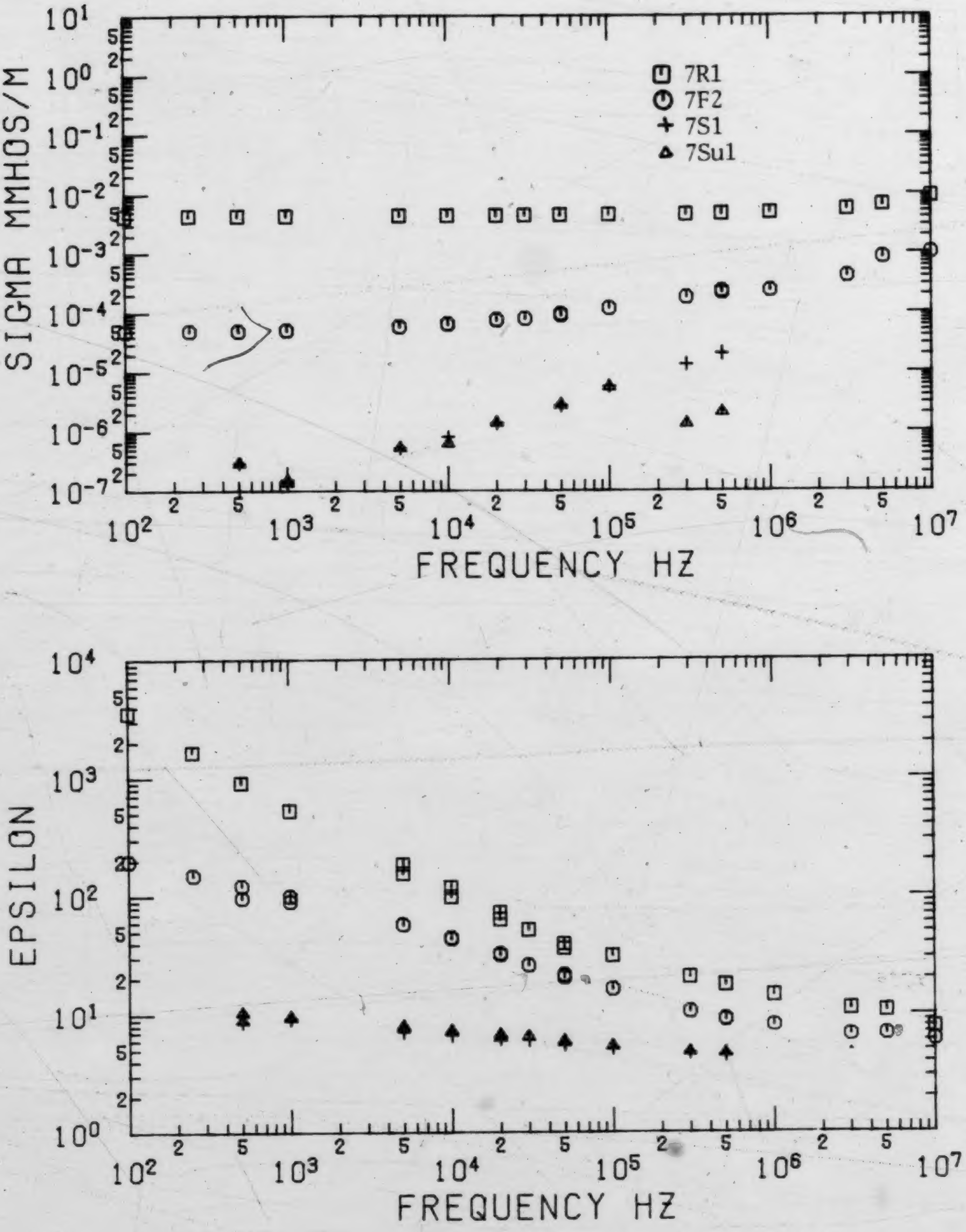

FIGURE(4.28) DRYING TEST SAMPLES 7R1 7F2 7S1 7SU1

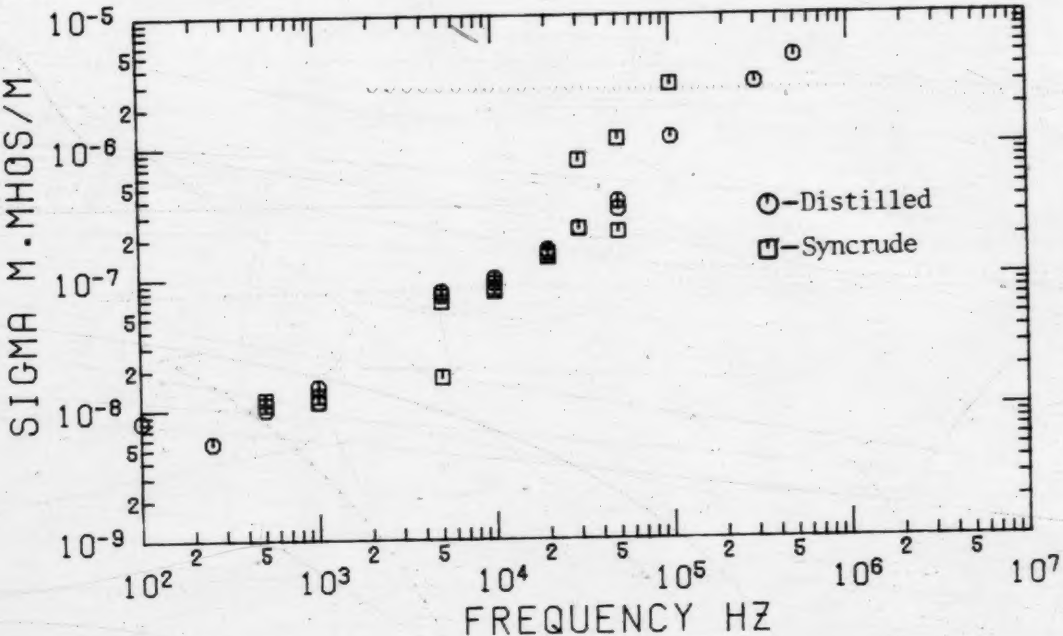

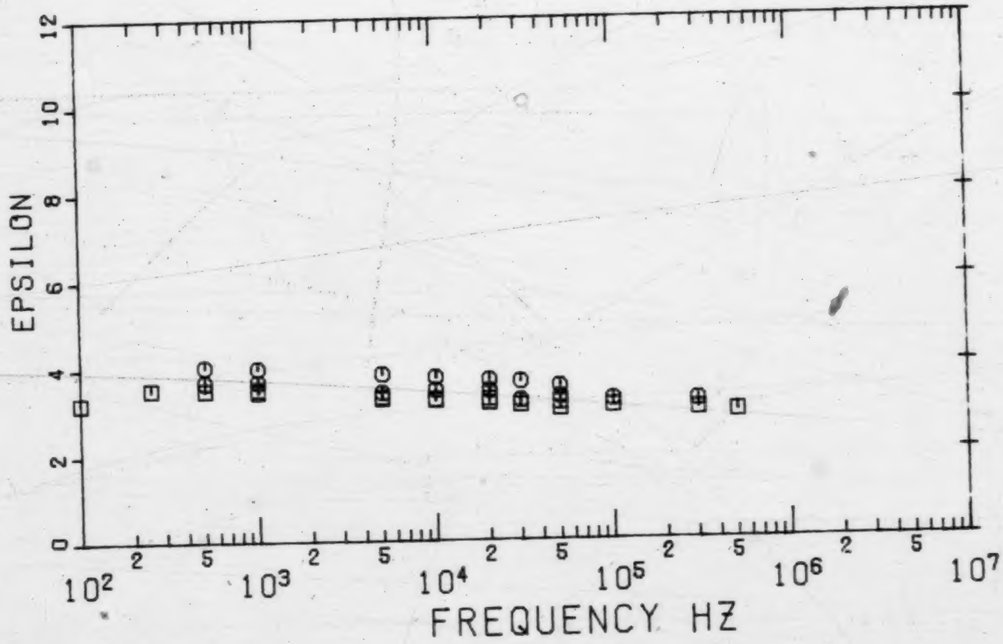

FIGURE(4.29) PURE BITUMEN SAMPLES

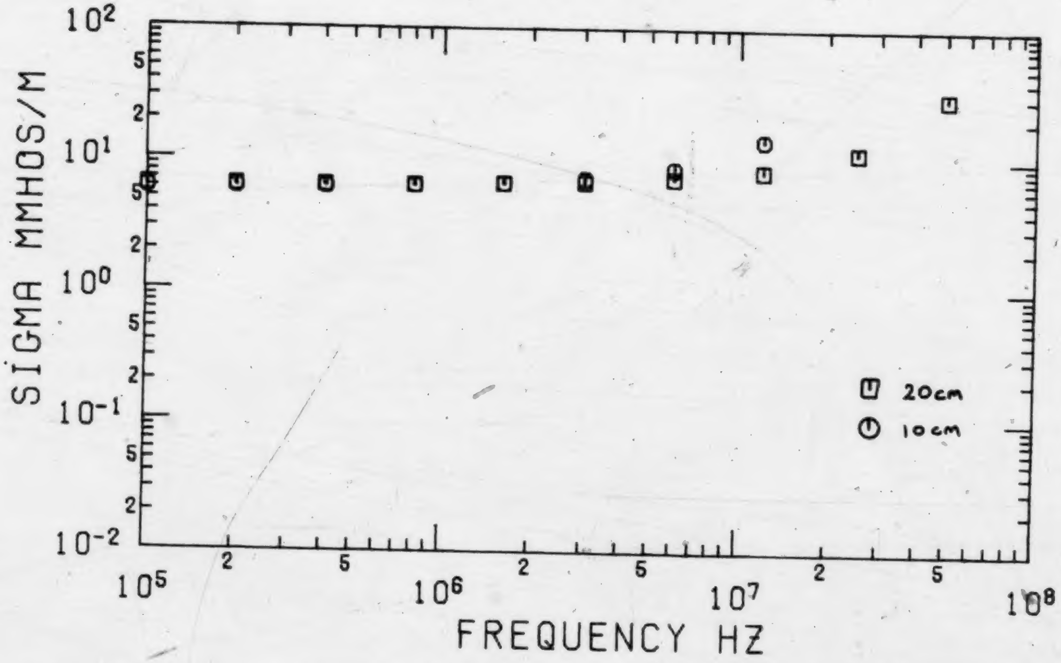

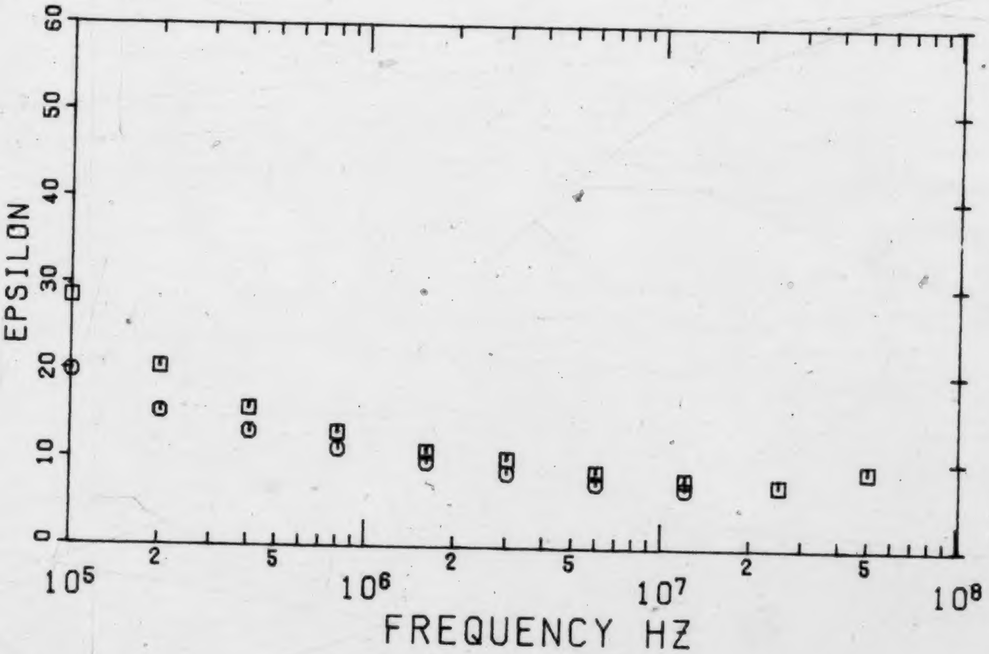

FIGURE(4.30) TAR SAND SAMPLE F1-1
Water Content F1-6.0%
Bitumen Content F1-16.6%

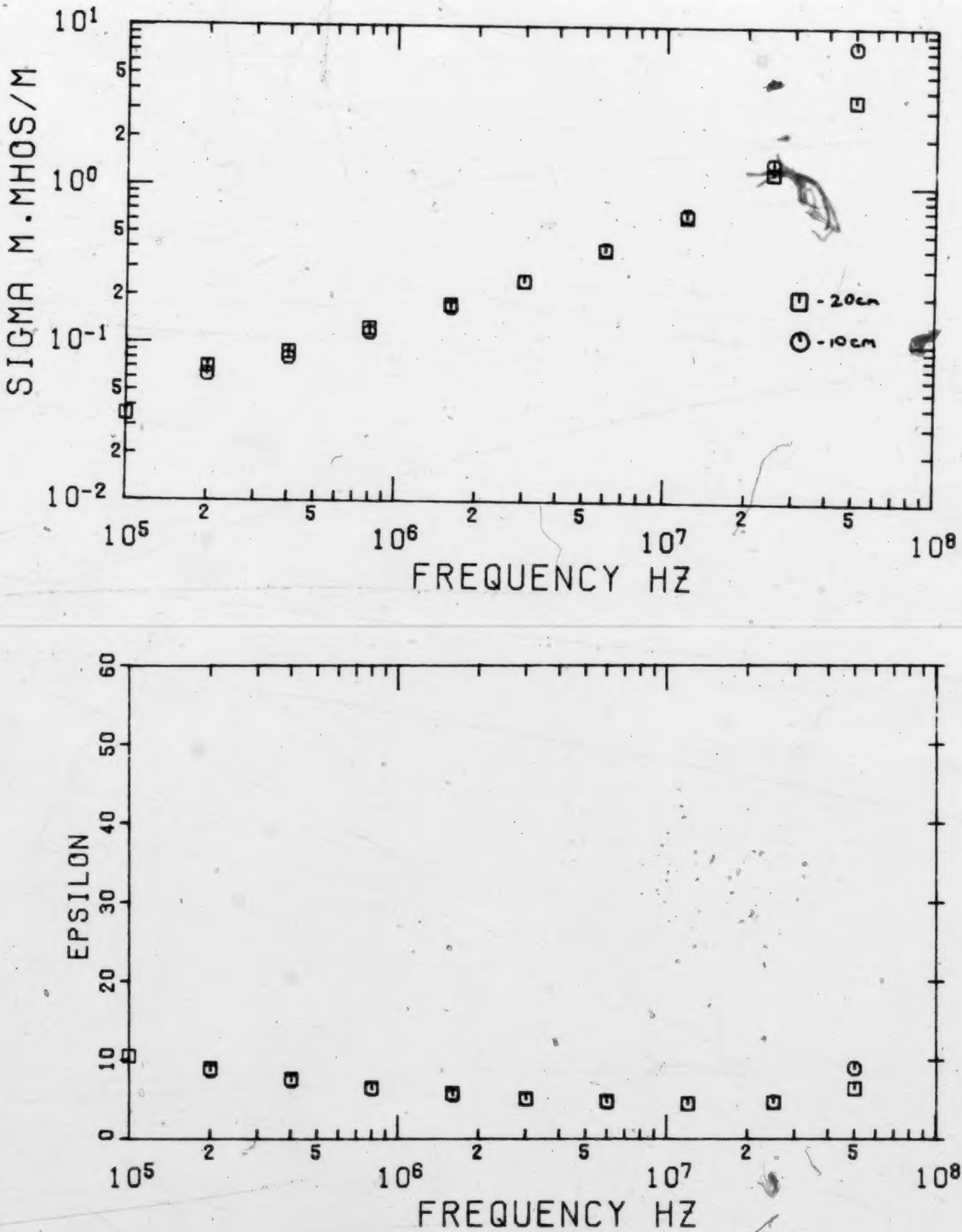

FIGURE(4.31) TAR SAND SAMPLE F3-1
Water Content F3-1 1.2%
Bitumen Content F3-1 14.1%

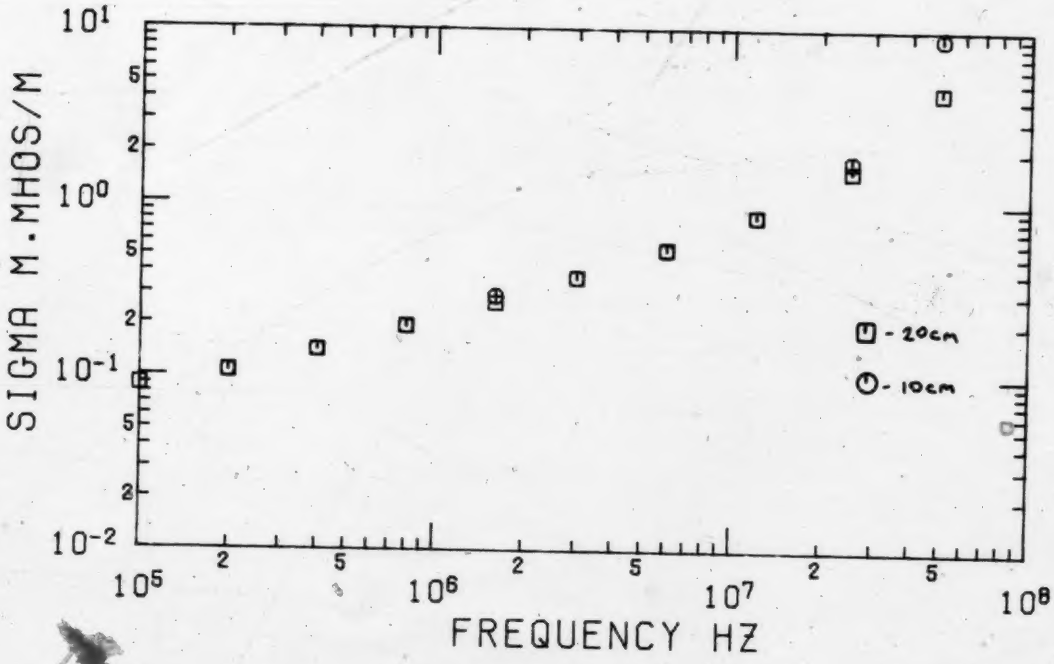

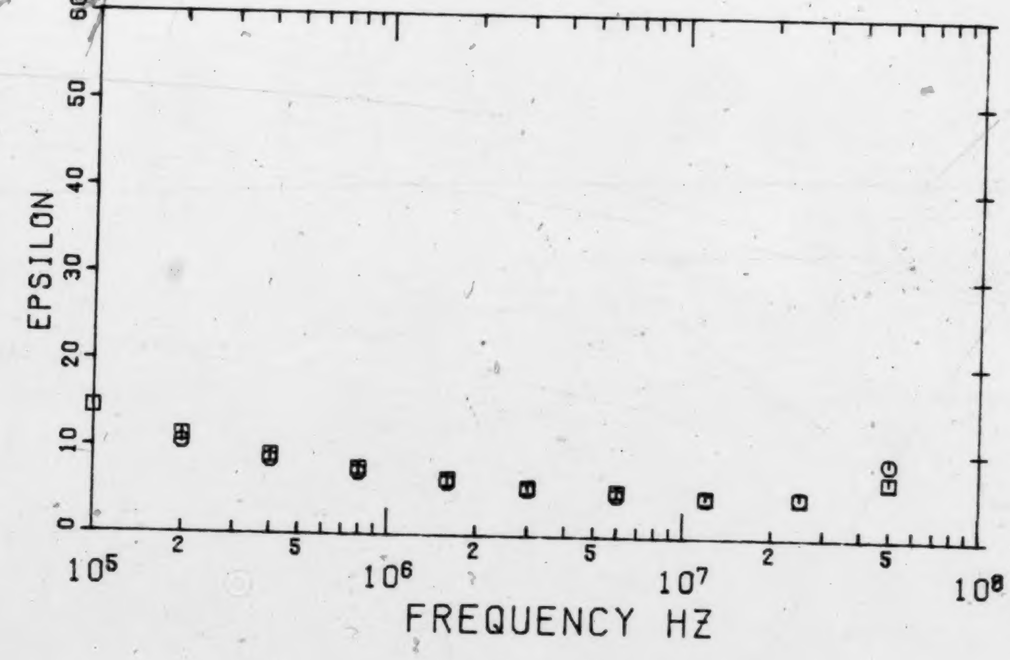

FIGURE(4.32) TAR SAND SAMPLE F3-2
Water Content F3-2 1.2%
Bitumen Content F3-2 14/1%

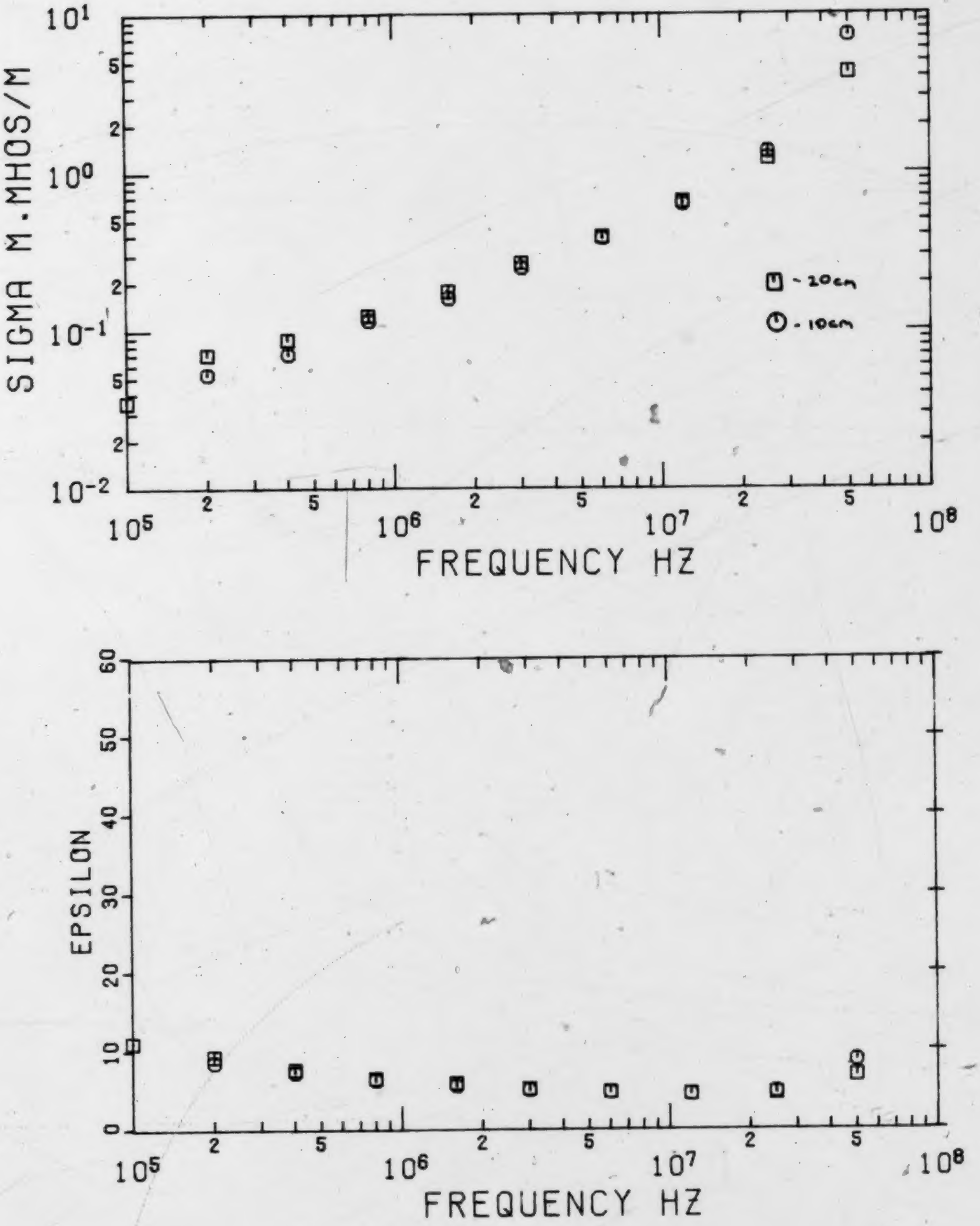

FIGURE(4.33) TAR SAND SAMPLE F3-3
Water Content F3-3 1.2%
Bitumen Content F3-3 14.1%

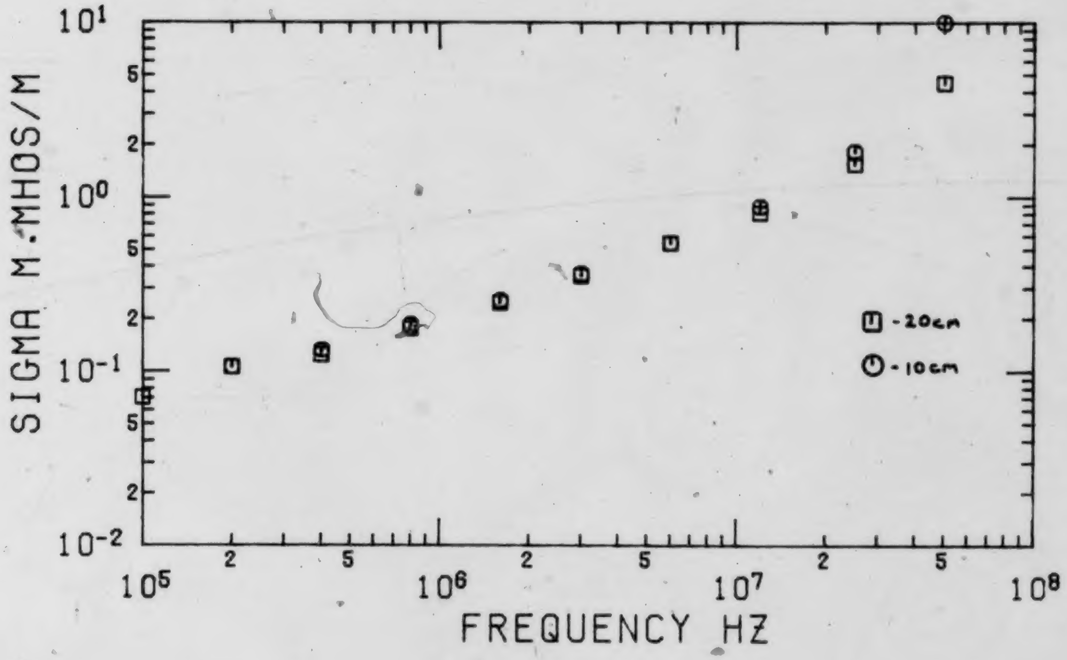

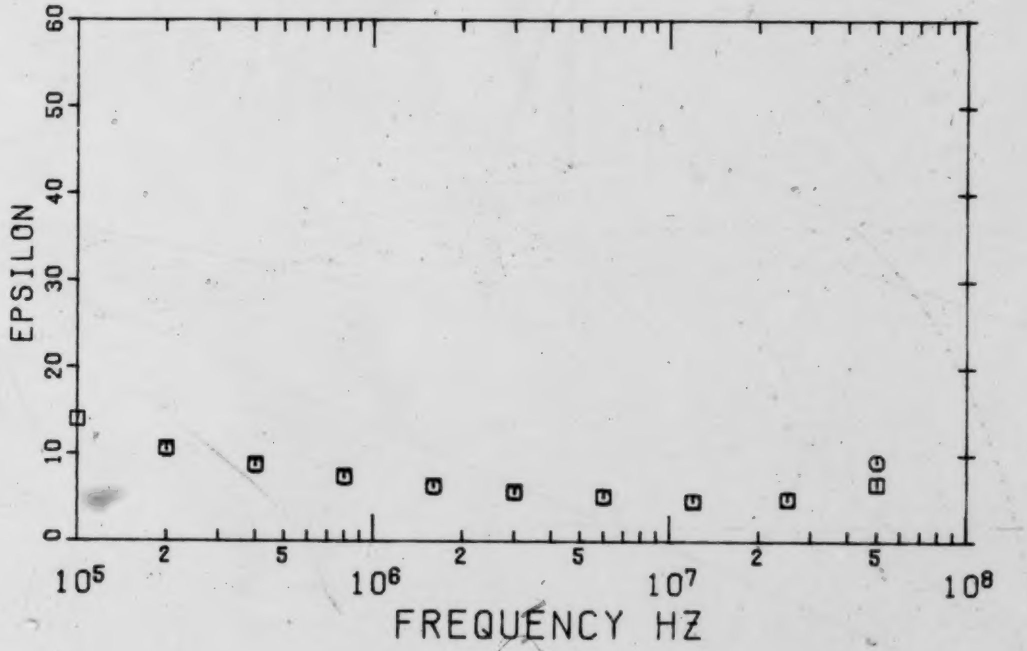

FIGURE(4.34) TAR SAND SAMPLE F3-4
Water Content F3-4 1.2%
Bitumen Content F3-4 14.1%

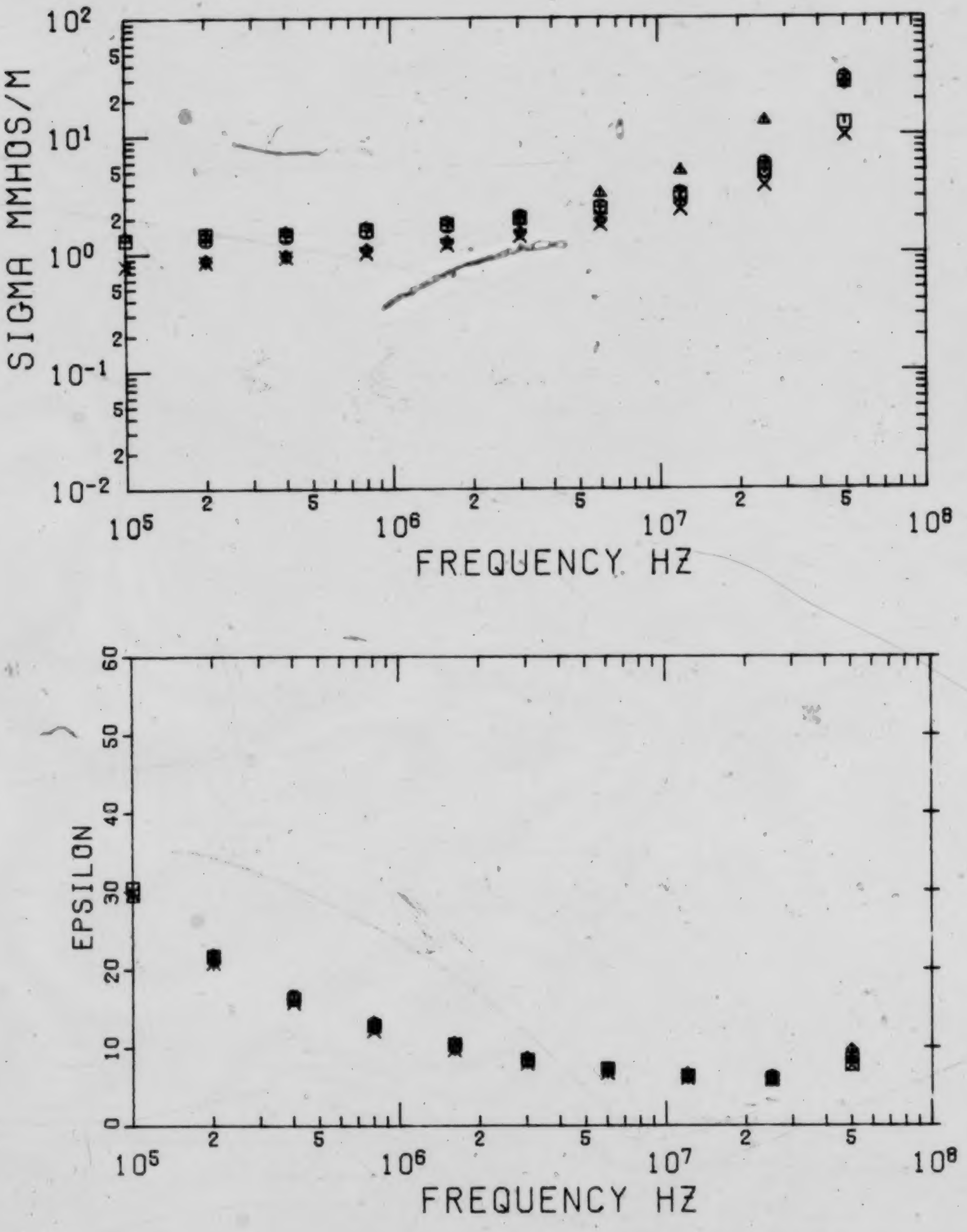

FIGURE(4.35) COMPOSITE GRAPH OF BATCH 4
Average Water Content 1.2%
Average Bitumen Content 14.1%

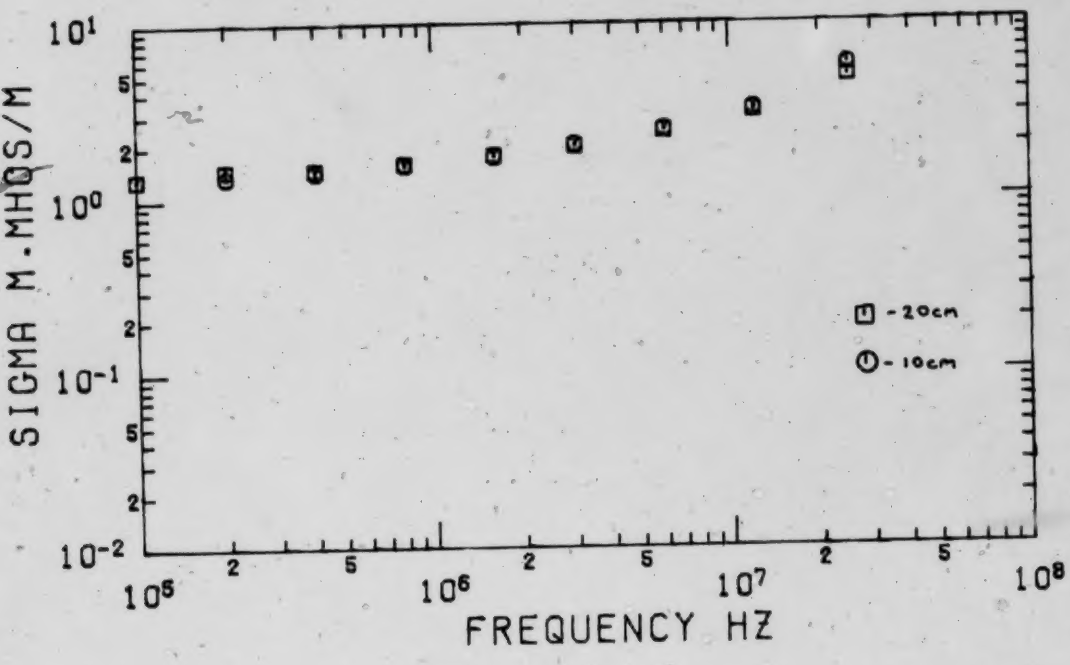

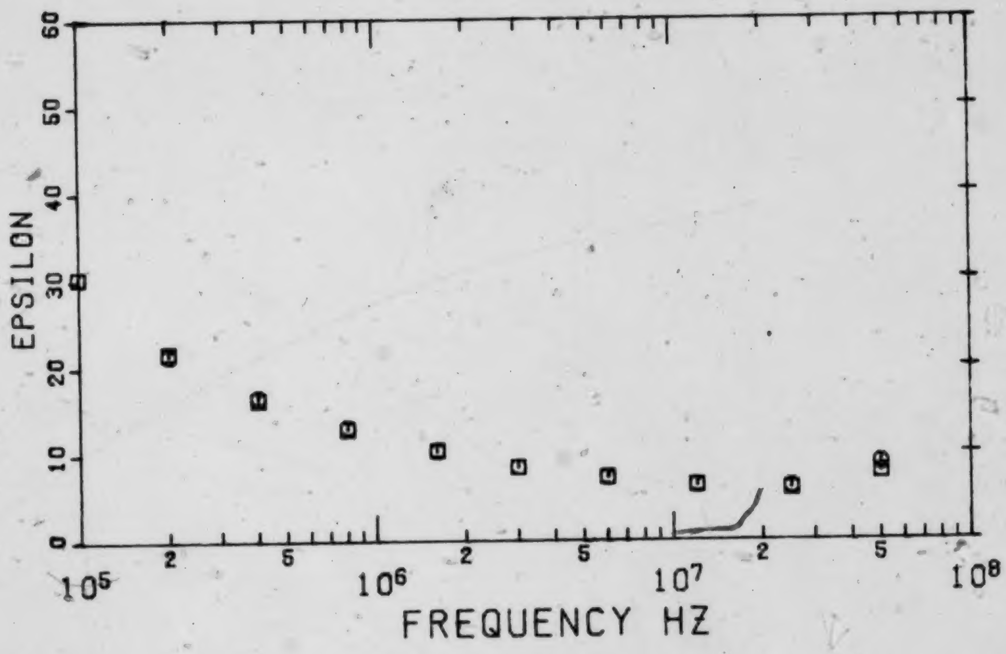

FIGURE(4.36) TAR SAND SAMPLE F4-1
Water Content F4-1 1.8%
Bitumen Content F4-1 13.5%

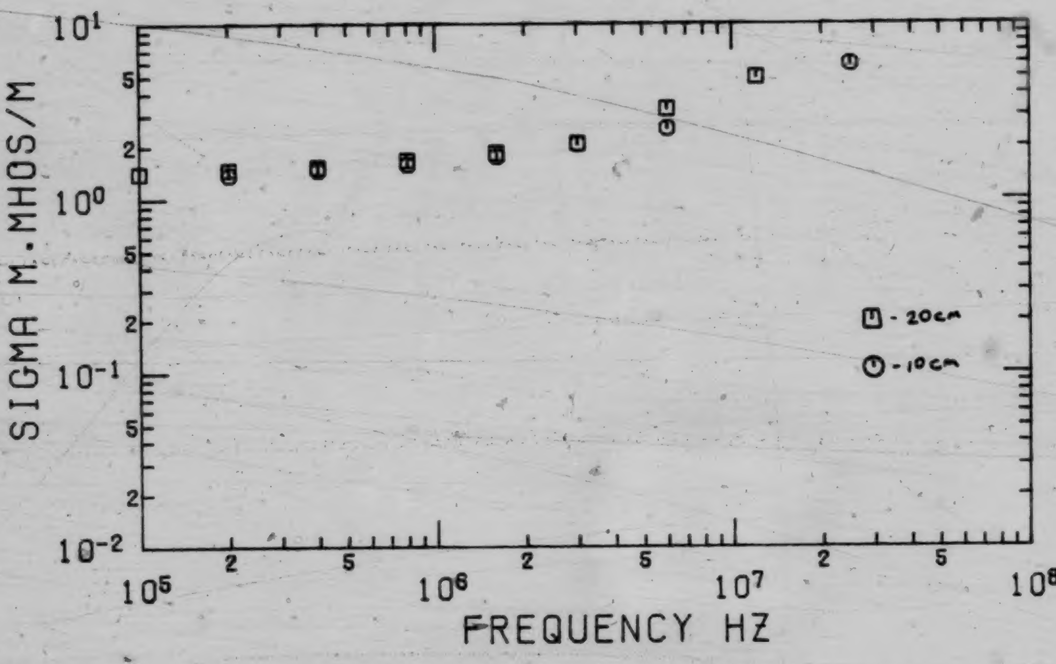

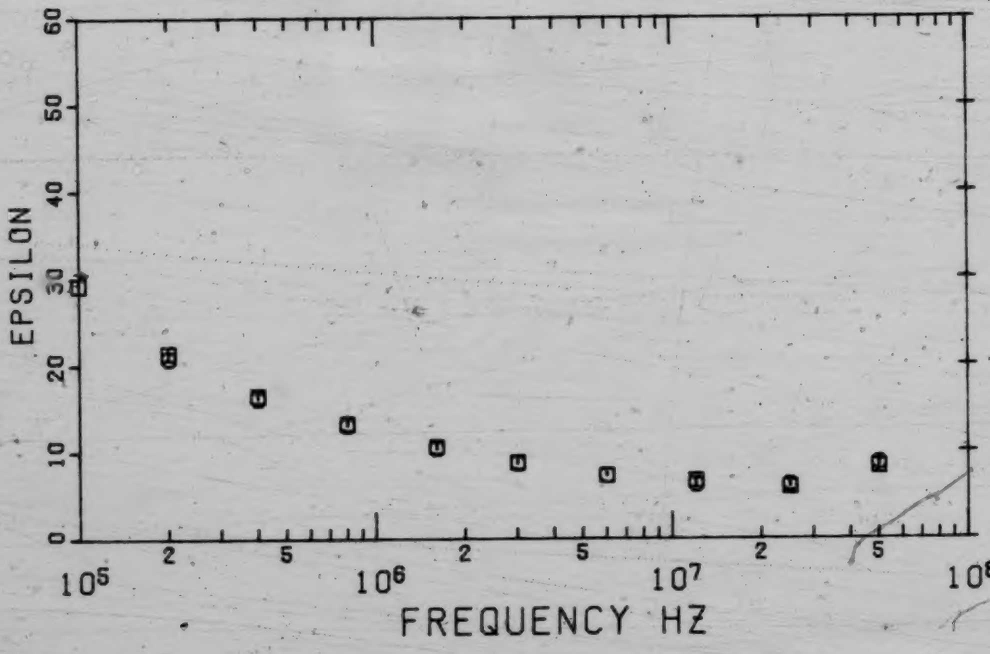

FIGURE(4.37) TAR SAND SAMPLE F4-2
Water Content F4-2 1.8%
Bitumen Content F4-2 13.5%

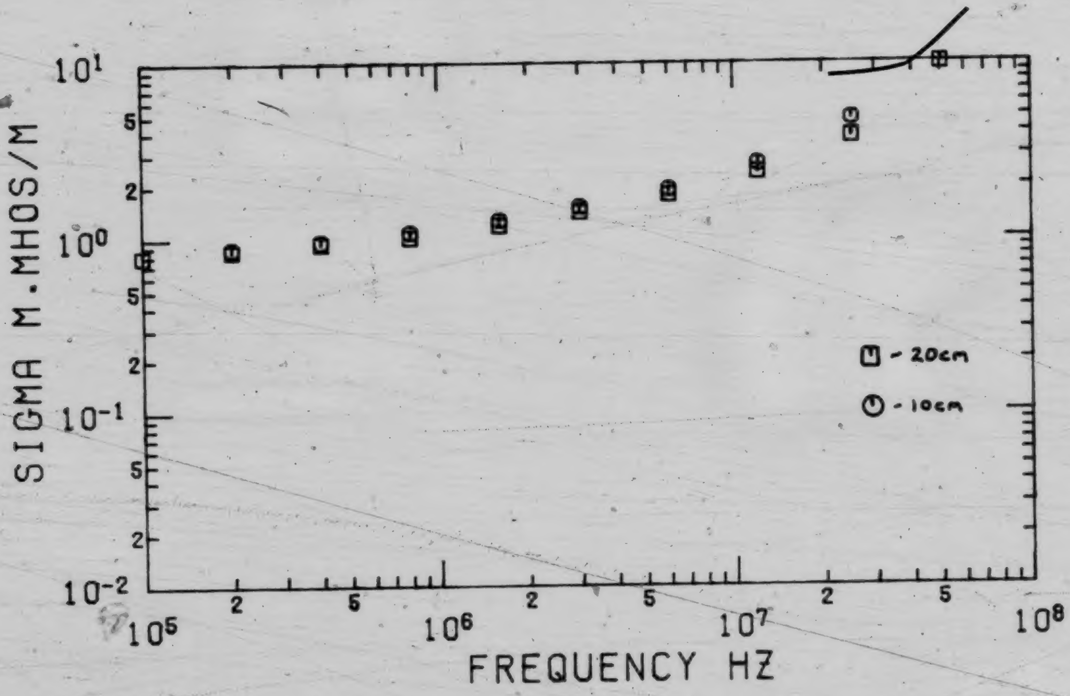

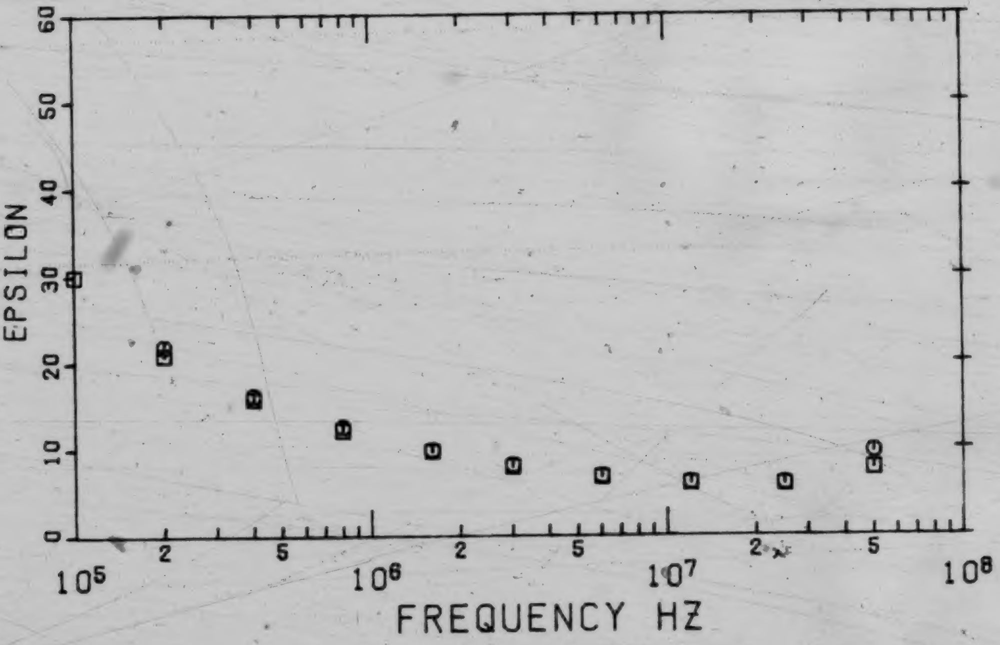

FIGURE(4.38) TAR SAND SAMPLE F4-3
Water Content f4-3 1.8%
Bitumen Content F4-3 13.5%

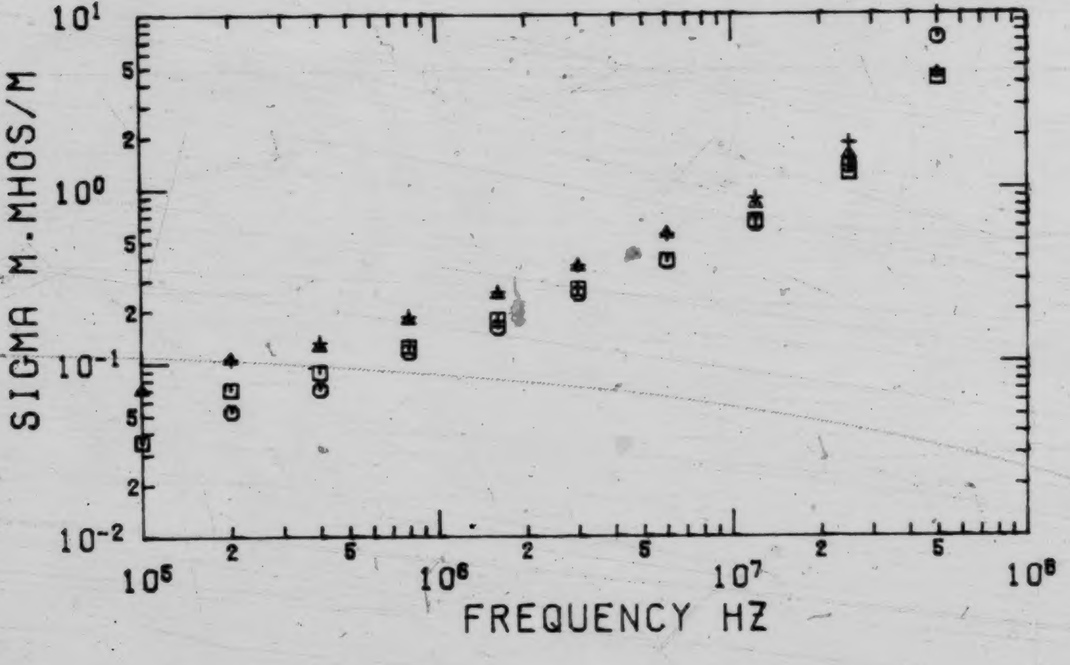

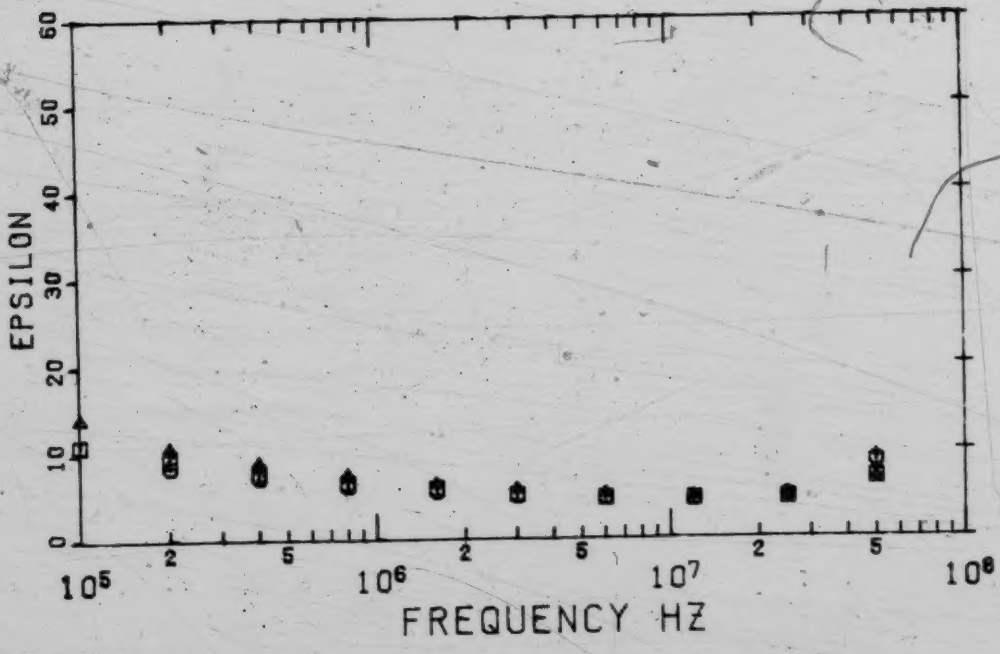

FIGURE(4.39) COMPOSITE GRAPH OF BATCH 5
Average Water content 1.8%
Average Bitumen Content 13.5%

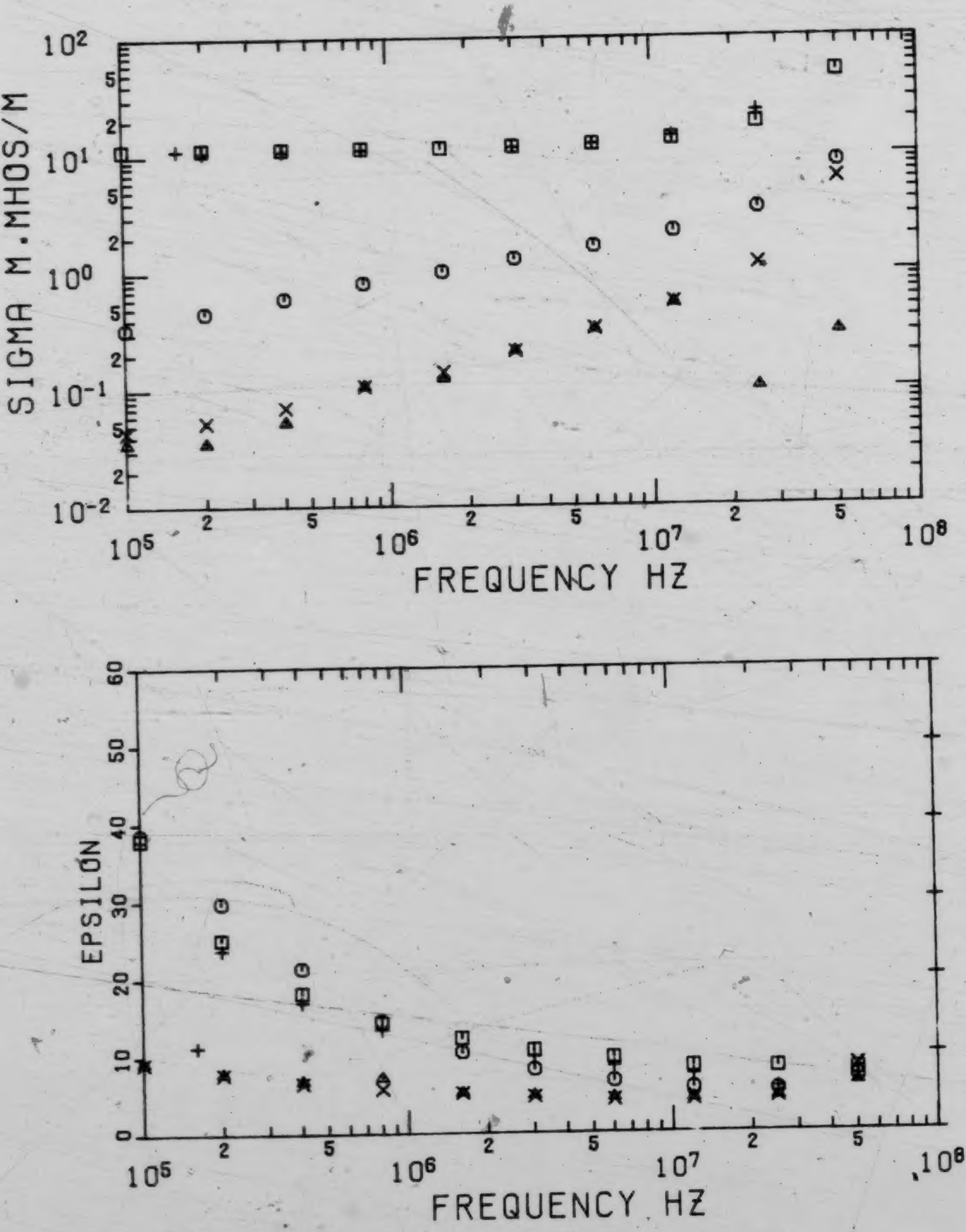

FIGURE(4.40) FIRST DRYING TEST
Initial Water Content 5.7%
Final Water Content 0%

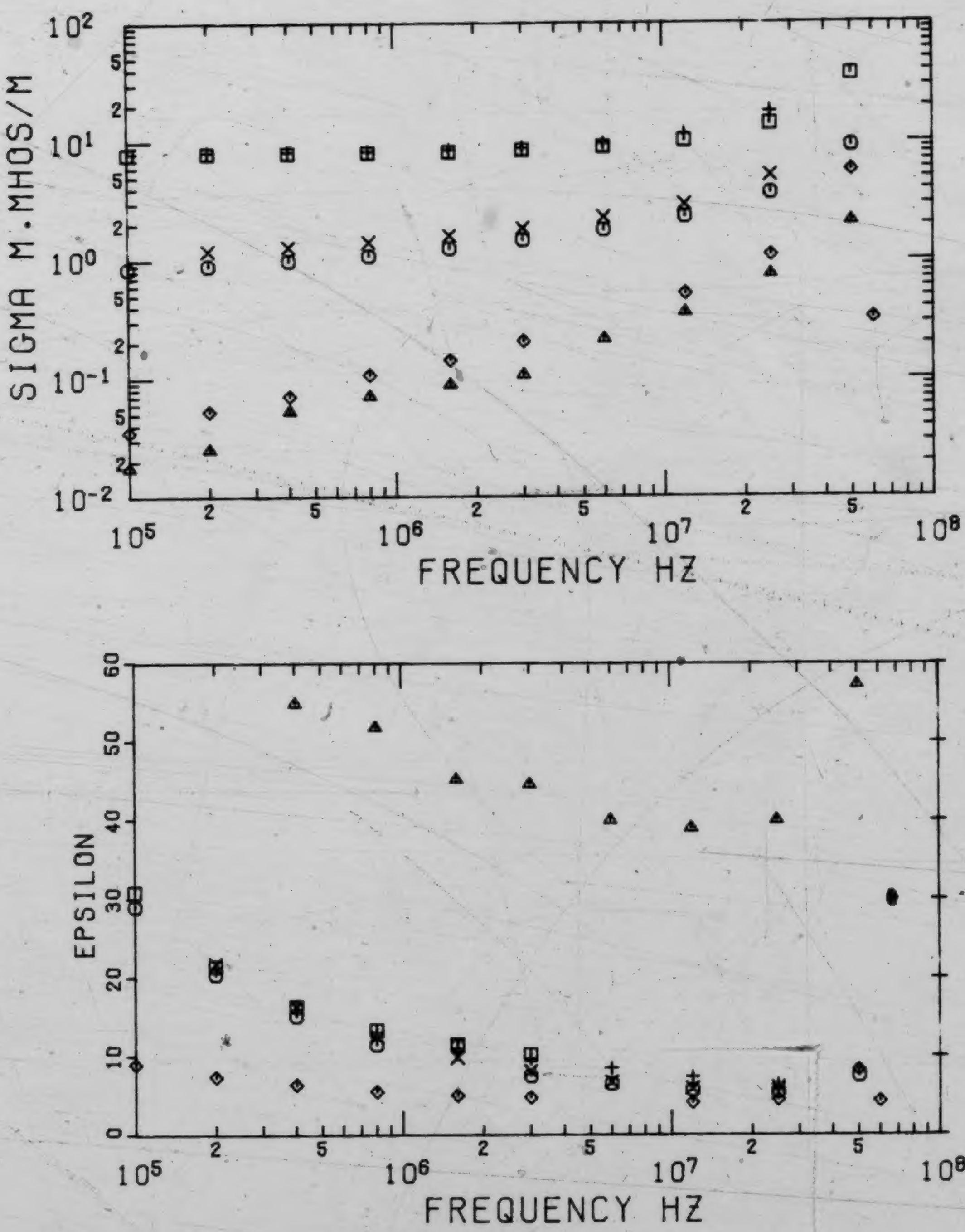

FIGURE(4.41) SECOND DRYING TEST
Initial Water Content 3.4%
Final Water Content 0%

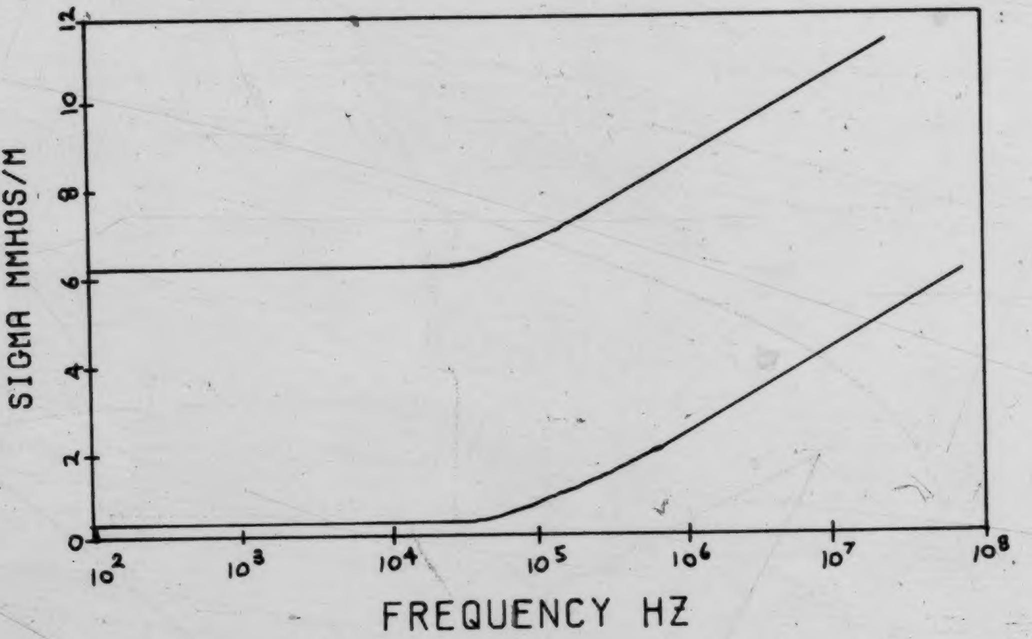

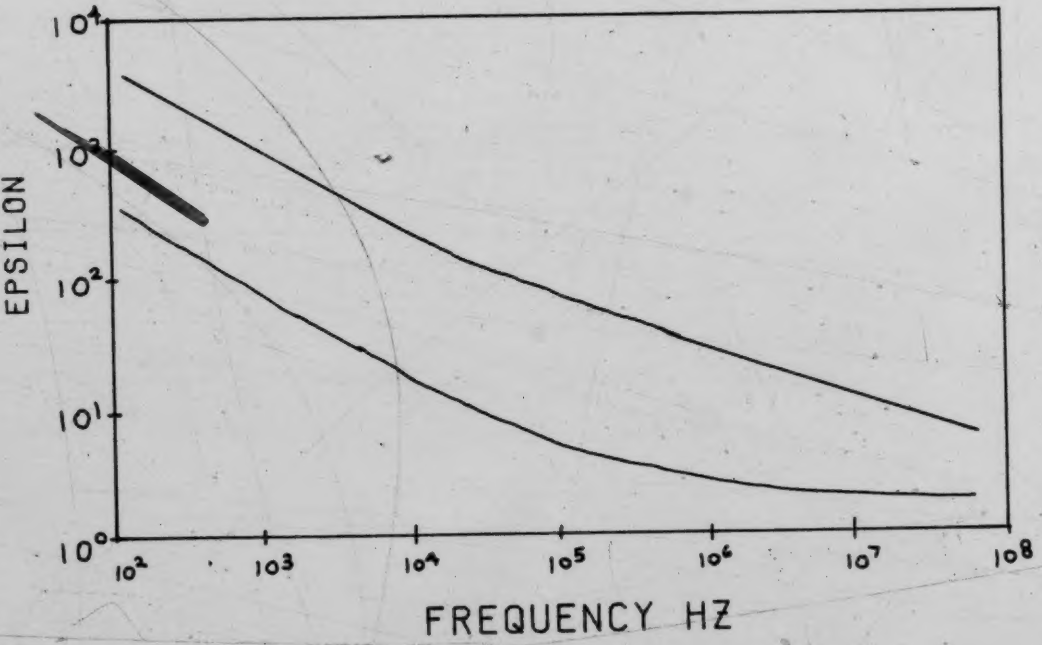

FIGURE(4.42) PARAMETER LIMITS

LIST OF REFERENCES

1 G. W. Govier, "The Athabasca Oil Sands", American Petroleum Institute, Division of Production, Annual Meeting Papers, 1972, Houston, Texas, 3/6-8/72, quoted in F. W. Camp, "The Tar Sands of Alberta, Canada", *Enclyclopedia of Chemical Technology*, s.v., Vol. 19, John Wiley and Sons, 1969.

2 T. M. Doscher, "Technical Problems in In-Situ Methods for Recovery of Bitumen from Tar Sands", *Proceedings of the Seventh World Petroleum Congress*, Vol. 3, Elsevier Publishing Co., Essex England, 1967, pp. 625.

3 H. J. Remey,Jr., "A Current Review of Oil Recovery by Steam Injection", *Proceedings of the Seventh World Petroleum Congress*, Vol. 3, Elsevier Publishing Co., Essex England, 1967, p. 471.

4 C. M. Davies, "Electrovolatization of Oil In Situ", *Proceedings of the Alberta Oil Sands Conference*, Kings Printer , Edmonton, 1951, p. 141.

5 D. L. Flock and J. Tharin, "Unconventional Methods of Recovery of Bitumen and Related Research Areas Particular to the Oil Sands of Alberta", Petroleum Society of CIM, Preprint.

6 E. R. Abernethy, "Production Increase of Heavy Crude Oils by Electromagnetic Heating", Paper No. 374007 presented by the May 7-10, 1974 Technical Meeting of the Petroleum Society of CIM in Calgary.

7 M. A. Carrigy, "The Physical and Chemical Nature of a Typical Tar Sand: Bulk Properties and Behavior", *Proceedings of the Seventh World Petroleum Congress*, Vol. 3, Elsevier Publishing Co., Essex England, 1967, pp. 573-581.

8 L. Hartshorn and W. Ward, "The Measurement of Permittivity and Power Factor of Dielectrics at Frequencies from 10^4 to 10^8 cps", J. IEE, Vol. 79, 1936, pp. 597-609.

9 H. P. Schwan and C. D. Ferris, "Four-Electrode Null Techniques For Impedance Measurement with High Resolution", Rev. Scientific Instruments, Vol. 39, No. 4, 1968, pp.481-485.

10 C. D. Ferris, "Four Electrode Electronic Bridge for Electrolyte Impedance Determinations", Rev. Scientific Instruments, Vol. 34, No. 1, 1963, p. 109.

11 H. H. Skilling, Electric Transmissions Lines. McGraw Hill Book Co., New York, 1951, p. 14.

12 E. J. Kirkscether, "Ground Constant Measurements Using a Section of Balanced Two Wire Transmission Line", IRE Trans. On A and P, May, 1960, pp. 307-313.

13 W. L. Everitt, Communication Engineering. McGraw Hill Book Co., New York, 1937, pp. 168-171.

14 A. R. Von Hippel, ed., Dielectric Materials and Applications. John Wiley and Sons, New York, 1954, pp. 67-69.

15 Ibid., pp. 88-103.

16 R. J. Lytle, "Measurement of Earth Medium Electrical Characteristics: Techniques, Results and Applications", IEEE Trans. On Geo. Science Electronics, Vol. GE-12, No. 3, pp. 81-101.

17 E. C. Jordan and K. G. Balmain, Electromagnetic Waves and Radiating Systems. Second edition, Prentice-Hall, New Jersey, 1968, pp. 654-655.

18 A. Sommerfeld, "On the Distribution of Waves in Wireless Telegraphy", quoted in, R. L. Smith-Rose, "Electrical Measurements on Soil With Alternating Currents", *J. IEE*, Vol. 75, 1934, p. 222.

19 G. H. Keller and F. C. Frischknecht, *Electrical Methods in Geophysical Prospecting*, Pergammon Press, New York, 1965, p. 14.

20 C. B. Feldman, "The Optical Behavior of Ground for Short Radio Waves", *Proc. IRE*, Vol. 21, No. 6, 1933, pp. 765-799.

21 F. S. Grant and G. F. West, *Intrepretation Theory in Applied Geophysics*, McGraw-Hill Book Co. New York, 1965, p. 385.

22 P. K. Bhattacharya and H. P. Patra, *Direct Current Geolectric Sounding*, Elsevier Publishing Co., Amsterdam, 1968, pp. 5-9.

23 Lytle, pp. 82-85.

24 von Hippel, pp. 295-425.

25 Smith-Rose, p. 228.

26 G. V. Keller and P. H. Licastro, "Dielectric Constant and Electric Resistivity cf Natural State Cores", *U. S. Geo. Survey Bulletin 1052-H*, p. 259.

27 B. F. Howell, Jr., and P. H. Licastro, "Dielectric Behavior of Rocks and Minerals", *American Mineralogist*, Vol. 46, 1961, p. 280.

28 J. H. Scott, R. D. Carroll, and D. R. Cunningham, "Dielectric Constant and Electrical Conductivity Measurements of Moist Rock: A New Laboratory Method", *Journal of Geophysical Research*, Vol. 72, No. 20, 1967, p. 5101.

29 H. Fricke, "The Electric Capacity of Suspensions With Special Reference to Blood", *Journal General Physiology*, Vol. 9, 1926, pp. 137-152.

30 G. C. Koops, "On the Dispersion of Resistivity and Dielectric Constant of Some Semi-conductors at Audio Frequencies", *Phys. Rev.* ,Vol. 83, No. 1, 1951, pp. 121-124.

31 A. G. Tarkhov, "Resistivity and Dielectric Constant of Rocks in Alternating Current Fields", as quoted in J. H. Scott et al., p. 5102.

32 A. R. Von Hippel, "Interfacial and Space Charge Polarization", *Dielectrics and Waves*. John Wiley and Sons, New York, 1954, pp. 228-234.

33 J. F. Johnson and R. H. Cole, "Dielectric Polarization of Liquid and Solid Formic Acid", *J. American Chemical Society*, Vol. 73, Pt. 4, 1951, pp. 4536.

34 B. F. Howell, Jr. And P. H. Licastro, pp. 285-286.

35 K. A. Valeev and E. L. Parkhomenko, "Electrical Properties of Rocks in Constant and Alternating Electric Fields", IZV. *Phys. Solid Earth*, Eng. Translation, 12, 1965, pp. 45-52.

36 J. H. Scott et al., p. 5105.

37 D. J. Marshall and T. R. Madden, "Induced Polarization, A Study of Its Causes", *Geophysics*, Vol. 24, No. 4, 1959, pp. 790-816.

38 G. V. Keller and P. H. Licastro, pp. 277-279.

39 B. D. Fuller and S. H. Ward, "Linear System Description of the Electrical Parameters of Rocks", *IEEE Trans. On Geo. Electronics*, Vol. GE-8, No. 1, 1970, pp. 7-17.

40 J. O. Bockris and A. K. Reddy, *Modern Electrochemistry*. Vol. 2, Plenum Press, New York, 1973, P. 895.

41 A. M. Dymond, "Characteristics of the Metal-Tissue Interface of Stimulation Electrodes", *IEEE Trans. On Biomedical Engineering*, Vol. BME-23, No. 4, 1976, pp. 274-279.

42 A. G. Tarkhov as quoted in J. H. Scott et al.

43 J. H. Scott et al., P. 5104.

44 R. Alvarez, "Complex Dielectric Permittivity in Rocks: A Method for Its Measurement and Analysis", *Geophysics*, Vol. 38, No. 5, 1973, pp. 920-940.

45 C. D. Ferris, *Introduction to Bioelectrodes*. Plenum Press, New York, 1974, p. 184.

46 L. Young, *Anodic Oxide Films*. Academic Press, New York, 1961, p. 216.

47 J. H. Scott et al., p. 5109.

48 K. A. Clark, Mimeo. Circ. 22 Edmontom Research Council of Alberta 1957.

49 S. M. Blair, *Report on the Alberta Bituminous Sands*, Government of the Province of Alberta, Edmontom, Canada, 1951, p. 36.

50 Alvarez, pp. 921-923.

51 G. V. Keller and P. H. Licastro, p. 265.

52 G. V. Keller and F. C. Frischknecht, *Electrical Methods in Geophysical Prospecting*, Pergamon Press, Toronto, 1966, pp. 436-452.

53 Fuller and Ward, pp. 7-9.